TELECOMMUNICATIONS

English Edition of

ЭЛЕКТРОСВЯЗЬ

LIBRARY
U. S. NAVAL
POSTGRADUATE SCHOOL
JAN 21961
MONTEREY, CALIFORNIA

No.1 January 1961

Published by the American Institute of Electrical Engineers
with the aid of a grant from the National Science Foundation

Translated and Produced by Royer and Roger, Inc.

AMERICAN INSTITUTE OF ELECTRICAL ENGINEERS

Established 1884

33 West Thirty-ninth Street
New York 18, New York

Warren H. Chase, President
N.S. Hibshman, Executive Secretary
C.E. Dean, Technical Vice President, Communications
W.F. Denkhaus, Director of Publications
L.G. Abraham, Chairman, Communications Division

The English edition of TELECOMMUNICATIONS is published by the American Institute of Electrical Engineers with the aid of a grant from the National Science Foundation. © 1961 by American Institute of Electrical Engineers. Also published under the same arrangement are the Russian electronic journals RADIO ENGINEERING AND ELECTRONICS and RADIO ENGINEERING.

TELECOMMUNICATIONS

(ЭЛЕКТРОСВЯЗЬ)

Publication of the
A.S. Popov Technical Society of Radio Engineering and Telecommunications

Translated and Produced
by
Royer and Roger, Inc.

Translation Editor: Jack Warren, Columbia University
Associate Translation Editor: Alfred Weiss, Radio Corporation of America

AIEE REVIEW COMMITTEE FOR TELECOMMUNICATIONS
H.F. May
Bell Telephone Laboratories, Inc.
Chairman

A.G. Cooley
A.D. Fowler
A.E. Frost
F.G. Hollins
A.E. Joel
A.D. Moore
W.B. Quirk
L.L. Robinett
R.B. Shanck
D.L. Solomon
F.W. Smith
G. Worthen

Subscriptions to Telecommunications should be sent to AIEE
Special Subscription Department
41 East 28th Street
New York 16, New York

1961 Subscription rates:

	$	£
Individuals	14.25	5
Libraries, institutes, govt. agencies	28.50	10

12 issues per annum comprising approximately 1100 pages

APPLICATION OF NULL-DEVIATION FOR THE EVALUATION OF NOISE AND DISTORTION

V.A. Smirnov

In the theory of potential interference stability, V.A. Kotel'nikov has shown that with ideal reception the a minimum of the quantity $\overline{[\chi(t) - A_f(t)]^2}$ is ensured. This article justifies the possibility of taking the condition of $\chi(t) - (t) = 0$ during practical calculations for an ideal receiver. From here the Kotel'nikov formulas are derived for the case of very small noise fluctuations and also some new general solutions for large noise.

It is proposed to use the above condition for the evaluation of several types of noise and distortion, for multi beam propagation and for other cases.

JUSTIFICATION FOR THE CONDITIONS OF NULL-DEVIATION

In the theory of potential interference stability, V.A. Kotel'nikov [1] has shown that in an ideal receiver the minimum condition of root mean square deviation is fulfilled:

$$\overline{[\chi(t)-A_F(t)]^2} = \frac{1}{T}\int_{-\frac{T}{2}}^{\frac{T}{2}} [\chi(t) - A_F(t)]^2\, dt. \tag{1}$$

In this expression

$$\chi(t) = A(t, F_0) + N(t), \tag{2}$$

where $A(t, F_0)$ is the useful signal at the receiver input, modulated by the signal $F_0 = F_0(t)$, and $N(t)$ is the fluctuating noise at the receiver input.

$A_F(t) = A(t, F)$ is also expressed formally, as the useful signal at the receiver input, but with the difference that it is modulated by the $F = F(t)$ signal, obtained at the receiver output and which includes noise.

Having proved the minimum condition in (1), V.A. Kotel'nikov does not utilize it as the starting point in calculating $F(t)$ and employs a different method to calculate the signal and corresponding component of noise at the ideal receiver output. The case where fluctuating noise plays a relatively small role at the receiver input, is solved by V.A. Kotel'nikov in a practical way to obtain concrete expression for calculation of noise. Nevertheless it is apparent that a formal mathematical solution can be sought for the minimum condition of integral (1) without imposing any limitations

on noise magnitude and its physical characteristics. This implies, that the minimum condition of integral (1) can be taken as an initial condition for ideal reception with the signal affected by any type of interference.

To find the integrand function which will yield the minimum definite integral is as it is known a problem in calculus of variations. Without imposing any other limitations upon the integrand function — but those required by calculus of variations — a general solution can be found. It is known [2] that the conditions for obtaining one unit of an interal of a form

$$I = \int_{t_1}^{t_2} \Phi [\varphi(t), \psi(t), \varphi'(t), \psi'(t)]\, dt \tag{3}$$

are the relations

$$\left.\begin{aligned} \frac{\partial \Phi}{dx} - \frac{d}{dt}\left(\frac{\partial \Phi}{\partial x'}\right) = 0 \\ \frac{\partial \Phi}{\partial y} - \frac{d}{dt}\left(\frac{\partial \Phi}{\partial y'}\right) = 0 \end{aligned}\right\} \tag{4}$$

Here

$$\left.\begin{aligned} x = \varphi(t) \\ y = \psi(t) \end{aligned}\right\}; \tag{5}$$

are the parametric representations of the desired line and $x' = \varphi'(t)$ and $y' = \psi'(t)$ are their derivatives with respect to parameter t.

In our case

$$\Phi(t) = [\chi(t) - A_F(t)]^2 \tag{6}$$

and in connection with fluctuating interference effects, we are interested in the relation between

$$x = N(t) \text{ and } y = F(t),$$

where N(t) is the fluctuating interference and F(t) is the sought function reproduced by the receiver.

Since in this problem the function $\Phi(t)$ does not clearly depend on $x' = N'(t)$ and $y' = F'(t)$, the conditions (4) take the following form

$$\frac{\partial \Phi}{\partial x} = \frac{\partial \Phi}{\partial y} = 0. \tag{7}$$

By applying condition (7) to function (6), which in a more expanded form is

$$\Phi(t) = [A(t, F_0) + N(t) - A(t, F)]^2, \tag{8}$$

we get

$$\frac{\partial \Phi}{\partial x} = \frac{\partial \Phi}{\partial N} = 2[A(t, F_0) + N(t) - A(t, F)] = 0,$$

$$\frac{\partial \Phi}{\partial y} = \frac{\partial \Phi}{\partial F} = 2[A(t, F_0) + N(t) - A(t, F)]\ \frac{\partial A(t, F)}{\partial F} = 0.$$

From which it is seen that the minimum condition for integral (1) in the most general case is the condition that

$$A(t, F_0) + N(t) - A(t, F) = 0. \tag{9}$$

This is the condition we shall call the condition of null deviation.[1]

SMALL NOISE FLUCTUATIONS

From (9) we obtain the Kotel'nikov formula which is applicable for small noise fluctuations.

Assuming

$$A(t, F) = A(t, F_0 + \Delta F), \tag{10}$$

where ΔF is an increment of the modulating signal resulting from relatively small noise at the receiver output. Since in such a case, ΔF is also small as compared to F_0, then by taking approximately

$$A(t, F_0 + \Delta F) = A(t, F_0) + \Delta F A'_{F_0}(t, F_0) \tag{11}$$

and substituting it into (9), we find

$$N(t) - \Delta F A'_{F_0}(t, F_0) = 0$$

and, hence,

$$\Delta F = \frac{N(t)}{A'_{F_0}(t, F_0)}. \tag{12}$$

Since $A(t, F_0)$ and $N(t)$ are functions independent of time, we can average ΔF successively and separately, and thus get that

$$\Delta F_c = \frac{N(t)}{\sqrt{\overline{\left(\frac{\partial A}{\partial F_0}\right)^2}}}, \tag{13}$$

where ΔF_c is the average with respect to the signal derivative only.

We get from (13) that the power spectrum of ΔF_c is equal to the spectrum of $N(t)$ divided by a constant quantity $\overline{\left(\frac{\partial A}{\partial F_0}\right)^2}$, in other words

$$\sigma_c^2 = \frac{\sigma_i^2}{\overline{\left(\frac{\partial A}{\partial F_0}\right)^2}}. \tag{14}$$

Expression (14) was found by Kotel'nikov, in it σ_i is the noise spectrum intensity at the input of an receiver and σ_c is the noise spectrum. Later by considering a more general case for spontaneous noise, we shall find more accurate relations for small noises.

---

[1]The obtained result is justified, at least for a finite but large interval of time T in (1). Besides, it can be visualized physically as an approximation, at least for relatively small noise. In order to appreciate the limits of its practical application, it is necessary to derive from condition (9) the formulas for noise calculations at the receiver output and to compare the calculated results from these formulas with the results obtained from previously known theoretical formulas and with experimental data as well. That is the aim of this article.

Let us find the significance of ΔF in (9), without making assumptions as to the small amplitude of noise. In this case it is convenient to solve the problem for different types of modulation.

AM: For this type of modulation, we may write

$$\left.\begin{aligned} A(t, F_0) &= A_0(1 + MF_0)\sin(\omega t + \alpha) \\ A(t, F) &= A_0(1 + MF_0 + M\Delta F)\sin(\omega t + \alpha) \\ N(t) &= A\cos\omega t + B\sin\omega t \end{aligned}\right\}, \tag{15}$$

where

$$E = \sqrt{A^2 + B^2} \tag{16}$$

is the noise envelope in the receiver range.

Substituting relations (15) and (9) we obtain

$$A\cos\omega t + B\sin\omega t = A_0 M\Delta F\sin\alpha\cos\omega t + A_0 M\Delta F\cos\alpha\sin\omega t.$$

This equation must be satisfied at all instants of time; therefore,

$$A = A_0 M\Delta F\sin\alpha$$
$$B = A_0 M\Delta F\cos\alpha.$$

Squaring and adding these equations, and taking into account (16), we obtain

$$\Delta F_{AM} = \frac{E}{A_0 M}. \tag{17}$$

It therefore follows that the power spectrum ΔF_{AM} is the power spectrum of the envelope of fluctuating oscillations, reduced at each point by $A_0^2M^2$; i.e.,

$$G_{\Delta F}(F) = \frac{G_E(F)}{A_0^2 M^2}. \tag{18}$$

The envelope spectrum may be found by first calculating the correlation coefficient of the envelope. In correspondence with (3) we have the following relation for the correlation coefficient of the envelope

$$R_E(\tau) = \frac{\pi}{4-\pi}\left[\left(\frac{1}{2}\right)^2 p^2 + \left(\frac{1}{2\cdot 4}\right)^2 p^4 + \left(\frac{1\cdot 3}{2\cdot 4\cdot 6}\right)^2 p^6 + \ldots\right]. \tag{19}$$

Using the first term of the expansion in (19) for simplicity we obtain

$$R_E(\tau) \approx \frac{\pi}{4(4-\pi)}\, p^2, \tag{20}$$

where

$$p = r(\tau) = \frac{\sin\pi w\tau}{\pi w\tau} \tag{21}$$

for an ideal rectangular form of receiver frequency characteristic with bandwidth ω.

The fluctuation spectrum will then be [3]

$$G_E(F)_1 = 4\sigma^2 \int_0^\infty R_E(\tau)_1 \cos\Omega\tau d\tau =$$

$$= \frac{4\sigma^2}{4-\pi}\int_0^\infty \frac{\sin^2\pi w\tau}{(\pi w\tau)^2}\cos\Omega\tau d\tau = \frac{\pi\sigma^2}{2(4-\pi)}\,\frac{1}{w}\left(1 - \frac{F}{w}\right). \tag{22}$$

For the frequency range of interest here $F \ll \omega$ we find from (18) that

$$G_{\Delta F}(F)_1 = \frac{\sigma^2}{A_0^2 M^2} \cdot \frac{\pi}{2(4-\pi)w}. \tag{23}$$

Further, taking into consideration that $\sigma^2 = \sigma_I^2 \omega$; then

$$G_{\Delta F}(F)_1 = \frac{\pi \sigma_i^2}{2(4-\pi) A_0^2 M^2} \approx \frac{1.82 \sigma_i^2}{A_0^2 M^2}. \tag{24}$$

The second term in (19) yields

$$G_{\Delta F}(F)_2 \approx \frac{0.08 \sigma_i^2}{A_0^2 M^2}. \tag{25}$$

It is not difficult to derive the other components. In the limit, we approach the relation

$$G_{\Delta F}(F)_{AM} = \frac{2\sigma_i^2}{A_0^2 M^2}, \tag{26}$$

known from the work of V.A. Kotel'nikov.

The above solution indicates that the independence of $G_{\Delta F}$ (F) from frequency F is justified only in the region where F has small values (22). When the ratio of F/ω approaches unity, $G_{\Delta F}$ (F) begins to decrease rapidly In this way, the given solution for ΔF in the form of (17) gives a more accurate evaluation of the process.

Expressions (24), (25), and (26) are justified for any signal to noise ratio at the receiver input.

This is characteristic of AM modulation.

Phase Modulation PM: In this case as it is known

$$A(t, F_0) = A_0 \sin(\omega t + \Delta\varphi F_0). \tag{27}$$

Condition (9) will be written in the following way:

$$A_0 \sin(\omega t + \Delta\varphi F_0) + N(t) - A_0 \sin(\omega t + \Delta\varphi F_0 + \Delta\varphi \Delta F) = 0. \tag{28}$$

Utilizing for N(t) the same expression as in (15) we obtain

$$A \cos \omega t + B \sin \omega t = A_0 [\sin(\Delta\varphi F_0 + \Delta\varphi \Delta F) - \sin(\Delta\varphi F_0)] \cos \omega t + A_0 [\cos(\Delta\varphi F_0 + \Delta\varphi \Delta F) - \cos(\Delta\varphi F_0)] \sin \omega t. \tag{29}$$

Since this equation must be satisfied for any t, then

$$\left.\begin{aligned} A &= A_0 [\sin(\Delta\varphi F_0 + \Delta\varphi \Delta F) - \sin(\Delta\varphi F_0)] \\ B &= A_0 [\cos(\Delta\varphi F_0 + \Delta\varphi \Delta F) - \cos(\Delta\varphi F_0)] \end{aligned}\right\}. \tag{30}$$

Squaring and adding A and B we obtain

$$E^2 = 4A_0^2 \sin^2\left(\frac{\Delta\varphi \Delta F}{2}\right).$$

From which

$$\sin\left(\frac{\Delta\varphi \Delta F}{2}\right) = \frac{E}{2A_0},$$

and hence,

$$\Delta F_{PM} = \frac{2}{\Delta\varphi} \arcsin \frac{E}{2A_0}. \tag{31}$$

Such, in general, is the expression for noise at the output of an ideal receiver for PM modulation, for any signal to noise ratio at the input. When noise at the receiver input is relatively small, i.e., $E/2A_0$, it follows from (31) that

$$\Delta F_{PM} = \frac{E}{\Delta\varphi A_0}. \tag{32}$$

This formula is analogous to (17) and, in this way, for spectrum density we obtain relation (26) in which instead of M we write $\Delta\varphi$ which is the modulation index, i.e.,

$$G_{\Delta F}(F)_{PM} = \frac{2\sigma_i^2}{A_0^2\Delta\varphi^2}. \tag{33}$$

This value for $G_{\Delta F}(F)_{PM}$ is known from the work of V.A. Kotel'nikov. FM: In this case

$$A(t, F_0) = A_0 \sin[\omega t + \Delta\omega_m \int F_0(t)\,dt]. \tag{34}$$

From which it can be seen, that in order to obtain ΔF_{FM}, it is necessary to take the derivative of (31) and $\Delta\omega_m$ instead of $\Delta\varphi$, where $\Delta\omega_m$ is the maximum deviation. With this it is easy to obtain

$$\Delta F_{FM} = \frac{E'}{A_0\Delta\omega_m\sqrt{1 - E^2/4A_0^2}} \tag{35}$$

and for small values of E/A_0

$$\Delta F_{FM} = \frac{E'}{A_0\Delta\omega_m}. \tag{36}$$

As known, the derivative spectrum is obtained from the spectrum of the original function through a multiplication by the square of the frequency:

$$G_{\Delta F}(F)_{FM} = \frac{2\sigma_i^2\Omega^2}{A_0^2\Delta\omega_m^2}. \tag{37}$$

We shall obtain more accurate results by calculating the E and E' spectrums through correlation coefficient $R_E(\tau)$, given in the form of expansion (19). Under these conditions we shall obtain a more complicated dependence relationship of $G_{\Delta F}(F)_{FM}$ upon frequency. Taking into account only the first term of the expansion, for FM we obtain

$$G_{\Delta F}(F)_{FM} = \frac{\pi\sigma_i^2\Omega^2}{2(4-\pi)A_0^2\Delta\omega_m^2}\left(1 - \frac{\Omega}{2\pi w}\right). \tag{38}$$

The solution of $G_{\Delta F}(F)$ for PM and FM in a more general case can be obtained by deriving the correlation coefficient from (31) which is a subject of a separate article.

Initial relation (9) may be employed to analyze fluctuating noise effects for any other types of modulation and manipulation.

CONCLUSION

We have justified the method of null-deviation in the form of relation

(9) which is useful for simple situations of practical problems in the theory of potential interference stability. Our solutions are more general than the previous ones obtained in this theory. They are justifiable for relatively large noise effects at receiver inputs, and give a more correct solution for noise spectrum density at the output of the receiver in the frequency range from 0 to ∞.

Relation (9) may be employed for a comparative analysis of any communication systems, with any forms of modulation and manipulation, and under the influence of any type of interference and distortion. In fact in expression (9), instead of N(t), we may employ expressions for noise of any type. Nevertheless, it is not always as easy to find the solution for ΔF, as it was for fluctuating interference.

It has also been proven that it is possible to effectively employ the method of null-modulation for the evaluation of distortion for multibeam propagation of radio waves, which is treated in a separate work.

Original article submitted May 13, 1960

LITERATURE

1. V.A. Kotel'nikov, Theory of Potential Interference Stability. GEI, 1956.
2. V.I. Smirnov, V.I. Krylov, and A.V. Kantorovich, Variational Calculus, KUBUCh, 1933.
3. V.I. Bunimovich, Fluctuation Processes in Radio Receivers. Izd. "Sovetskoe Radio," 1951.

LOW FREQUENCY REGENERATIVE DIVIDER

V.S. Andreev, B.P. Burdzeiko, V.I. Vasil'ev

This article describes the characteristics of a low frequency regenerative divider circuit, employing RC-amplifiers with twin T bridge networks for its selective elements. This divider utilizes a new scheme of frequency multiplication which insures greater coefficients of division under wide synchronization ranges. With a division by 20, the synchronization band reaches 9.3%. Experimental results and oscillography pictures are supplied. This article also shows the desirability of connecting an ordinary RC-filter at the divider output.

INTRODUCTION

Known harmonic frequency divider networks, using LC tank circuits for frequency selection, are working successfully at frequencies of 100 cps and above.

Even in dividers with an output frequency of about 100 cps difficulties are encountered. The difficulties are connected with the deterioration of the shape of the output signal due to the decreasing Q of the LC circuits, their increasing overall size, and the fact that continuous tuning within their frequency range is impossible.

To obtain sinusoidal oscillations of lower frequencies by means of division, it is desirable to use RC-amplifiers or oscillators as the elements which determine the frequency and form of the oscillations.

Notwithstanding the self evidence of the above, sufficiently good low frequency harmonic dividers have not as yet been developed. Article [1] describes a frequency division scheme utilizing an RC phase shift oscillator synchronized to its subharmonic. The output signal of this divider is not sinusoidal, and the required control voltage is in tens of volts.

Consequently, this divider did not become popular. In the interesting work of Schlichting [2] are given the results of research on synchronization to a subharmonic of the input signal of an oscillator followed by a parallel RC-network. In this work considerable synchronization bands were obtained, but at a sacrifice of the shape of the output signal. (Oscillographs of the output voltage are not supplied). Article [3] describes a key-type low frequency divider with one selective RC-amplifier with a double T-shaped bridge. Key-type dividers, while having much in common with regenerative frequency dividers, are less complex than the latter. However, they are inferior to the previously mentioned dividers as far as phase stability and non-linear distortions of the output signal are concerned. In connection with this the attempt of creating a regenerative divider of low frequencies was undertaken. Design and test results of such a divider are described below.

THE FREQUENCY DIVIDER

The schematic diagram of a regenerative low frequency divider with selective RC arrangements is shown in Figure 1. It consists of a mixer, which uses one half of tube 6Н1П; a frequency multiplier — the second half of the tube — and two selective RC amplifiers. In ordinary two-tube regenerative frequency dividers, the necessary tuning and selectivity of the stages is obtained by connecting the required resonant circuits in the plate circuits of the mixer and multiplier tubes [4].

When using selective RC-amplifiers, the placement of the selectivity circuit and the mixer (or multiplier) functions in one stage is undesirable. In order to obtain maximum selectivity the operating region must be selected in the linear portion of the grid-plate characteristics, corresponding to maximum transconductance; and in order to obtain the most efficient mixing stage (or multiplication) which determines circuit sensitivity the operating point must be selected in the non-linear portion of the characteristic curve or even in the cutoff region. Therefore, in order to insure enough network sensitivity and selectivity it was necessary to introduce independent selective RC amplifiers. The amplifier, following the mixer, was tuned to frequency f, which is the subharmonic of the input signal $f_{in} = nf$, and the amplifier following the multiplier was tuned to a frequency $(n - 1)f$. Each

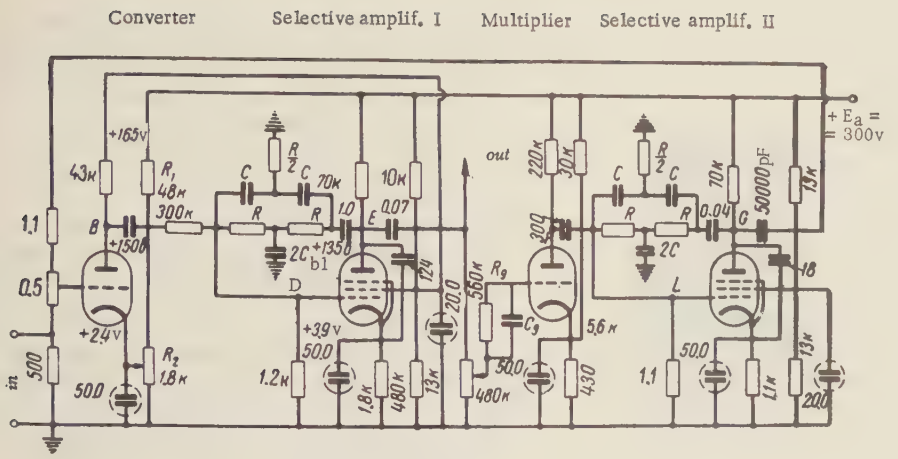

Figure 1

amplifier was constructed around a 6Ж4 tube with a twin T bridge, in the negative feedback loop. Since the amplifiers are fed from high impedance sources, a shunt bridge feeding arrangement was employed. However, in view of insufficient "high-impedance" of these sources, — which could cause considerable decrease in the selectivity of the RC-amplifiers which follow — their resistance was increased by connecting an additional 1-megohm resistor in series. Optimum resistance was determined experimentally for each stage so as to obtain maximum amplifier selectivity.

It is known, that selection of elements (R and C) for a twin bridge with an insufficient degree of accuracy of the resonant frequency, may result in two consequences: either negative feedback — thus reducing network selectivity, or positive feedback which will reduce the amplifier operating stability up to the point of oscillation. With the aim of insuring normal operation of these amplifiers, the parameters of the twin T bridges were determined with high degree of accuracy (0, 1%), and were not regulated later. Nevertheless, this precaution alone was insufficient to prevent the amplifiers from self-excitation. Self-excitation was eliminated by connecting a small capacitor between the plate and the cathode of each amplifier tube. This resulted in a slight reduction of amplifier selectivity.

The frequency converter uses a single grid to perform the frequency conversion. To obtain the optimum operating point — which corresponds to the best efficiency as far as the beat frequency is concerned — the operating point was selected in the region near tube cutoff by means of potentiometer R_1 to R_2 (Figure 1). At the mixer input, frequency nf beats with frequency (n - 1)f from the frequency multiplier network. The mixer output voltage (point B in Figure 1), is shown in Figure 2. This is an oscillograph diagram for n = 10. It contains the corresponding frequency difference f and feeds its following tuned amplifier.

The schematic in Figure 1 was investigated for frequency division by n = 5, 10 and 20 times, which required corresponding frequency multiplication by 4, 9 and 19 times. At the start, an ordinary tube network of a

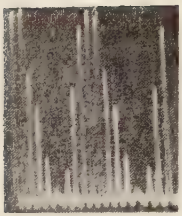

Figure 2

multiplier was tried, but eventually this was found to be ineffective, especially for large multiplication coefficients. The latter is caused by a rapid decrease in amplitude as the number of the harmonic increases, as well as the fact that it is impossible to insure optimum grid bias, above cutoff, while retaining network operation without introducing special trigger arrangements. Therefore, a new frequency multiplication network was developed which utilizes a ringing circuit excited by short timed impulses. The RC amplifier following the multiplier network was utilized as this circuit. This multiplier operates between two limiting conditions produced by the absence and presence of grid currents. The operation of the frequency multiplier is clarified by Figure 3. As a result of the large amplitude of the sinusoidal input of frequency f, impulses of an almost trapezoidal form (Figure 3a) are generated in its plate circuit. The width, and slope of the edges of these impulses are dependent on the initial bias and amplitude of the input voltage. A differentiating network is connected to the plate of the multiplier. This network is formed by the blocking capacitor[1] C = 300 pF and a parallel

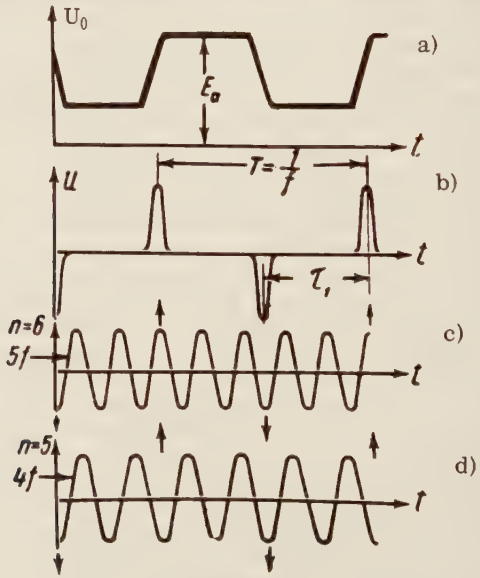

Figure 3

[1]The capacity C also serves to increase the output impedance of the multiplier, which — as already noted — is necessary in order to increase the sensitivity of the next stage.

connection of the input bridge resistance and the grid leak resistance of the next tube R = 1.1 meg.

The output of the differentiating network consists of narrow pulses of frequency 2f. These pulses support the oscillations in the amplifier which is tuned to the (n - 1)f frequency. The oscillations decay in the intervals between the impulses. The rate of decay is determined by the equivalent Q of the tuned amplifer. To effectively operate such a frequency multiplier, it is important that the impulses be sufficiently narrow and strong, and the interval τ_1 between the negative and positive impulses be completely determinable, thus insuring impulse action at the time of largest negative or positive voltage of the signal (n - 1)f at the grid of the amplifier. The magnitude of τ_1 may be regulated by varying the bias as well as the parameters of Rg and Cg in the grid circuit of the multiplier. By interpolating graphs b, c and d in Figure 3, it can be easily seen that for the case $\tau_1 = \frac{T}{2}$ the most desirable conditions exist for an even numbered division, and that division by an uneven number is impossible. In Figure 4, the oscillograph picture of the signal strength at the output of the differentiating network with the divider operating and n = 10, the arrows indicate the action of the first negative and the second positive impulse.

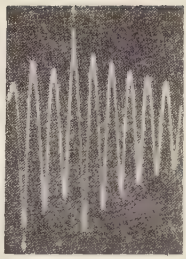

Figure 4

ANALYSIS OF THE CIRCUIT BASED ON EXPERIMENTAL DATA

In the following table are supplied the facts about the frequency and the coefficients of division at which the divider was tested; the size of the capacitors in the twin T bridges, and also the largest synchronization bands obtained expressed in percentages relative to the frequency of the input signal (П%).

Table 1

Coefficient of division	Frequency		Tuning frequency of selective amplifier, cps		Capacitance C of twin-T bridge		П%
	f , cps	f, cps	multiplier	converter	multiplier	converter	
5	200	40	160	40	3 680	14 700	17
10	178	17.8	160	17.8	3 680	33 200	7.3
20	356	17.8	338	17.8	1 740	33 200	9.3

All resistances R, in the twin T bridge networks in both tuned amplifiers were equal to 220 K.

The divider amplitude characteristics, i.e., dependence of the output voltage V_{out} on the amplitude of the input signal V_{in} were taken with the network tuned to resonance for n = 5, these are illustrated in Figure 5; and for n = 10 and 20 in Figure 6.

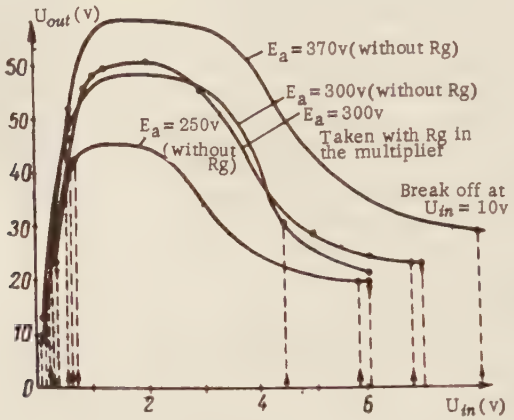

Figure 5

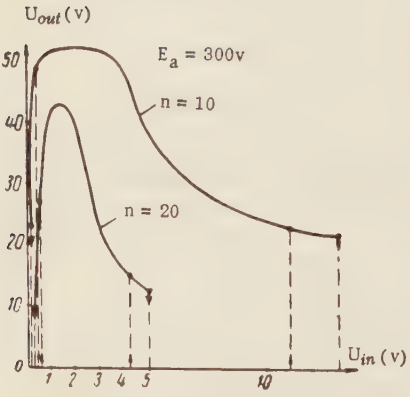

Figure 6

The shape of all characteristics is the same: the divider excitation begins when the input signal exceeds a certain threshold value $V_{in\,1}$. Further increase of V_{in} to a magnitude of approximately 1 v results in a sharp — almost linear — rise in V_{out}. After that an increase in V_{in} does not result in any appreciable rise of V_{out}, and may even reduce its magnitude. At a certain level of $V_{in\,2}$ the network ceases to oscillate. Consequently, the network realizes frequency division only if the amplitude of V_{in} is within certain limits.

In Figures 7 and 8, the divider frequency characteristics corresponding to n = 5 and n = 20 are supplied. These characteristics relate the amplitude of output voltage V_{out} and the frequency of the input voltage V_{in} as the parameter. The region corresponding to the transition from the linearly increasing region of amplitude characteristics to the curved region (in our case for $V_{in} \approx 1$ to 1.5 v) should be taken as the most advantageous region of operation for the regenerative frequency divider under consideration. In this region, the output signal has the best form, and the synchronization band is close to its maximum. When n = 5, the largest synchronization band is obtained with V_{in} = 2.5 v; however

for this case the output waveform was slightly inferior. With n = 20, the largest synchronization band was obtained for V_{in} equal to approximately 1.5 v.

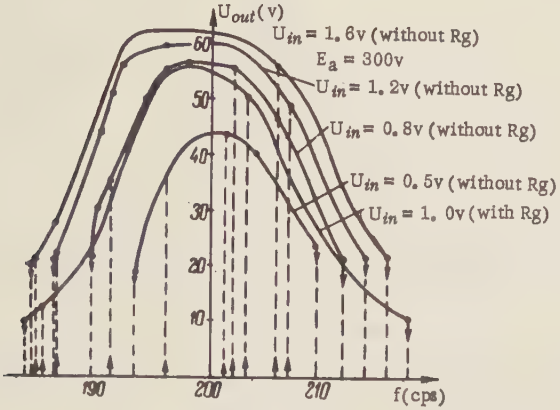

Figure 7

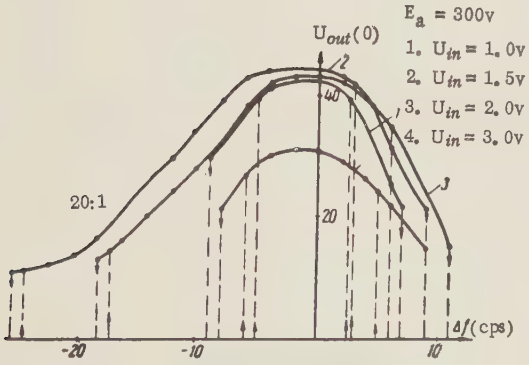

Figure 8

Resistance Rg, connected to the grid of the multiplier, has considerable effect on the divider characteristics due to the fact that the latter operates on grid currents. For n = 5, the amplitudes and frequency characteristics were taken with Rg = 560 K-ohms and without it (Figures 5 and 7). For n = 10 and 20, capacitance C was connected in parallel with Rg = 560 K-ohms. The connection of R reduces the shunt effect of the frequency multiplier upon the tuned RC-amplifier proceding it, with the result that its gain and selectivity increases. This results in: a decrease in the lower limit of V_{in1}, an increase in the range of V_{in} where the divider operation is stable, as well as an increase in the synchronization band.

Among the merits of the described network are the wide synchroniza-

tion bands (table 1). If we assume that division by any given number n can take place, as long as the frequency of the input signal f_{in} does not exceed the limit of half the frequency interval between nf and $(n \pm 1)f_0$[2], where f_0 is the frequency to which the ouput network is tuned — then the synchronization band must not exceed

$$\Pi_{max}\,\% \approx \frac{100}{n}. \qquad (1)$$

For the case where n = 20 the largest synchronization band was found to be greater than that defined by expression (1). This apparently is a consequence of a good selection of the frequency multiplier operating region, which permits multiplication by 19 and impedes multiplication by 18 and 20. Such a situation is analogous to the one illustrated in Figure 3c and d. It is possible that an increase in the synchronization bands obtained for n = 5 and 10 could be realized with a more finely adjusted network.

The effect of the supply voltage on the operation of the divider was checked by varying the supply voltage E_a from 370 to 250 v, and in some cases to 180 v. In all cases the operation of the divider was relatively stable. An increase in E_a, increases the gain of all stages, and consequently, the selectivity of the RC-amplifiers. The output voltage V_{out} increases, the input voltage V_{in1} decreases, the range of V_{in} is widened and the wave form of the output voltage shows some improvement. The synchronization band does not change greatly.

Within the operating ranges, the equivalent quality factor Q_e for the tuned amplifiers which was determined from the .707 points of the frequency response was not very large ($Q_e \approx 20 - 30$). This is a consequence of utilizing capacitors in the amplifiers to eliminate self excitation. Nevertheless the divider output voltage closely approximated a sinusoid (as may be seen from oscillograph diagrams illustrated in Figure 9a for n = 10 and in Figure 9b for n = 20). Both oscillograph diagrams were obtained for V_{in} = = 1 v. Despite the low selectivity of the RC-amplifiers, the output signal from such a divider is considerably better than the signal obtained for the same n at the output of a key-type low frequency RC divider [3].

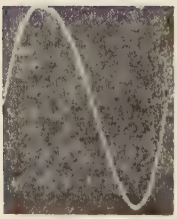

a)

b)

c)

Figure 9

[2]Such assumption is more or less justified, if the considered operating range is equally applicable to division by an even as well as uneven number of times.

To increase the waveform of the output signal from the divider, an ordinary single mesh RC filter ilustrated in Figure 10 was connected. Since the derivation from a sinusoid of the output signal from the divider is largely the result of the "leak through" of signals throught the converter, such a filter performs best as n increase. It may be easily shown that if filter elements R and C are selected from the condition

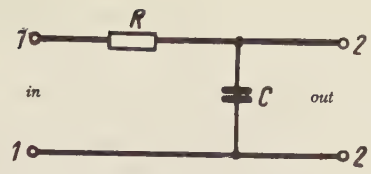

$$R \gg \frac{1}{2\pi f_{in} C}, \qquad (2)$$

then for larger n, the filtering coefficient approaches n. As oscillograph diagram for the output voltage from the filter, for n = 20 and V_{in} = 1v, is illustrated in Figure 9c.

CONCLUSION

The output frequency range for the above considered low frequency divider is determined by the operating frequency range of the tuned RC-amplifiers with twin T bridge networks and covers the range from several tens of kilocycles to 10 cycles and lower. Use of constant current amplifiers will permit the construction of dividers for even lower frequencies. Despite the comparatively low selectivity of the RC-amplifiers, the output oscillations were almost sinusoidal. The experiments carried out in the present work, and in work [3], have shown that; increasing the equivalent Q-factor of the selective amplifiers gives better output waveform with a simultaneous narrowing of the synchronization bands and vice versa. This is found to be in complete agreement with work [2], in which it has been proven that for harmonic dividers, the broader the phase characteristics of the frequency selective elements, the wider the synchronization band. Usually, the lower the Q-factor of the tuned network the lower the steepness of the phase characteristics. Consequently, from our point of view, in order to fully describe the characteristics of any harmonic frequency devider (especially for cases of large n) it is necessary to indicate not only the synchronization bands, but it is also important to supply oscillograph diagrams of the output voltage or to supply facts about its spectrum.

Low frequency regenerative divider possesses good sensitivity, has stable operation for a wide range of power supply and amplitude of the incoming signal, provides large coefficients of division with wide synchronization bands, and a good output signal waveform. With large coefficients of division, the synchronization band is wider then that obtained up to the preent by other type of dividers. With large coefficients of division a considerable improvement of output signal waveform may be obtained by means of an ordinary RC filter (Figure 10). This is true for regenerative as well as key type dividers.

Application of the new frequency multiplying network in the divider has, in our opinion, an independent significance.

Original article submitted April 29, 1960

LITERATURE

1. Smidt, Frequency division with phase-shift oscillators. Electronics. V. 23, VI, 1950.
2. Schlichting, "Untersuchungen an harmonischen Frequenzteilern zur Ermittlung der Voraussetzungen für die Erzeilung hoher Teilerverhaltnisse und grober Mifnahmebereckte bei hohen Frequenzen." Zeitschrift fur augewande Physik. Bnad IX, Heft 9, 1957.
3. V.S. Andreev, E.M. Soshnikov, "Low-frequency divider," Elektrosvyaz, No. 2, 1960.
4. V.S. Andreev, "Operation of a two-tube regenerative frequency divider with multiplier." Radiotekhnika No. 1, 1954.

INTERFERENCE EFFECTS ON A TWO-CHANNEL RECEIVER INSTALLATION WITH AGC

V.V. Shirokov

This article considers the random processes within a two-channel installation with AGC. It determines the statistical characteristics at the channel outputs, which allows the choice of the AGC parameters, and also determination of the effect of channel unbalance.

INTRODUCTION

In present day radio systems, a two-channel receiver setup with AGC (Figure 1) is utilized for the determination of angular coordinates. Strict conditions are imposed on the equality of channel characteristics, since on it depends the accuracy of the determined angular coordinates. This is especially true in the presence of different types of interferences.

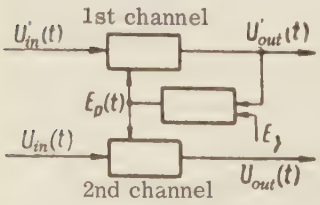

Figure 1

The present article analyses the effects of signal and noise fluctuations, when random modulated, on a two-channel installation with AGC. This analysis permits calculation of the characteristics of the random processes at the outputs of the receiver channels, determination of their dependence on the AGC parameters

and the effect of unbalance of channel regulating characteristics.

SOLUTION OF THE INTEGRAL EQUATION WHICH DESCRIBES AGC

The first channel of the AGC receiver constitutes a closed loop (Figure 1). Random processes in a closed AGC system are analysed in [1], and we shall utilize to a great extent the results there obtained. In order to compare the output interference characteristics, of the channels under consideration, it is necessary to analyse the random processes in the second channel, which constitutes an open loop in the AGC system.

In view of the extreme slow response, property of an AGC system, the regulated amplifier may be considered to have instantaneous response, and we may take for the input excitation the amplitude of the incoming signal, even for the case where it is in the form of an impulse [2]. Let us consider the steady state operation of AGC. The approximate regulating characteristic of the amplifier in the vicinity of the operating point is assumed to be the following straight line:

$$\kappa(E_p) = \kappa_0 - bE_p(t).$$

Here k_0 and $b_0 = \tan\alpha$ are the parameters of the regulated characteristic (Figure 2), $E_p(t)$ is the regulation potential. Then the signal at the output of the second channel $U_{out}(t)$ depends on the amplitude of its input signal in the following manner:

$$U_{out}(t) = U_{in}(t)[\kappa_0 - bE_p(t)]. \quad (1)$$

and for the case under consideration, the input signal from the first channel is related to the input signal of the second channel by expression

$$U'_{in}(t) = \mu U_{in}(t),$$

where μ is a positive quantity.

Then the first channel output signal $U'_{out}(t)$ will be justly expressed by:

$$U'_{out}(t) = \mu U_{in}(t)[\kappa'_0 - b'E_p(t)], \quad (2)$$

where k_0 and b' are parameters of the regulation characteristics of the first channel.

It is known that a stationary random process may be expressed by a Fourier integral [3, 4]

$$U_{out}(t) = \int_{-\infty}^{\infty} e^{i\omega t}\, dZ(\omega), \quad (3)$$

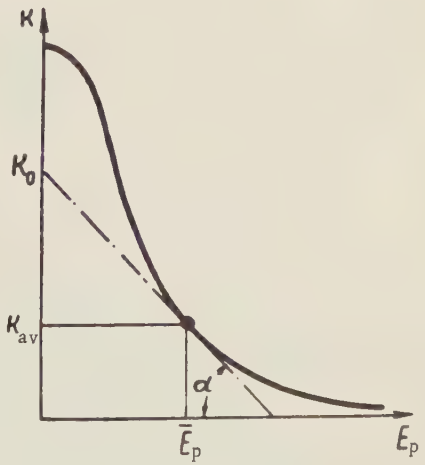

Figure 2

where $Z(\omega)$ is a random function. If the δ-function approach is employed, then it may be assumed that a derivative of this function $\frac{dZ(\omega)}{d\omega}$ does exist. Then integral (3) may be written in the ordinary Fourier integral form

$$U_{out}(t) = \frac{1}{2\pi}\int_{-\infty}^{\infty} C(\omega)\, e^{i\omega t}\, d\omega, \quad (4)$$

where $C(\omega) = 2\pi \frac{dZ(\omega)}{d\omega}$ may be naturally called the spectrum of the random process. From the mathematical point of view, such an expression cannot be considered rigorous since the introduction of the δ-function is not entirely rigorous. However this scheme permits manipulation with ordinary Fourier integrals which are common in technical applications.

If the solution for $C(\omega)$ can be found, then it is not difficult to determine the random process characteristics at the output. The expectation will be found from the relation

$$\overline{U_{out}(t)} = \frac{1}{2\pi} \int_{-\infty}^{\infty} \overline{C(\omega)}\, e^{i\omega t}\, d\omega, \tag{5}$$

where the line above the expression signifies the ensemble average of the random process outputs.

The expression for the random process spectrum deviation from the value of expectation has the form

$$C(\omega) - \overline{C(\omega)} = \int_{-\infty}^{\infty} \Delta U_{out}(t_2)\, e^{-i\omega t_2}\, dt_2, \tag{6}$$

where $\Delta U_{out}(t) = U_{out}(t) - \overline{U_{out}(t)}$, and its conjugate quantity will take the following form:

$$C^*(\omega') - \overline{C^*(\omega')} = \int_{-\infty}^{\infty} \Delta U_{out}(t_1)\, e^{i\omega' t_1} dt_1. \tag{7}$$

Multiplying (6) by (7) and taking the ensemble average we obtain

$$\overline{[C(\omega) - \overline{C(\omega)}][C^*(\omega') - \overline{C^*(\omega')}]} = \int_{-\infty}^{\infty}\int \overline{\Delta U_{out}(t_1)\Delta U_{out}(t_2)}\, e^{i\omega' t_1 - i\omega t_2}\, dt_1 dt_2.$$

Introducing a new variable $\tau = t_2 - t$, we obtain the following expression

$$\overline{[C(\omega) - \overline{C(\omega)}][C^*(\omega') - \overline{C^*(\omega')}]} = \int_{-\infty}^{\infty} R(\tau)\, e^{-i\omega\tau} d\tau \int_{-\infty}^{\infty} e^{i(\omega-\omega')t_1}\, dt_1,$$

where $R(\tau)$ is the correlation function $U_{in}(t)$.

After integrating, we shall find the expression which will permit the determination of the random process spectrum density at the output $g_{out}(\omega)$, if the solution for $C(\omega)$ is known

$$\overline{[C(\omega) - \overline{C(\omega)}][C^*(\omega') - \overline{C^*(\omega')}]} = 2\pi\delta(\omega - \omega') g_{out}(\omega). \tag{8}$$

Let us determine the solution for $C(\omega)$. We take the output signal from the first channel to be analogous to (4), and the input signal to be

$$U_{in}(t) = A + \frac{1}{2\pi} \int_{-\infty}^{\infty} a(\omega)\, e^{i\omega t}\, d\omega, \tag{9}$$

where $A = \overline{U_{in}(t)}$ is the expectation of the input signal.

Then, with the assumption that the AGC feedback network is linear, we shall obtain the following expression for the regulation potential:

$$E_p(t) = \frac{\kappa_1}{2\pi} \int_{-\infty}^{\infty} C'(\omega) H(\omega)\, e^{i\omega t} d\omega - \kappa_1 E_s. \tag{10}$$

here $C'(\omega)$ is the random process spectrum at the output of the first channel; $k_1 H(\omega)$ is the feedback coefficient $[H(0)] = 1$; E_Z the retardation potential. Substituting (10), (9) and (4) into (1) and (2), we obtain equations which relate the voltage spectrums at the output of the channels with the spectrum of the input channel,

$$C'(\omega) = [2\pi A\delta(\omega) + a(\omega)] \frac{\mu(\kappa_0' + b'\kappa_1 E_e)}{1 + \mu A b'\kappa_1 H(\omega)} - \\ - \frac{b'\kappa_1}{2\pi} \int_{-\infty}^{\infty} \frac{C'(s)\,\mu a(\omega - s) H(s)\,ds}{1 + \mu A b\kappa_1 H(\omega)}, \tag{11}$$

$$C(\omega) = [2\pi A\delta(\omega) + a(\omega)]\,(\kappa_0 + b\kappa_1 E_e) - Ab\kappa_1 H(\omega) C'(\omega) - \\ - \frac{b\kappa_1}{2\pi} \int_{-\infty}^{\infty} C'(s) H(s) a(\omega - s)\,ds, \tag{12}$$

where $\delta(\omega)$ is the delta function.

The solution of equation (11), which describes a closed AGC system of any order, was obtained in [1], [assuming that $\frac{\sigma^2}{A^2} < 1$, where σ^2 is the dispresion of U (t)] in the form of repeated approximations

$$C'(\omega) = C_0'(\omega) + C_1'(\omega) + C_2'(\omega) + C_3'(\omega) + \ldots,$$

where

$$\left.\begin{aligned} &C_0'(\omega) = \kappa_{av}' \mu A 2\pi\delta(\omega); \quad C_1'(\omega) = H_e'(\omega)\,\mu a(\omega) \\ &C_2'(\omega) = -H_e'(\omega) \frac{\mu^2 b\kappa_1}{2\pi} \int_{-\infty}^{\infty} a(s)\, a(\omega - s)\, H_p'(s)\,ds \\ &C_3'(\omega) = H_e'(\omega)\,\mu^3 \left(\frac{b\kappa_1}{2\pi}\right)^2 \int_{-\infty}^{\infty}\int a(s')\, a(s - s')\, a(\omega - s) H_p'(s)\, H_p'(s')\,ds\,ds' \end{aligned}\right\}. \tag{13}$$

Here

$$\kappa_{av}' = \frac{\kappa_0' + b'\kappa_1 E_e}{1 + Ab'\kappa_1 \mu} \tag{14}$$

the average coefficient of amplification of the first channel

$$H_e'(\omega) = \frac{\kappa_{av}'}{1 + \mu A b'\kappa_1 H(\omega)}, \tag{15}$$

$$H_p'(\omega) = H(\omega)\, H_e'(\omega) \frac{1}{\kappa_{av}'}. \tag{16}$$

Utilizing the obtained results, it is natural to seek a solution of equation (12) also in the form of repeated approximations

$$C(\omega) = C_0(\omega) + C_1(\omega) + C_2(\omega) + C_3(\omega) + \ldots \tag{17}$$

Then the zero approximation for $C(\omega)$ will be written in the form

$$C_0(\omega) = 2\pi\delta(\omega) A (\kappa_0 + b\kappa_1 E_e) - Ab\kappa_1 H(\omega) C_0'(\omega).$$

By substituting $C_0'(\omega)$ from (13) we shall find

$$C_0(\omega) = \kappa_{av} A 2\pi\delta(\omega), \tag{18}$$

where

$$\kappa_{av} = \frac{\kappa_0 + Ab'\kappa_1\kappa_0\mu - Ab\kappa_1\kappa_0'\mu + b\kappa_1 E_e}{1 + \mu Ab'\kappa_1}$$

is the average coefficient of amplification of the second channel.

In the same manner the corrections to this approximation are obtained:

$$C_1(\omega) = a(\omega)(\kappa_0 + b\kappa_1 E_e) - Ab\kappa_1 H(\omega) C_1'(\omega) -$$

$$- \frac{b\kappa_1}{2\pi} \int_{-\infty}^{\infty} C_0'(s) H(s)\, a(\omega - s)\, ds = H_e(\omega)\, a(\omega), \tag{19}$$

where

$$H_e(\omega) = \kappa_{av} \frac{1 + \mu A\kappa_1 H(\omega) \left(b' - b \frac{\kappa_{av}'}{\kappa_{av}}\right)}{1 + \mu Ab'\kappa_1 H(\omega)}, \tag{20}$$

$$C_2(\omega) = -\frac{\mu b\kappa_1 H_e'(\omega)}{2\pi} \int_{-\infty}^{\infty} a(s)\, a(\omega - s)\, H_p'(s)\, ds, \tag{21}$$

$$C_3(\omega) = \frac{bb'\mu^2\kappa_1}{(2\pi)^2} H_e'(\omega) \int_{-\infty}^{\infty}\int a(s_1)\, a(s - s_1)\, a(\omega - s)\, H_p'(s) H_p'(s_1) ds\, ds_1. \tag{22}$$

The obtained solution permits the possibility of determining the signal envelope at the output of the second channel for any input envelope. Application of this solution to random input problem, permits determination at the statistical characteristics of the signal at the output of the second channel.

RANDOM PROCESS CHARACTERISTICS AT THE OUTPUT OF THE SECOND CHANNEL

We shall determine the expectation of the output signal by substituting in the equation (5) the solution for C (ω), as obtained in (17). Then the expectation for the second channel output signal, to the third approximation, will have the form

$$\overline{U_{out}(t)} = \kappa_{av} A \left\{1 - \frac{\kappa_{av}' b\mu\kappa_1}{\kappa_{av} 4(1 + \mu Ab'\kappa_1) 2\pi} \int_{-\infty}^{\infty} g(s) H_p'(s)\, ds\right\}. \tag{23}$$

In deriving this expression, we take into account that for a stationary random process the following equation holds $\overline{a(s)\, a(\omega - s)} = 2\pi g(s)\, \delta(\omega)$ where g (s) is the spectrum density of the input signal. This can be proven in a manner analogous to the one employed in proving relation (8).

We shall determine the spectrum density of the output signal by substituting the solution in the form of (17) into formula (8). Since in this case

$$C_0(\omega) = \overline{C_0(\omega)},\ \overline{C_1(\omega)} = \overline{C_3(\omega)} = 0 \text{ and } \overline{C_1^*(\omega)[C_2(\omega) - \overline{C_2(\omega)}]} = 0,$$

then

$$2\pi g_{out}(\omega)\, \delta(\omega - \omega') = \overline{C_1(\omega) C_1^*(\omega')} + \overline{C_2(\omega) C_2^*(\omega')} + \overline{C_1(\omega) C_3^*(\omega')} +$$

$$+ \overline{C_3(\omega) C_1^*(\omega')} - \overline{C_2(\omega) C_2^*(\omega')} + \ldots = 2\pi [g_1(\omega) + g_2(\omega) + \ldots]\, \delta(\omega - \omega').$$

In connection with formula (19) we obtain

$$\overline{C_1(\omega)\,C_1^*(\omega')} = H_e(\omega)\,H_e^*(\omega')\,\overline{a(\omega)\,a^*(\omega')} = 2\pi g_1(\omega)\,\delta(\omega-\omega'),$$

where $g_1(\omega)$ is the first approximation to the spectrum density at the output.

Since $\overline{a(\omega)\,a^*(\omega')} = 2\pi g(\omega)\,\delta(\omega-\omega')$, then

$$g_1(\omega) = |H_e(\omega)|^2\, g(\omega). \tag{24}$$

In this manner, the first approximation of the AGC system in the second channel is equivalent to a linear system with a transfer ratio determined by formula (20).

From [1] it follows, that an analogous transfer ratio for a linear system, at an equivalent AGC system in the first channel, is determined by formula (15).

The obtained formulas permit the determination to the first approximation of the spectrum densities of the output of a receiver channels and to evaluate the effect of an unbalance in their characteristics. From expressions (15), (20), (18) and (14) it follows that with identical regulated characteristics of the channels (i.e., with $k_0 = k_0'$ and $b = b'$) the expressions for the equivalent frequency characteristics of the first and second channel, coincide completely. A correction to the first approximation for spectrum density of the second channel output, will be found from relation

$$\overline{C_2(\omega)\,C_2^*(\omega')} + \overline{C_1(\omega)\,C_3^*(\omega')} + \overline{C_3(\omega)\,C_1^*(\omega')} - \overline{C_2(\omega)\,C_2^*(\omega')} = 2\pi g_2(\omega)\,\delta(\omega-\omega').$$

By utilizing formulas (19), (21), (22) we find in the same manner as employed in [1] the following expressions for $g_2(\omega)$:

$$g_2(\omega) = \frac{b^2\mu^2\kappa_1^2}{2\pi}\,|H_e'(\omega)|^2 \int_{-\infty}^{\infty} g(s)\,g(\omega-s)\left[|H_p'(s)|^2 + H_p'(s)\,H_p'^*(\omega-s)\right]ds +$$

$$+ g(\omega)\,\frac{bb'\kappa_1^2\mu^2}{\pi}\,\mathrm{Re}\left\{\left[H_e^*(\omega)\,H_e'(\omega)\right]\left[H_p'(0)\int_{-\infty}^{\infty} g(s)\,H_p'(s)\,ds + \right.\right.$$

$$\left.\left. + \int_{-\infty}^{\infty} g(s)\,H_p'(\omega+s)\,H_p'(s)\,ds + \int_{-\infty}^{\infty} g(\omega-s)\,H_p'(\omega)\,H_p'(s)\,ds\right]\right\}. \tag{25}$$

And so, in the described manner we obtain general expressions for the statistical characteristics of interference at the output of the second channel, which are justified for an AGC system of any order. By utilizing the formulas derived in [1], we can determine the interference characteristics at the output of the first channel as well as evaluate the effect of channel unbalance on the noise-proof features the receiving system.

INTERFERENCE CHARACTERISTICS AT THE OUTPUT OF A TWO-CHANNEL RECEIVER WITH AN AGC SYSTEM OF THE FIRST ORDER

As an example of application of the general expressions for the random process characteristics, we shall examine a case, frequently encountered in practice, of an AGC system whose feedback network has cotransfer ratio

$$\kappa_1 H(\omega) = \frac{\kappa_1}{1 + i\omega T}. \tag{26}$$

We shall take the spectral interference density at the input of the second channel in the form

$$g(\omega) = \frac{2\alpha\sigma^2}{\alpha^2 + \omega^2}, \tag{27}$$

where σ^2 is the dispersion, and $\frac{1}{\alpha} = T_k$ is the correlation time for $U_{in}(t)$. Then, by substituting (27) and (16) into (23) and taking into account (26) we shall obtain as the expectation for the interference at the output of the second channel, the following expression:

$$\overline{U_{out}(t)} = \kappa_{av} A \left\{ 1 - \frac{\kappa_{av} b \kappa_1 \sigma^2 \mu}{\kappa_{av} A (1 + \mu A b' \kappa_1)^2 (1 + \alpha T_e)} \right\}, \tag{28}$$

here $T_e = \frac{T}{1 + \mu A b' k_1}$ is the equivalent time constant of the AGC.

Since $\mu A b' k_1 \gg 1$, the second term in formula (28) may be with sufficient accuracy for practical purposes be disregarded

$$\overline{U_{out}(t)} \approx \kappa_{av} A. \tag{29}$$

In a similar manner, the expectation for the interference at the first channel output is written in the form

$$\overline{U_{out}(t)} \approx \kappa'_{av} \mu A. \tag{30}$$

Comparison of formulas (29) and (30) indicates, that if we are only interested in the average potentials at the outputs of the channels, then in order to make the paths identical it is sufficient to maintain (by means of additional regulation) their average coefficients of amplification equal in the entire range of input signal or interference. It should be pointed out, that equating the average amplification coefficients for any one single value of input signal may prove to be an insufficient means for making the channels identical. In fact, the regulating characteristics for each channel may greatly vary, because with a changing signal strength, the parameters of k_0 and k'_0, b and b', will change in a different manner. From the above, and also from formula (14) and (18) it follows, that the average amplification coefficients of the channels will differ depending on the expectation for the input signal. It may therefore be necessary to maintain them equal in the whole range of the input signal strength.

If we limit ourselves to the first approximations, then the spectral density at the output of the second channel for this case will have the form

$$g_1(\omega) = \frac{2\alpha\sigma^2\kappa_{av}^2}{(\alpha^2 + \omega^2)} \frac{(N^2 + \omega^2 T_e^2)}{(1 + \omega^2 T_e^2)}, \tag{31}$$

where

$$N = \frac{1 + \mu A \kappa_1 \left(b' - b \frac{\kappa'_{av}}{\kappa_{av}} \right)}{1 + \mu A b' \kappa_1}. \tag{32}$$

The first approximation for the dispersion of the random process at the output of the second channel is obtained as a result of integrating expression (31) with respect to ω

$$\sigma_1^2 = \kappa_{av}^2 \sigma^2 \frac{N^2 + \alpha T_e}{1 + \alpha T_e}. \tag{33}$$

As was shown in [1], the dispersion process at the output of the first channel is determined to the first approximation by the expression

$$\sigma_1^{2'} = \kappa_{av}^{'2} \mu^2 \sigma^2 \frac{\frac{1}{(1 + \mu A b' \kappa_1)^2} + \alpha T_e}{1 + \alpha T_e}. \quad (34)$$

A comparison of expressions (33) and (34), and bearing in mind (32) shows, that even when means are taken to secure equality of the average amplification coefficient for both channel, the dispersion of the random processes at the outputs may still differ greatly from the case of complete channel identity. For example, for $k_{av} = k'_{av}$, $b = 2b'$, (which may take place for unequal regulating characteristics of the channels), the dispersion process at the output of the second channel will have the form

$$\sigma_1^2 \approx \kappa_{av}^{'2} \sigma^2. \quad (35)$$

From equation (34) and (35) it follows, that for identical channel characteristics, the faster the fluctuation response of an AGC system for the first channel, i.e., the greater the inequality $\alpha T_e < 1$, the more the dispersions at the output will differ.

Analogously, higher order approximations can be found for the output random process characteristics.

The given analysis indicates that succeeding approximations will rapidly converge for $\frac{\sigma^2}{A_2} < 1$ and that for practical purposes the obtained expressions can be frequently sufficient.

CONCLUSION

On the basis of the obtained results, the following conclusions can be made:

1. As far as the transmission of signal envelope is concerned the AGC system is equivalent (in the first approximation) to a linear system, for which the transfer ratio in the first channel is determined by formula (15), and for the second channel by formula (20).

2. The average signal at the channel outputs does not depend on the random component of the input voltage. If only average signal values at the channel outputs are of interest, then it is sufficient, by means of supplementary regulation, to maintain their average amplification coefficients equal in the entire range of input amplitude variation.

3. Even if measures are taken to equate the average amplification coefficients of the channels in the receiving system, fluctuating components of output voltages may greatly differ due to the inequality of the regulating characteristics. This difference will be the more pronounced, the faster the response of the AGC system.

Thus we have analyzed the effect of a changing amplitude signal on a two-channel setup with AGC with a filter of any order. In the article are obtained and solved integral equations for the spectrums of output potentials. Also obtained are formulas for the expectations and spectrum densities of the output potentials. As an example, an AGC system with a filter at the first order is analyzed in detail.

By utilizing the above methods, the effects of other type signals (for example, a sinusoidally modulated signal of fluctuating amplitude, and others) may be analyzed. However, analysis of these cases is beyond the scope of this work.

Original article submitted May 31, 1960

LITERATURE

1. V.V. Shirokov, V.G. Repin, "Interference effects in AGC systems," Radiotekhnika, No. 4, 1959.
2. G.P. Tartakovskii, Dynamics of AGC Systems, Gosenergoizdat, 1957.
3. B.V. Gnedenko, Course in the Theory of Probability, Gostekhizdat, 1954.
4. M.S. Bartlett, Introduction to the theory of Random Processes, IIL, 1958 (translated from English by B.A. Sebast'yanov).

SELECTION OF NETWORK ELEMENTS TO COMPENSATE FOR FREQUENCY CHANGES DUE TO TEMPERATURE IN QUARTZ-CRYSTAL OSCILLATORS

G.B. Al'tshuler and V.A. Prokhorov

Compensation for frequency changes due to temperature by means of reactive-resistive networks is considered. Frequency relations for the crystal controlled oscillator are supplied. Also determined are the equivalent parameters of the compensating networks as well as their interrelationships. The experimental data obtained confirms the derived relations.

INTRODUCTION

In oscillators operating under large temperature gradients, the frequency drifts are caused mainly by temperature instability of the network elements. Such conditions prevail in oscillators operating in airborne, portable and other radio aparatus. Temperature stabilization is found to be the most accurate way of frequency stabilization. However it consumes additional energy from the power sources and also increases weight and overall size of the equipment. In connection with this, in many cases when high accuracy of frequency stabilization is not required, it is advantageous to employ thermal compensation. Thermal compensation has received wide application in non-quartz oscillators, where it is accomplished by connecting in the network reactive elements with temperature coefficients of opposite polarity.

In quartz oscillators the frequency instability due to temperature is largely determined by the temperature-frequency coefficient (TFC) of the

quartz resonator, and does not greatly depend on the temperature coefficients of the remaining network elements. Therefore, for quartz oscillators, the usual manner of frequency compensation is not effective. Connection of reactances even with high temperature coefficients (as for example certain types of ceramic capacitors) does not yield the frequency changes required for compensation, since the magnitude of the reactances does not change sufficiently.

One way of obtaining large changes in reactive impedance (which depend on temperature), is by utilizing thermistor controlled XR-networks. If a parallel network constructed from inductances or capacitances and thermal-resistance is connected following the quartz resonator, then the reactance which constitutes the impedance of such parallel network (considered following the quartz oscillator) may be visualized as a variable quantity which depends on thermal resistivity, i.e., on temperature. For example the equivalent inductance of a parallel LR-network is equal to

$$L_e = \frac{L}{1+\left(\frac{\omega L}{R}\right)^2}.$$

In a similar manner, we may change the frequency of the quartz oscillator by connecting in parallel with the quartz crystal an inductor or capacitor network and a thermistor. With the aid of the described networks, the possible limits of frequency change are analyzed below in more detail.

The given method of thermal compensation for frequency deviations is described in [1]. However, the author does not give any concrete suggestions as to the selection of network elements for thermally compensated oscillators and does not consider the problem of losses which are introduced in the network by the XR-network.

Theoretical consideration of the compensation problem for frequency changes in quartz oscillators due to temperature variations is completely justifiable, since it will facilitate the practical matching of network elements.

Thermal compensation of frequency in quartz oscillators actually constitutes frequency control by means of reactive impedances. Therefore, relations which characterize controlled oscillators are also applicable to a thermally compensated quartz oscillator. General problems of frequency control in quartz oscillators, as applied to radiotelegraphy and frequency tuning, are considered in our own as well as foreign literature (for example [2]). Below we shall pause on one such general problem only insofar as it is necessary to establish the underlying relations in a thermally compensated quartz oscillator.

FUNDAMENTAL RELATIONS IN A CRYSTAL CONTROLLED QUARTZ OSCILLATOR

Let us consider two most widely used quartz oscillator networks: the network with a quartz resonator between the grid and the anode, and the network with a quartz resonator between the grid and the cathode. Both of these networks may be reduced to an equivalent network of a Hartley oscillator [3] (Figure 1). In accordance with the theory of a generalized Hartley oscillator the network frequency relations, in the steady state, are determined by the phase balance equation

$$X_1 + X_2 + X_3 = 0, \qquad (1)$$

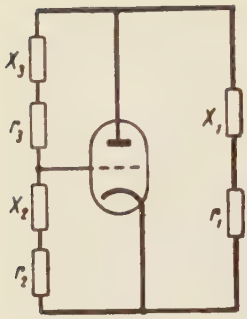

Figure 1

The amplitude relations are determined by the amplitude balance equation

$$S_1 R_y = 1, \tag{2}$$

where S_1 is the transconductance for the first harmonic,

$$R_y = \frac{X_1 X_2}{r_1 + r_2 + r_3} \tag{3}$$

the impedance of the oscillator control.

It is convenient to visualize the quartz resonator as a series connection of a reactive and active impedance:

$$X_k = |X_{c0}| \frac{e}{1-e}, \tag{4}$$

$$R_k = \frac{r_k}{(1-e)^2}, \tag{5}$$

where r_k is the resistive loss of the quartz resonator, $x_{C0} = -\frac{1}{\omega C_0}$ is the static capacitive reactance of the quartz resonator, $e = \frac{f - f_k}{F}$ is the given detuning of the quartz resonator calculated from the series resonant frequency f_k, and F is the frequency difference between the series and parallel resonant frequency.

It is desirable that the formulas of frequency change, for parallel as well as series connection of the control reactances, should have a convenient and similar form. Therefore, for parallel connection, it is necessary to employ the control admittance B_y, and the detuning of the quartz oscillator e; and for the series connection, take X_y as the control reactance and $\eta = 1\text{-}e$ as the detuning i.e., detuning $\eta = \frac{f_0 - f}{F}$ is calculated from the frequency of parallel resonance f_0.

Taking into account the above, we find for the network in Figure 2a that the change in detuning Δe for parallel control in agreement with equation (1) is equal to

$$\Delta e = e - e_0 = \frac{e_0^2 b_y}{1 - e_0 b_y}, \tag{6}$$

where

$$e_0 = \frac{X_r}{X_g - X_{c0}} \tag{7}$$

is the detuning of the quartz resonator without the control admittance B_y, e is the detuning of the quartz resonator with the control admittance, X_g is the peak input impedance of the oscillator with respect to points 1.1 (Figure 2a, b), $b_y = B_y |X_{C0}|$ is the given control admittance.

For series control (Figure 2b) the change in detuning $\Delta\eta$ in accordance with equation (1) is equal to

$$\Delta\eta = \eta - \eta_0 = \frac{\eta_0^2 x_y}{1 - \eta_0 x_y}, \tag{8}$$

where

$$\eta_0 = \frac{X_{c0}}{X_{c0} + X_g} \tag{9}$$

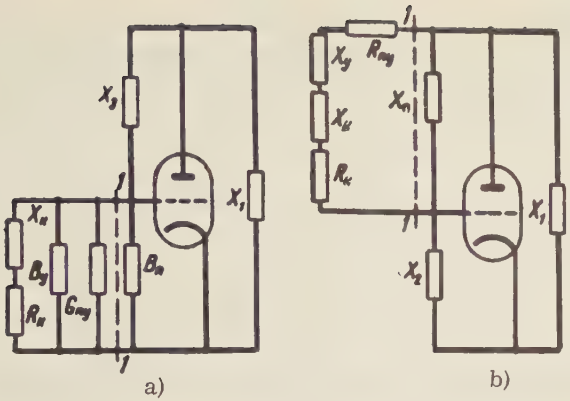

Figure 2

is the quartz resonator detuning without the control reactance X_y, η is the detuning with the control reactance, X_y, $x_y = \frac{X_y}{|X_{c0}|}$ is the given control reactance.

Accordingly, the frequency change Δf for series and parallel control is equal:

$$\Delta f = -F\Delta\eta, \tag{10}$$

$$\Delta f = F\Delta e. \tag{11}$$

Analyzing equations (6) and (8), we see that the oscillator control increases with the increase in detuning e_0 and η_0, for parallel as well as series control. In this manner, in the case of parallel networks for thermal compensation of frequency changes it is necessary to operate with small oscillator input capacitances C_g; and for a series network, with large input capacitances C_g. The latter conclusions follow from equations (7) and (9), and are physically understandable.

Connection of compensating elements is necessarily associated with introduction of additional losses in the oscillator network. Therefore it is of interest to evaluate the control impedance of the oscillator R_y. In our case, when the change in the reactive component of the network is performed by changing its resistive part, such evaluation acquires a first class significance. Only by considering the decrease of the impedance control of the oscillator will permit the determination of the allowable limits of variation of the reactive-resistive network elements and the selection of their correct values.

For the quartz oscillator networks under consideration, the total resistive loss $r = r_1 + r_2 + r_3$ (2) is determined by the impedance of quartz resonator branch. In this branch are included the compensating networks. The equivalent networks of the quartz resonator branch for parallel and series connection of the compensating elements are shown in Figure 2a, b in that order. Calculating the network for the series connection of Figure 2b, we obtain that the loss resistance r is equal

$$r \approx (R_{ny} + R_x)\left(\frac{X_n}{X_x + X_y + X_z}\right)^2. \tag{12}$$

where R_{ny} is the resistive impedance of the compensating network, $X_n = -\frac{1}{\omega C_n}$ is the reactance due to parasific capacitance C_n in the loop.

By considering equations (4), (8), and $\eta = 1-e$, we have

$$X_x + X_y \approx X_{x0} = \frac{1-\eta_0}{\eta_0} | X_{c0}$$

where X_{k0} is the reactance of the quartz resonator with initial detuning η_0.

By substituting $X_k + X_y$ by X_{k0} and simple manipulations equation (12) takes the form

$$r = \left[R_{ny} + \frac{r_x}{\left(\eta_0 \frac{1}{1-\eta_0 x_y} \right)^2} \right] \frac{1}{\left(1 - \frac{1-\eta_0}{\eta_0} \frac{C_n}{C_0} \right)^2}, \tag{13}$$

In a similar manner, we find the resistive loss for parallel control

$$r \approx \frac{\frac{R_x}{X_x^2} + G_{ny}}{\left(\frac{1}{X_x} + B_y + B_n \right)^2}, \tag{14}$$

where G_{ny}, B_y are the corresponding resistive and reactive admittances of the compensating network, $B_n = \omega C_n$ is the admittance due to the parasitic capacitance of the loop.

FREQUENCY CONTROL BY MEAN OF REACTIVE-RESISTIVE NETWORKS

To calculate the possible frequency deviations of the quartz oscillator with the aid of XR-network, let us find the size of the reactive and resistive impedances.

The transformation formulas from parallel to series networks are as follows:

$$r_p = R_p \frac{X_p^2}{R_p^2 + X_p^2}, \tag{15}$$

$$x_p = i X_p \frac{R_p^2}{R_p^2 + X_p^2}, \tag{16}$$

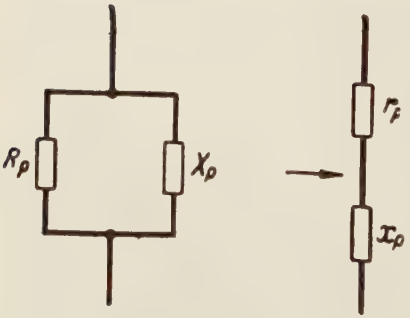

Transformation of a series network $x_s r_s$ into a parallel network $R_s X_s$ gives

$$R_s = \frac{r_s^2 + x_s^2}{r_s}, \tag{17}$$

$$X_s = i \frac{r_s^2 + x_s^2}{x_s}. \tag{18}$$

The recalculated values of $r_p x_p$ and $R_s X_s$ are functions of the impedances R_p and r_s for which thermistors with large temperature coefficients are used. It is not difficult to see that frequency control with the aid of a series chain $r_s x_s$ may be accomplished by connecting it in parallel with the quartz resonator; and with the aid of a

parallel chain R_pX_p by connecting it in series with the resonator.

Let us put the expressions for the calculated impedances in a form useful for substitution in the formulas for frequency deviations (6), (8) and for the resistive loss r of the oscillator (13), (14). For series control:

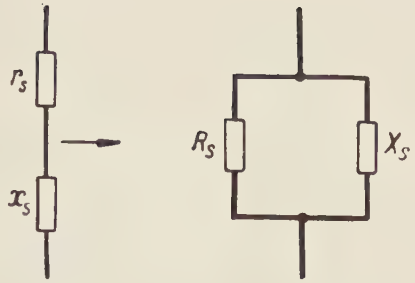

$$x_y = \frac{x_p}{|X_{c0}|} = \gamma \frac{1}{1+y^2} \qquad (19)$$

is the control impedance,

$$r_y = \frac{r_p}{|X_{c0}|} = \gamma \frac{y}{1+y^2} \qquad (20)$$

is the resistive loss, where

$$\gamma = \frac{X_p}{|X_{c0}|}, \quad y = \frac{X_p}{R_p}. \qquad (21)$$

For parallel control

$$b_y = \frac{|X_{c0}|}{X_s} = \gamma \frac{1}{1+y^2} \qquad (22)$$

is the control admittance,

$$g_y = \frac{|X_{c0}|}{R_s} = \gamma \frac{y}{1+y^2} \qquad (23)$$

is the loss admittance, where

$$\gamma = \frac{|X_{c0}|}{x_s}, \qquad (24)$$

$$y = \frac{r_s}{x_s}. \qquad (25)$$

By comparing equations (19) with (20), and (22) with (23), we have

$$\left.\begin{aligned} r_y &= x_y \frac{1}{y} \\ g_y &= b_y \frac{1}{y} \end{aligned}\right\}. \qquad (26)$$

Figure 3 gives the dependence of x_y, b_y and r_y, g_y on y with γ as a parameter.

Since the formulas for reactive and resistive control impedances in a series compensating network, and admittances in the parallel network have the same form, future analysis is carried out for the example of series control.

It can easily be seen that the maximum loss resistance, introduced by the control network $R_{ny} = r_y |X_{c0}|$, corresponds to the equality of the reactive impedance with the control thermistor (y = 1). The rate at change of the reactive control impedance, and consequently, the rate of frequency change increases with increasing reactive impedance, i.e., with increasing $\gamma = \frac{X_p}{|X_{c0}|}$ (for the same thermistor magnitude). However with this, the loss resistance R_{ny}, introduced by the XR network also increases.

Formula (19) was employed to calculate the curves of the frequency dependency on y. The calculated values for x_y are substituted into formula (8). In Figure 4 are given the calculated as well as the experimental dependencies of the change is detuning $\Delta\eta$ from the relation y, for different values of γ for a practical oscillator and a quartz crystal resonator:

C_f 49 pF, C_0 = 7 pF,

F = 9150 cps, f = 4 Mc.

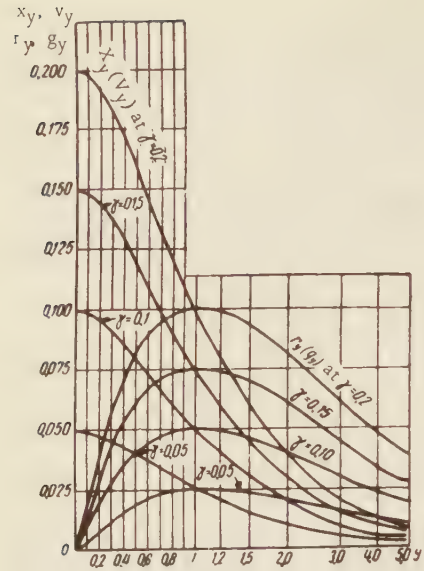

Figure 3

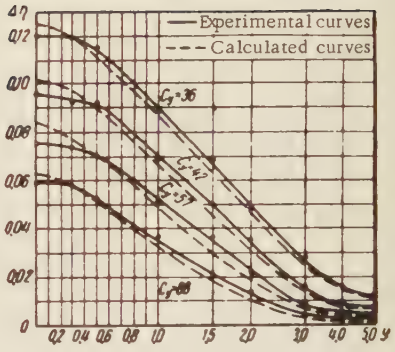

Figure 4

The calculated results are well substantiated by the experimental ones.

In Figures 5, 6 are given the experimentally determined curves of the dependencies of the output voltage and frequency change of the oscillator with resistance R_p. These curves are given for different values of capacitance for or series control with a parallel XR-network. From the voltage change graph, it can be seen that for large γ (small capacitance) the frequency change increases, the output voltage falls until oscillators cease. We shall determine the allowable value for the control reactance x_y from the condition of oscillator self excitation

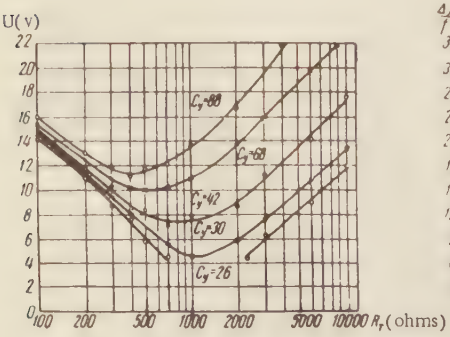

Figure 5

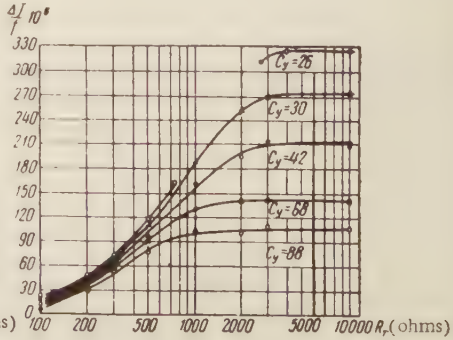

Figure 6

$$S_0 R_y > 1, \tag{27}$$

where S_0 is the initial tranconductance.

According to equations (2) and (13) the control impedance of the oscillator R_y is equal to

$$R_y = \frac{X_1 X_2 \left(1 - \frac{1-\gamma_0}{\gamma_0}\frac{C_n}{C_0}\right)^2}{\left[R_{ny} + \frac{r_k}{\left(\gamma_0 \frac{1}{1-\gamma_0 x_y}\right)^2}\right]}. \tag{28}$$

By substituting into (28) instead of R_{ny} its value from (26), we obtain

$$R_y = \frac{X_1 X_2 \left(1 - \frac{1-\gamma_0}{\gamma_0}\frac{C_n}{C_0}\right)^2}{\left[|X_{c0}| \frac{1}{y} x_y + \frac{r_k}{\left(\gamma_0 \frac{1}{1-\gamma_0 x_y}\right)^2}\right]}. \tag{29}$$

Since y = 1 corresponds to the maximum introducable resistance R_{ny}, from equation (29) and $S_0 R_y = 1$ the value of the control reactance x_y, corresponding to y = 1, can easily be determined.

With x_y known corresponding to y = 1 we find from equation (19) the maximum allowable value for the relation γ_{max} (operation close to the point of interrupted oscillations).

$$\gamma_{max} = 2x_y. \tag{30}$$

In practice it is necessary to operate with γ smaller than $2x_y$.

CHARACTERISTICS OF THERMAL COMPENSATION IN "BT" AND "AT" CUT CRYSTALS, EXPERIMENTAL PART

The law of frequency change (compensated by a network in quartz oscillator) and its value is determined by the type and the parameters of the quartz resonator. We shall briefly stop on two quartz crystals AT and BT which are utilized at high frequencies. It is known that in the AT cut quartz crystals the frequency varies as the cube of temperature while in the BT cut crystals their relationship is parabolic. It is obvious that the frequency change under the influence of the compensating network must be in a reverse direction from the quartz temperature characteristics. To compare the required limits of the change in the compensating reactance it is convenient to employ the (TFC) temperature frequency coefficient of the quartz resonators α_t in the interval of temperature Δt.

From the point of view of the quartz oscillator frequency control, another parameter of the quartz resonator has an important significance. This parameter is the value of the relative frequency separation for series and parallel resonance, equal to $\frac{1}{2}\frac{C_k}{C_0}$. According to equations (10) and (11), the frequency change produced by the connection of a reactive impedance is proportional to the interval

$$F \approx \frac{1}{2}\frac{C_k}{C_0} f_k.$$

The value of $\frac{1}{2}\frac{C_к}{C_0}$ depends on the type of connection and other factors [5]; nevertheless it is quite constant for a group of quartz resonators of the same construction with the same technique of slab manufacture.

For the bulk at high frequency quartz crystals we have

$$\text{AT cut} \quad \begin{cases} \frac{1}{2}\frac{C_к}{C_0} = (1000 - 2\,500)\,10^{-6}, \\ \alpha_f = (0.4 - 1{,}2)\,10^{-6}\,\frac{1}{\text{deg.}} \end{cases}$$

$$\text{BT cut} \quad \begin{cases} \frac{1}{2}\frac{C_к}{C_0} = (500 - 1\,000)\,10^{-6}, \\ \alpha_f = (1.2 - 2{,}0)\,10^{-6}\,\frac{1}{\text{deg.}} \end{cases}$$

Since the (TFC) of the BT cut resonator is greater than that of the AT cut resonator at each side of the parabola, while the relation $\frac{1}{2}\frac{C_к}{C_0}$ is smaller, it follows that if the remaining conditions are held the same it is more difficult to regulate the frequency of a BT cut resonator than that of an AT cut resonator.

The direction of frequency change depends on the method of connecting the reactances and on their character. It is known that a series connection of inductance and a parallel connection of capacitance decreases the frequency of oscillation; while a parallel connection of inductance and a series connection of capacitance increases it. The foresaid takes into account equations (6) and (8).

The majority of AT cut quartz crystals possess a positive TFC for which the frequency change by means of thermistors is simplified and the compensating networks are also simpler. The semiconductor thermistors manufactured by industry [4] have a negative TCR (Temperature Coefficient of Resistance). With increasing resistance in a parallel LR-circuit the equivalent inductance increases while in an RC-circuit the equivalent capacitance decreases (the reverse is true in series circuits). Therefore for compensation of frequency change in an AT cut quartz resonator with a positive TFC a series connection of a parallel RC-circuit or a parallel connection of a series LR-circuit is necessary.

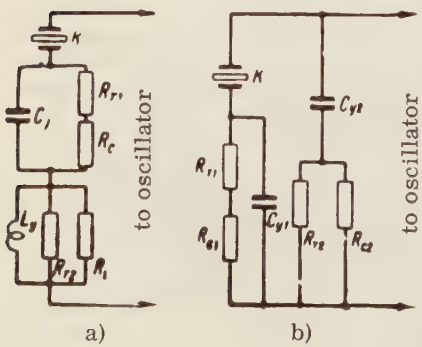

a) b)

Figure 7

In connection with the parabolic form of frequency-temperature dependence in BT cut quartz crystals, it is necessary to realize a parabolic (or close to it) temperature characteristic of the frequency change of the thermistor. Such dependencies may be obtained by one of the networks in Figure 7a, b. In the network of Figure 7a, resistance R_C limits the action of the CR-network for temperatures higher than the temperature corresponding to the top of the parabola. The significance of resistances R_{C1} and R_{C2} in network 7b is anolgous.

An experimental check of the described method of thermal compensation was performed on a breadboard

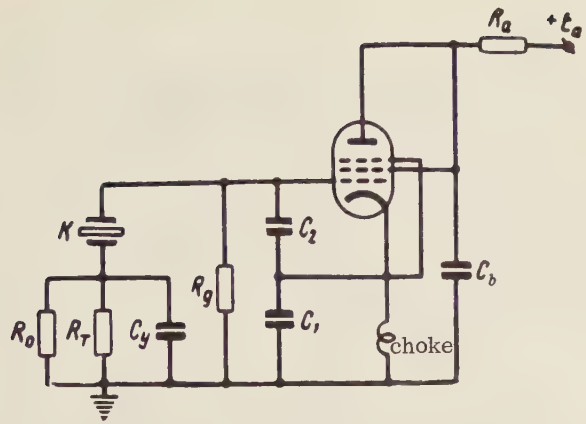

Figure 8

corresponding to Figure 8. The experiments were conducted for an AT cut resonator with a frequency of r Mc, C_0 = 7pF, F + 9150 cps. The input capacity of the oscillator was C_g = 49pF. The Thermocompensating elements were tuned for an interval of positive temperatures +20° C - +70° C and in the wide temperature interval -60° C - +60° C.

In Figure 9 are shown the temperature frequency dependencies for a non-compensated and a thermally compensated oscillator in the temperature interval +20° C - +70° C; in Figure 10 the same is shown for a temperature interval -60° C - +60° C.

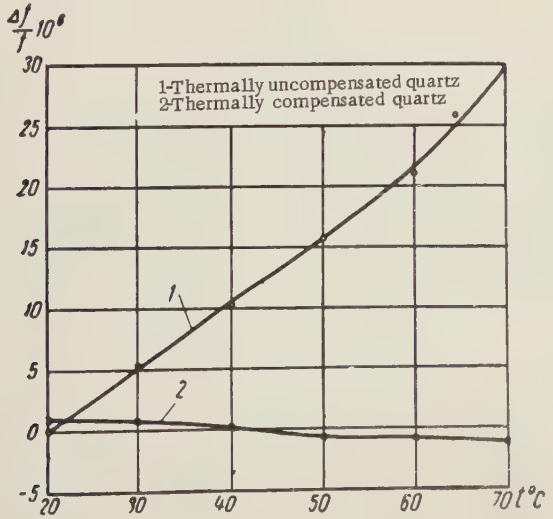

Figure 9

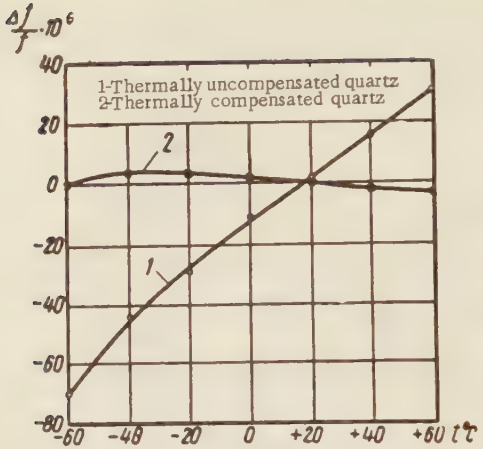

Figure 10

Introduction of thermal compensation increases the frequency stability; temperature instability in the interval +20° C - +70° C did not surpass $2.5 \cdot 10^{-6}$, as compared to $30 \cdot 10^{-6}$ in a non-compensated oscillator. Instability in the interval -60° C - +60° C did not surpass $7 \cdot 10^{-6}$ without thermal compensation.

The output voltage in the temperature interval -60° C - +60° C varies from 16 to 7 volts.

Original article submitted February 16, 1960

LITERATURE

1. Spears, "Thermally compensated crystal oscillators." The journal of the British Institute of Radio Engineers, Vol. 18, No. 10, 1958.
2. A.A. Magazanik, Control of Oscillator Frequency with a Quartz Stabilizer, Information Bulletin. Svyaz'izdat, 1955.
3. S.I. Evtyanov, Radio Transmission Devices. Svyaz'izdat, 1950.
4. N.P. Udalov, Semiconductor Temperature - Controlled Resistors, Oborongiz, 1955.
5. G.B. Al'tshuller, "Possibility of controlling a high-frequency quartz resonator by a capacitive network." Elektrosvyaz', No. 8, 1960.

INVESTIGATION OF THE EFFECT OF PHASE DISTORTION ON INSTANTANEOUS SIGNAL VALUE IN A RADIO TRANSMISSION CHANNEL

A.A. Glukhov

In this article are given the results of an experimental investigation of the effect of phase distortion instantaneous signal value in a radio transmission channel, utilizing an unloaded cable as a junction between the transmission stations.

INTRODUCTION

Well known automatic control setups (ACS) in transmitting systems permit control (within averaged values) of the transfer coefficient, the noise level, and isolated points of the frequency characteristic, by a comparison of the rectified input and output signals. However, the setup, working on the principle of deviation comparison, does not permit the direct control of nonlinear distortions. Since nonlinear distortions are an important factor in determining the quality of transmission, it would be important to develop an instantaneous signal value comparator which would permit the control of nonlinear distortions in the system. However, it is known that in channels containing lone circuit lines (to which belong the overwhelming majority of transmitting channels), there are phase distortions which can change the shape of a complex signal at the output as compared to the shape of the input signal.

As far as we know, there is no data containing information on the character of distortions of concrete transmission signals caused by phase distortions. The following article presents the result of an experimental investigation of this problem.

EXPERIMENTAL PATH

The examination of the effect of phase distortion on the instantaneous complex signal values was carried out on an experimental path whose parameters are characteristic of most cable transmissio channels. Its block diagram is shown in Figure 1.

High quality linear amplifiers (LA_1, LA_2, LA_3) were selected with identical parameters; the frequency characteristic in the range of 30 - 15000 cps had a variation of ± 0.5 db. At $U_{out} = 3.1$ v, used for conducting the experiment, and at the rated load, their coefficient of nonlinear distortion

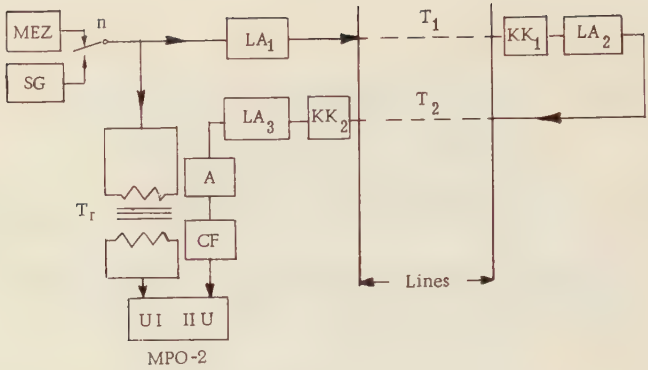

Figure 1

does not exceed 0.5% in the entire frequency range. The phase characteristic typical of all three amplifiers was obtained experimentally and is shown in Figure 2.
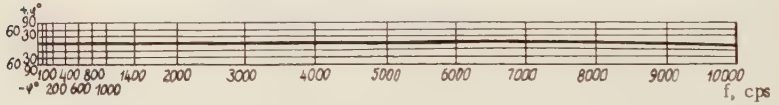
Figure 2

The unloaded cable lines (L_1, L_2) had a conductor diameter of 0.9 and 0.5 mm. Since it was possible to vary the length of the cable lines, three experimental sections were formed: two homogeneous with length $L_{0.9}$ = 15 km and $L_{0.9}$ = 30 km, and one nonhomogeneous with an over-all length of 30 km ($L_{0.9}$ = 15 km and $L_{0.5}$ = 15 km). The experimentally obtained phase and frequency characteristics of the homogeneous route are shown in Figures 3 and 4, where curve 1 corresponds to the 15 km route, and curve II to the 30 km route.

The frequency correction networks (KK_1, KK_2) have a series impedance. To achieve symmetry of the experimental path a type EST-1 transformer was connected at the input of each frequency-correction network. Experiment has shown, that in the frequency band of 50 to 15000 cps these transformers do not practically introduce any phase distortions.

In order to match the input and output path impedance (600 ohms) with the input impedance (3 ohms) of the circuit oscilloscope as well as to obtain the necessary current amplitudes (25-30 ma), matching arrangements were set up: a cathode follower CF and a high quality low frequency step-down transformer T_r. With this arrangement, a linear amplitude characteristic of the path was assured in the required frequency range. Experiment showed that these arrangements do not introduce phase distortions.

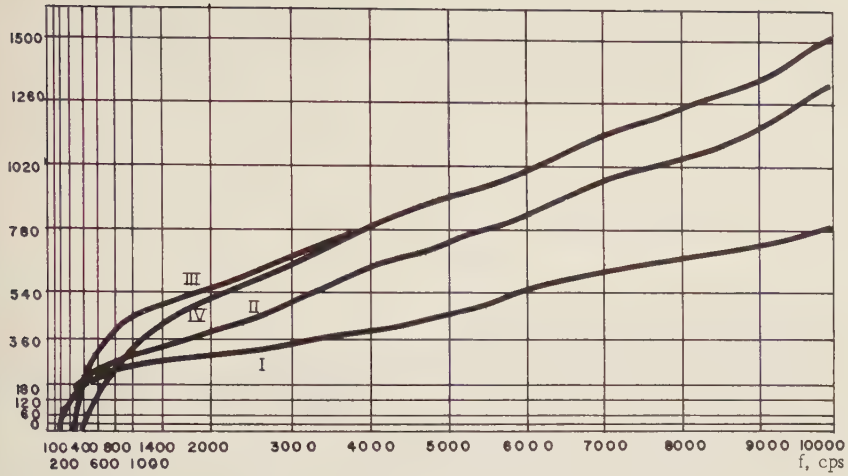

Figure 3

The signals under consideration were recorded on standard film with the aid of two identical oscilloscopes MPO-2 circuits with a natural frequency of 10 kc. The speed of the film was 1000 mm/sec.

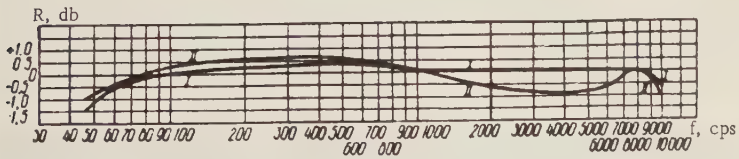

Figure 4

The coefficient of linear distortion does not exceed 1% in the entire range of the generated frequencies (50 - 10,000 cps). The noise level is under -60 db.

Since according to Figure 3, the phase distortions largely take place in the frequency range of 50-600 cps, portions of the transmission programs under consideration were selected with components of the above frequency in their spectra. On the other hand, analysis of signals which do not contain low frequency components in their spectra is of definite interest in the design of automatic control setups. After consideration of the desired spectra for the transmission program [1], portions of instrumental music (symphonic orchestra, violin, piano, organ), as well as vocal music and speech, both male and female were selected.

Method of analysis. The range was adjusted in such a manner that with a frequency of 1000 cps, the amplitudes of the currents in circuits I

and II (Figure 1) were equal and their initial phase coincided. The program was fed from a magnetic sound recorder MEZ-15. To facilitate analysis with the oscilloscope (for each given path condition), the starting time for the recording of each program portion was made coincident.

RESULTS OF THE ANALYSIS

As is known from [2], the path phase distortions will be absent if the following condition is fulfilled:

$$\varphi = 2k\pi + \omega\tau, \tag{1}$$

where α is the phase coefficient; k = 0.1, 2, 3, ..., τ is a certain constant, and ω is the angular frequency.

From inspection of phase characteristics in Figure 3, it can be seen that they do not satisfy condition (1) in the frequency range from 50 to 10,000 cps. Since the corrective elements introduce only insignificant phase distortions, it has been established that the above discrepancies are mainly introduced by lines L_1 and L_2. This can be seen in the phase characteristics illustrated in Figure 5 (obtained as a result of measurements of different types of amplification setups with the aid of an interference method [3]). Curve I is the phase characteristic of an ordinary corrective amplifier. Curve II is the amplifier phase characteristic in the central amplifying station (CAS) of the Moscow city radio relay net (MCRN), and curve III is the phase characteristic of the SAS, 25 kw amplifier.

Experiments show that the degree of the effect of path frequency correction upon it phase characteristic becomes more apparent on the edges of the transmitted frequency range, and more so in the range of 50 - 600 cps. In spite of the absence of frequency distortions in this range, a complete disappearance of the phase distortions is not observed. This is because with nonminimal path phase characteristics (which can be assumed for the path under consideration), the conditions for the absence of amplitude-frequency and phase distortions cannot be simultaneously satisfied at the end of the frequency band.

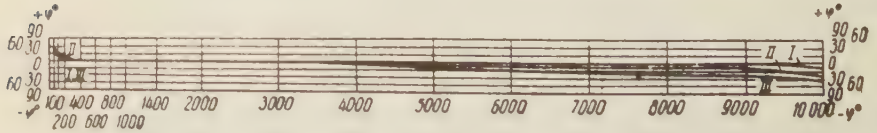

Figure 5

The effect of phase distortions on the signal form of the selected programs becomes more apparent in the musical portions of the symphonic orchestra and the piano. The value of the ratio |A| (expressed in db) of the peak signal values obtained at the input and output of the experimental route for portions of speech and symphonic music is given in Table 1. From this it can be seen that for the cases under consideration, the absolute value of ratio |A| may change considerably.

The intensity oscillogram in Figure 6a represents the portion of

symphonic music during its path transmission (length $L_{0.9}$ = 30 km but maintaining approximately the same frequency distortions for the indicated portion of the program, the measured value of |A| increases up to 7.0 v 8 db. This may be observed for the same markings 10, 12 in Figure 6b. In Figures 6a and b, as well as in the remaining figures, the upper oscillograms represent the input signal, and the lower, the output signals. The time axis goes through point 0.

Table 1

Sample	Sampling time (sec)	Magnitude of |A|, db		
		for homogeneous route of length		for inhomogeneous route, 30 km long
		$L_{0.9}$ = 15 km	$L_{0.9}$ = 30 km	$L_{0.9}$ = 15 km and $L_{0.5}$ = 15 km
Speech (male and female)	22	3 - 3.5	3.5 - 4.4	5.5 - 6
Symphonic orchestra	8	4.5 - 6	7.5 - 8	7.8 - 9

The data in the last column of Table 1 corresponds to the case where the 30 km route is nonhomogenous. Its frequency characteristic in the range of 50 - 4000 cps has a variation of +1.3 db to -6.4 db, and a continuous fall of 10 db at a frequency of 6000 cps. Here, the deviation in the peak value of the signals due to phase distortion is even more apparent. In addition, a delay of up to 1.5 - 1.7 μsec. of the peak signal value was observed on the oscillograms. These delays do not exceed 0.1 - 0.3 μsec. for homogenous routes.

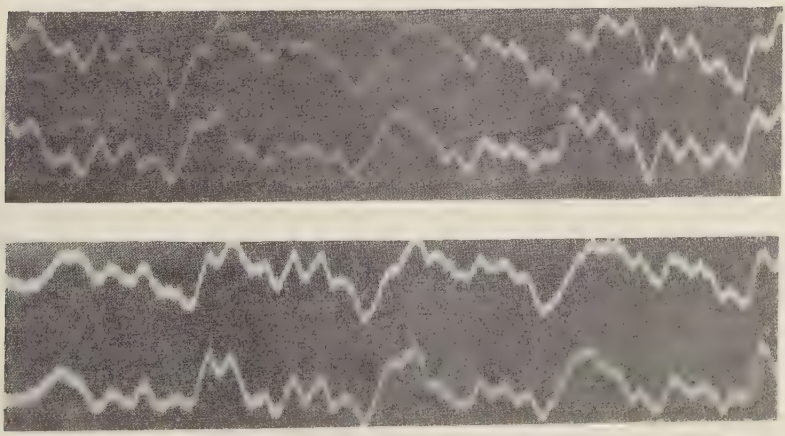

Figure 6

For engineering calculations of the control systems operating on the principle of instantaneous signal value comparison, the value of |A| and its frequency must be known for different radio transmission signals; since these quantities determine the selection of the time constants for the intergating networks in ACS. Certain statistical data on the deviation of the two musical performances (symphonic orchestra and piano) are given in Table 2.

Table 2

Sample	Sampling time (sec)	Number of measurements	Frequency and magnitude of the deviation of the peak value of the signal voltage (U) at output of the line ($L_{0.9}$ = 30 km) from the peak value at the input									
			Range: 0.5U - U					Range: 0.05U - 0.5U				
			Magnitude of deviation, db									
			|A| = 0	|A| < 2	|A| = 2÷4	|A| = 4÷6	|A| = 6÷8	|A| = 0	|A| < 2	|A| = 2÷4	|A| = 4÷6	|A| = 6÷8
Symphonic orchestra	1.0	961 (100%)	Frequency deviation, %									
			22	29.2	9.2	2.9	1.8	14.0	7.6	7.2	4.3	1.8
Piano. . .	1.0	1058 (100%)	Frequency deviation, %									
			12.9	35.3	18.0	5.5	0.9	8.0	6.9	7.8	3.7	1.0

From a consideration of Table 2, it follows that the greatest number of distortions of the instantaneous signal values attributable to phase distortion is observed in the range from 0.5 U to U (for a symphonic orchestra, out of 64% of all distortion cases, included in this interval the phase distortion constituted about 43%; and for the piano, out of 79% of all cases, phase distortion constituted about 60%). Thus, distortions with a value of |A| = = 4 to 6 db and |A| = 6 to 8 db are encountered extending over large time intervals; the duration of a single distortion did not exceed 1 to 10 μsec. The deviation of 2 to 4 db for the given program intervals should be considered as fundamental.

In Figure 7 are given the most typical phase characteristics of certain operating radio transmission channels of MCRN. Curve I is for the path of the supporting amplifier station (SAS) with intermediate frequency corrective elements in the programing and control circuits. Curves II and III correspond to the paths in which the correctors of frequency characteristics are connected at the input of SAS and the station amplifying unit SAU correspondingly at the input of CAS. Curve IV corresponds to the route for the transformer substation TS. Certain technical characteristics of the above channels are given in Table 3.

Upon inspecting the curves in Figure 7, we see that, in frequency range from 600 to 10,000 cps, the phase characteristics of real channels have approximately a linear dependence upon frequency; with small deviations in the range of 8 to 10 kc. In practice, these deviations need not be considered, since in this frequency range the signal power level is extremely small. In the low-frequency range (50 to 600 cps), where a large part of the signal power is concentrated, considerable phase distortion is inherent in real as well as experimental channels.

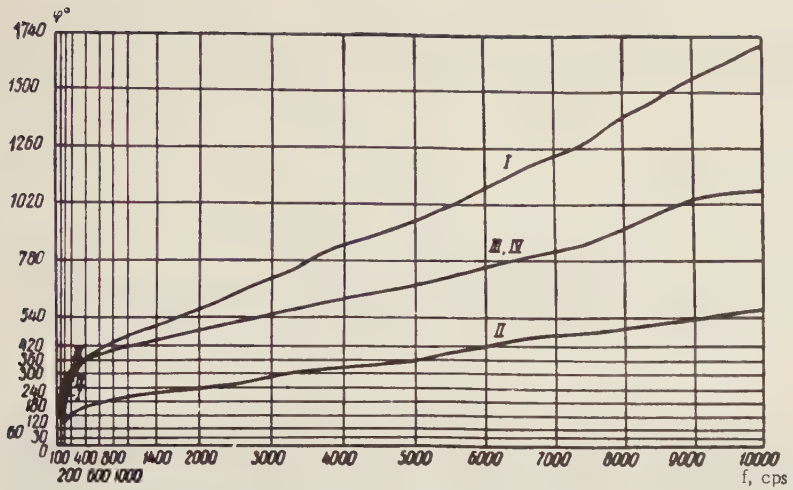

Figure 7

It is of definite interest to find out how much the peak signal values will change at the output of the control channel, if a low frequency band in which phase distortions occur is cut out at its input. Experiment showed that on elimination of low frequencies up to 200 cps from the signal spectrum of symphonic music, with the aid of a filter in which the downgrade slope of the frequency characteristic is at least 22 db per octave, and in the absence of other distortions, no distinction can be observed between the input and output peak signal values. For the remaining selected transmission band, the difference does not exceed 0.5 - 1 db. On increasing the cutoff frequency of the filter up to 400 cps, the quantity $|A|$ is practically equal to zero for all portions selected for transmission. Supporting this statement are the oscillograms of the intensity corresponding to the same transmission

Table 3

Amplifier power (TS) in the channel kw	Length, km		Variation of frequency characteristic in the 60 - 10,000 cycles band, db	Corresponding curve in Figure 7
	cable-linked line CAS (SAS, SAV, TS) CAS (core diameter 0.5 mm)	high-voltage bimetal feeder 4 mm		
SAS, 25	27	—	+2 -0.5	I
SAS, 25	9.5	—	0 -1.45	II
SAU, 5	18.4	—	+1.3 -0.7	III
TS, 5	18.4	1.0	+1 -4.3	IV

portion of the symphonic orchestra for the following conditions of the control channel $L_{0.9}$ = 15 km in length:

a) Figure 8a corresponds to the broadcast signal in the 50 - 10,000 cps frequency range and an +0.4 - 1.0 db variation of the frequency characteristics.

b) Figure 8b corresponds to the case where the input frequency is cut-off up to 200 cps.

The peak signal values in Figure 8a, as for example at markings 27 and 30, differ by 4.5 - 6 db. On the other hand it can be easily seen that no phase distortions are present in Figure 8b.

The phase distortions in the control channel, $L_{0.9}$ = 30 km in length, with subsequent connections of the above-mentioned filters are given in Figure 3 (Curves III and IV).

Figure 8

In Figures 3 and 7 the displacement of phase characteristics on the axis of ordinates is dependent on the phase displacement of the balancing transformers.

CONCLUSIONS

1. Due to considerable signal distortion, automatic control with the aid of an instantaneous signal value comparator in the frequency range of 50 - 10,000 cps cannot be realized without thorough phase correction of the channel.

2. The control channel may be utilized as an instantaneous signal value comparator if its bandpass is cut off below 400 cps, since the phase distortions thus have little effect upon the signal form. However such control is only useful for the transfer coefficient and noise level and is not useful for nonlinear distortions.

3. Conclusions applicable to cable transmission may be extended to

a radio broadcasting channel, since the connecting cable to the modulator is analogous to the cable transmission path.

I consider it my duty to express deep gratitude to Professor I.E. Goron for his valuable suggestions.

Original article submitted July 1, 1960

LITERATURE

1. Investigation of Distortions in Radio Transmission Channels. Information Bulletin, edited by I.E. Goron, Svyaz'izdat, 1959.
2. S.N. Evlanov, Correction Networks in Telegraph-Telephone Circuits. Svyaz'tekhizdat, 1937.
3. B.P. Aseev, Phase Relations in Radio Engineering, Svyaz'izdat, 1959.

QUANTUM PARAMAGNETIC AMPLIFIERS OF ULTRAHIGH FREQUENCIES[1]

PART II

V.B. Shteinshleiger

RESONATING PARAMAGNETIC QUANTUM AMPLIFIER

The physical operating principles of quantum paramagnetic amplifiers are analyzed in part I of this work. Below are considered different types of such amplifiers, and the noise interrelations within them.

The elementary resonator, in which the paramagnetic crystal is placed, is tuned to the frequency of the signal as well as to the brightening frequency in order to obtain intense brightening. The paramagnetic crystal is placed in the resonator in such a place where the magnetic field of the signal and the bias lighting or pump frequency have sufficient intensity. The main scheme of the paramagnetic amplifier resonator is illustrated in Figure 1a. Here the signal frequency resonator is formed by the deformed quarter wave length coaxial line, called the strip line, in which the inner

---

[1]Part II. See Part I in Telecommunications No. 12, 1960. References to formulas and drawings of Part I are marked by Roman I.

conductor is comprised of line 1, and the outer conductor of waveguide 2. The paramagnetic crystal is placed in contact with wall 4 where the bunching of the magnetic field and of the bias lighting are encountered. The magnetic lines of force encounter the strip line and have their greatest intensity at the wall 4. A picture of the magnetic lines of force is illustrated in Figure 1b. Connection with the outside line is realized by means of loop 5. The bias lighting resonator is formed by the cut section of the rectangular waveguide, in which the main waveguide oscillation of type H_{101} is formed. Communication at the frequency of the bias lighting is conveniently realized with the aid of openings, if the intensity of the bias lighting is supplied by the waveguide; or by means of a pin or hinge of the brightening route if by means of a coaxial cable. In Figure 1a contact is realized by means of the opening within the end wall. Tuning of the resonator to the bias lighting frequency may be realized by changing the position of this wall; with this, the waveguide section between the wall and end of strip 1 constitutes the limit of the signal frequency, which is considerably lower than the frequency of the lighting bias. Consequently, the wall position does not affect the tuning of the resonator to the frequency of the signal.

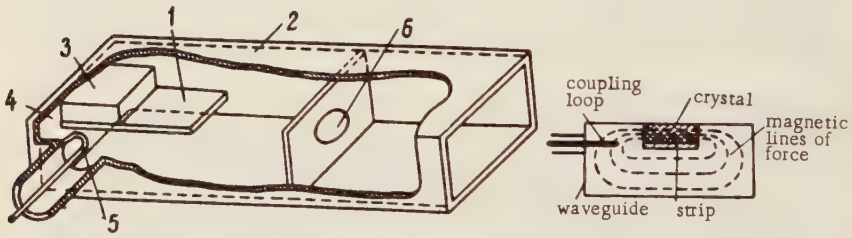

a) b)

Figure 1

The equivalent network of the resonator for the frequency of the signal is illustrated in Figure 2. The active element — paramagnetic — is represented as a negative resistance — r_m; this resistance compensates not only the resonator self loss resistance r_0, but what is more important, the resistance r_{in} which is introduced into the resonator from the line, and is connected with loading. The intensity of radiation from the paramagnetic crystal besides compensating the resonator self losses, radiates energy into the outside line. Such an amplifier is regenerative.

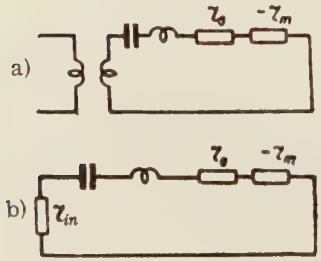

Figure 2

Analogous to the manner in which the energy losses within the resonator are characterized by self decrement d_0 — determined from the known formula

$$d_0 = \frac{P}{2\pi f_c E} \qquad (1)$$

(where P is the loss intensity and E is the stored energy within the resonator), the effectiveness of the paramagnetic substance, which radiates energy, may be characterized by a certain negative decrement — "magnetic decrement" — d_m

$$d_m = \frac{P_{irr}}{2\pi f_c E}, \tag{2}$$

where P_{irr} - is the intensity of radiation from the paramagnetic crystal. By utilizing formulas (8) I, (9) I, and (2) we may obtain

$$d_m = a \frac{f_n}{T} \xi, \tag{3}$$

here a is proportionality multiplier, which contains the constants of the substance and which depends on the operating region.

ξ is the coefficient of "saturation" which is equal to the ratio of the stored magnetic energy within the paramagnetic crystal, to the magnetic energy stored within the resonator which is tuned to the frequency of the signal.[2] With complete "saturation" of the resonator the quantity ξ is equal to unity.

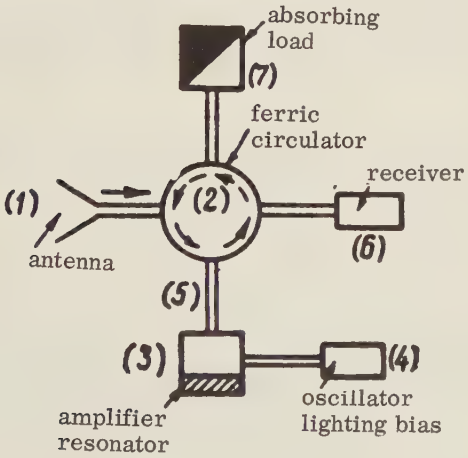

Figure 3

As we see, the effectiveness of the magnetic substance increases as its absolute temperature T decreases. This circumstance is mainly responsible for the use of liquid helium within paramagnetic amplifiers. Use of high bias lighting frequency, as may be seen from formula (3), also

---

[2] ξ also depends on the field orientation which is not indicated here for simplicity. More correctly this quantity could be called the coefficient of resonator magnetic field utilization.

increases the amplification factor. The amplifier resonator may be connected as a dipole or as a quadrupole. In scheme one the amplified and the source wave are transmitted along the same line. A ferric circulator (Figure 3) is employed for the separation of these two waves. The output signal from antenna 1 is applied through the ferric circulator 2 and line 5 to the amplifier resonator 3, into which oscillations from the bias oscillator 4 are applied simultaneously. The amplified resonator wave is sent along the same line 5 to receiver 6. In order to overcome self oscillations, when the receiver is poorly matched to the antenna, the power which is reflected from the receiver is absorbed by the matched load in load 7. The ferric circulator, also performs another important function by directing the noise, radiated by the receiver input, to the absorbing load; and thus prevents penetration of noise into the amplifier. In case of absence of such a non-mutual element, the noise characteristics of the amplifier would sharply decrease in quality.

If the resonator self losses are neglected (i.e., assuming $d_0 \ll d_m$), the equivalent network in Figure 2 is utilized, it is not difficult to obtain the following relations for the amplifier amplitude amplification factor in the case of resonance.

$$G = \left(\frac{d_{in} + d_m}{d_{in} - d_m}\right)^2, \tag{4}$$

here d_{in} is the decrement introduced by the resonator lines. With strong regeneration, when the regeneration parameter $\beta = \frac{d_m}{d_{in}}$ is near unity and $G \gg 1$, we obtain

$$G \approx \frac{4}{(1-\beta)^2}. \tag{5}$$

The bandpass of the amplifier Δf is determined by formula

$$\Delta f = (d_{in} - d_m) f_c. \tag{6}$$

From formulas (5) and (6) we obtain

$$\sqrt{G}\,\Delta f \approx 2 d_m f_c. \tag{7}$$

The effectiveness of the resonator amplifiers is commonly characterized by the product of the quantities $\sqrt{G}\,\Delta f$. In the amplifiers covered by literature [1], this product has a magnitude of an order of 50 Mc in the centimeter wavelength range; with a 20 db amplification this corresponds to ~5 Mc band. We note, that by connecting the resonator in a quadrupole scheme, the quantity of the product $\sqrt{G}\,\Delta f$ is cut in half, as compared to the described scheme. This is explained by the fact, that in this case, the radiation from the paramagnetic crystal, is not only consumed by the load but is also consumed in the output impedance of the signal source.

As has already been indicated, the quantum paramagnetic amplifier necessitates the use of liquid helium (temperature 4.2° K, and lower). Recently, the quantum amplifier effect was obtained with a 3 cm wavelength using the temperature of liquid nitrogen (77° K) [2]. With this, the value of the product $\sqrt{G}\,\Delta f$ was about 14 Mc.

A practical paramagnetic amplifier of the resonator type is accomplished in the following manner: the resonator together with the feedlines, which we constructed from stainless steel of white copper in order to reduce thermal conductivity, is placed in a specially constructed vessel — a cryostat — which contains liquid helium. The cryostat constitutes a Dewar vessel with liquid helium, which is placed, in order to minimize the helium evaporation, into a second vessel analogous to the first and filled with liquid

nitrogen. In recently developed amplifiers [1], metallic cryostats are employed, which constitute the connection of two metallic Dewar vessels in a single structure. In such cryostats the liquid helium may remain for days — even weeks — without additional filling. The lower end of the cryostat, where the resonator is located, is placed between the poles of an electromagnet or a permanent magnet.

Recently, constructions in which the magnet is located within the cryostat and is submerged in the liquid helium [3], (or nitrogen [2]), have appeared. Due to this, the gap of the magnet decreases and its weight sharply diminishes.

QUANTUM PARAMAGNETIC AMPLIFIER OF WAVEGUIDE TYPE (Traveling Wave Amplifier)

The resonator type amplifiers possess a number of disadvantages which are due to the regenerative character of amplification within them. The main disadvantage lies in the fact that the bandwidth is considerably narrower than the resonance bandwidth of the paramagnetic substance (the latter has a magnitude of an order of 100 Mc). Further, the amplification coefficient, for large degree of regeneration, is quite sensitive to small magnetic changes or to changes of the introduced decrement. By employing an amplification scheme with several resonators [4], connected between each other or separated by ferric circulators, the bandwidth and stability of amplification may be increased. However, in this case, a quantum waveguide type amplifier (a traveling wave amplifier) is the most effective.

In such an amplifier the paramagnetic substance is spread along the length of the waveguide through which the signal is transmitted. The signal increases along the path due to the radiation of the paramagnetic substance. However, calculations point out that with existing effectiveness of the paramagnetic substances a practically unattainable length of the waveguide amplifier is necessary.

In connection with the above, in the arrangements employed, waveguide delay systems, in which the wave is considerably delayed with group velocity, are employed. This permits the accomplishement of the same effect with a correspondingly smaller physical length of the waveguide.

The intensity ΔP_{irr} of paramagnetic substance radiation in the line section Δl of such a system, will be (from formula 2)

$$\Delta P_{\text{irr}} = 2\pi d_m f_c E \Delta l, \tag{8}$$

where E is the energy per unit length of the system.

The intensity of the wave propagating along the waveguide,

$$P = E v_g, \tag{9}$$

where v_g is the group velocity.

From (8) and (9) we find that the intensity amplification G along length l is equal to

$$G = e^{\frac{2\pi d_m f l}{v_g}}. \tag{10}$$

From which it is clear that by reducing the group velocity v_g the same amplification may be achieved with a smaller system length . Here the bandpass is determined by the dependence of quantity d_m upon frequency,

i.e., in the end calculation by the bandwidth Δf_β of the paramagnetic resonator. The expression for the bandpass of a traveling wave amplifier[3] may easily be obtained from formula (10):

$$\Delta f = \Delta f_\beta \sqrt{\frac{3}{G_{db} - 3}}, \tag{11}$$

where G_{db} is the coefficient of amplification in the center of the band and is expressed in db.

Here the quantity Δf is obtained of a greater order than in a resonator-type amplifier: several tens of Mc instead of several Mc. Also a greater amplification stability is obtained.

A crest type delay system, employed in the traveling wave paramagnetic amplifier [5], is illustrated in Figure 4a. A picture of the magnetic lines of force in such a system is shown in Figure 4b. The input and output of the given delay system are connected to coaxial cables.

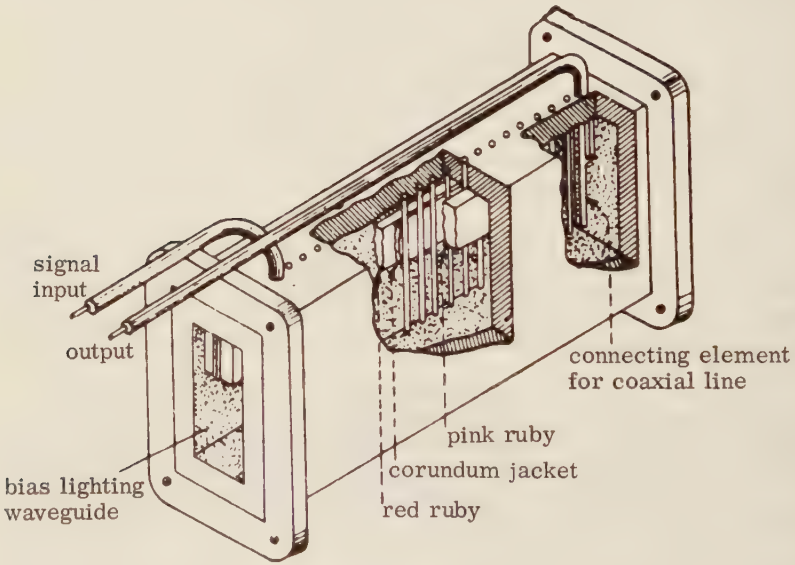

Figure 4a

The oscillations of the bias lighting frequency propagated along the waveguide, which surrounds the crest, are in the main wave form H_{10} of this waveguide, upon which the crest does not exert appreciable effect.

In order to prevent regeneration of the amplifier due to reflection from the system ends, the non-mutual properties of ferrites or of the

---

[3]It is assumed that the shape of the paramagnetic resonance curve has the shape of the resonance contour.

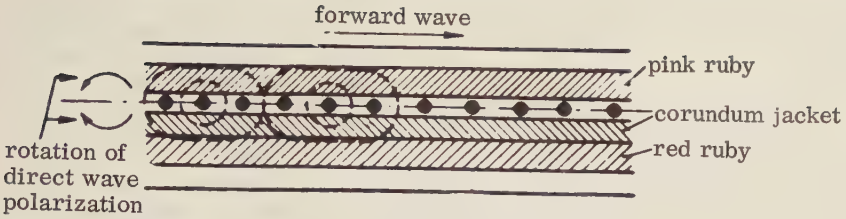

Figure 4b

paramagnetic substance itself are utilized. These properties become apparent with the varied action of such substances upon waves with opposite direction of rotation of angular polarization.

In the traveling wave amplifier shown, this is realized in the following manner: the paramagnetic ruby crystal, (in the form of a rectangular bar) designed for the amplification of a directly incident wave, is placed at one end of the crest (for example on top, as shown in Figure 4b). This crystal has a normal concentration of chrome ions ("pink ruby") and therefore with the given intensity of the oscillator bias lighting frequency the transition at the brightening frequency is saturated. A second paramagnetic crystal of analogous configuration, with a higher concentration of chrome ions ("red ruby'), is placed at the opposite side of the crest, where the wave, propagating in the forward direction has an opposite direction of rotation of polarization (see arrows in Figure 4b). As a consequences of the direction of polarization rotation, the mutual interaction of such a wave with the "red ruby" will be weak. Approximation to this may be understood by utilizing the classical model for a paramagnetic amplifier described in the first part of this work (Figure 4-1). An analogous effect is widely employed at ultra-high frequencies in ferrite units.

By the same token, the reflected wave intensity, having an opposite direction of rotation of polarization with respect to the incident wave, will slightly interact with the first ruby ("pink ruby") and strongly interact with the second ruby ("red ruby"). However, the latter will not increase the intensity of the reflected wave, but will absorb it. This is explained by the increased concentration of chrome ions (and in connection with this a small relaxation time). Consequently, the "red ruby" will not saturate with transition of bias lighting. In this ruby no change in the "population sign" of the signal transition will take place, which corresponds to absorption of the reflected wave. An analogous effect may be attained by substituting in place of the "red ruby" a special ferrite [6].

It is important to point out that since the non-mutual element is contained within the amplifier, no outside ferrite arrangements are necessary. This permits complete realization of an exceptionally low noise level which is inherent in quantum paramagnetic amplifiers (see below).

In the quantum traveling wave amplifier described in literature [5] an amplification of ~23 db is obtained with waves of ~5-6 cm and with a band of ~25 Mc (for noise see below).

NOISE IN QUANTUM AMPLIFIERS

The noise properties of low noise generating amplifiers is conveniently

characterized by the so-called noise temperature T_n. This quantity, by computation, is numerically equal to the absolute temperature of the equivalent antenna circuit, connection of which to the input of the amplifier would lead to a double increase of noise strength at its output as compared to the case of zero absolute temperature of the equivalent circuit.

The quantity T_n is connected with the commonly employed characteristics of the noise coefficient F, and relation $T_n = (F - 1) T_0$; where T_0 is the standard absolute temperature equal to 290° K.

Noise sources in quantum amplifiers are primarily the spontaneous radiations of the particles, found at the highest of the two energy levels, which form the quantum transition at the frequency of the signal; and, also, the temperature radiation of the amplifier elements which absorb the energy. We shall consider the noise in quantum waveguide type amplifiers.

The increment ΔP_n of the spectral noise density P_n, at the signal frequency f_c, for the element of length Δl of the amplifier is noted as

$$\Delta P_n = \alpha P_n \Delta l - \alpha_\beta P_n \Delta l + \alpha_\beta P_T \Delta l + B n_2 \Delta l. \tag{12}$$

Here the first term characterizes the noise amplification in the element Δl, and

$$\alpha = A(n_3 - n_2) \tag{13}$$

is the experimental index of amplification; n_3 and n_2 corresponds to the number of particles per unit length of the system, found at levels (3) and (2), and forming the quantum transition of the signal; A is a proportionality constant.

The second term in formula (12) corresponds to noise decrease due to temperature losses in the amplifier energy consuming elements (for example the walls of the waveguide); α_β is the equivalent index of damping. The third term determines the noise, due to temperature radiation of these elements, found at absolute temperature T (black body radiation); with this P is the spectral density of such radiation[4] and equal to $\frac{hf_c}{\exp\left(\frac{hf_c}{kT}\right) - 1}$, which with $hf_c \ll kT$ yields $P_T = kT$.

Finally, the last term in formula (12) yields the noise of spontaneous radiation; B is a proportionality constant.

The proportionality constants A and B are related by

$$B = hf_c A. \tag{14}$$

(This may be proved through formula (12) by considering the case of thermodynamic equilibrium for which the ration $\frac{n_3}{n_2}$ is determined by the Boltzmann distribution (3) I, and the quantity ΔP_n is equal to zero).

By integrating the relation (12) and noting that the quantity $\exp(\alpha - \alpha_\beta) l$ is the amplifier gain coefficient G, which we shall consider much greater than unity, the following formula may be obtained for the temperature noise T_n (assuming that $hf_c \ll kT$):

$$T_n = \frac{hf_c}{\kappa} \frac{n_3}{(n_3 - n_2)} \frac{\alpha}{\alpha - \alpha_\beta} + \frac{\alpha_\beta}{\alpha - \alpha_\beta} T. \tag{15}$$

---

[4]See [7]. In the subsequent equations k is the Boltzmann constant.

In this formula the first term is related to the spontaneous radiation (spontaneous noise), and the second term to the temperature radiation of the energy absorbing elements of the amplifier found at absolute temperature T.

By analogy with the case of thermal equilibrium,

$$n_3/n_2 = e^{-\frac{hf_c}{\kappa T_{eff}}} \tag{16}$$

Since in the operating amplifier $n_3 > n_2$, the quantity T_{eff}, called the effective temperature of signal transition, is negative. Assuming $hf_c < k|T_{eff}|$, formula (15) may be written in the following manner:

$$T_n = |T_{eff}| \frac{\alpha}{\alpha - \alpha_\beta} + \frac{\alpha_\beta}{\alpha - \alpha_\beta} T. \tag{17}$$

By assuming $\alpha_\beta \ll \alpha$, we may consider that the amplifier generates noise in such a manner as if the equivalent negative resistance introduced by the active particle system was found at temperature T_{eff}.

We shall evaluate this quantity for a tri-level quantum amplifier. By utilizing Equation (7) I, we may obtain

$$|T_{eff}| \approx T \frac{2f_c}{f_n - 2f_c}, \tag{18}$$

(the formula is written by assuming equal relaxation probabilities between all transitions).

The quantum amplifier operates at the temperature of liquid helium, i.e., the quantity T is composed of an integral number of Kelvin degrees. Therefore, in the radio frequency range the thermal noise T_n of the amplifier itself does not exceed several units of Kelvin temperature, i.e., is negligibly small.

In an analogous manner we may obtain the formula for the thermal noise of a resonator amplifier. This may be more simple done if a temperature T_{eff} is assigned to r_m in scheme of Figure 2. For the above given condition of this scheme it is not difficult to obtain a formula analogous to (17); the self decrement d_0 and the magnetic decrement d_m should be substituted in place of quantities α_β and α correspondingly.[5]

If the coefficient of losses of the elements before the amplifier is L (the ratio of the input to the output intensities), then the complete noise temperature of the amplifier together with its input rank may be calculated from the formula

$$T'_n = (L-1)T_0 + LT_n. \tag{19}$$

With L = 1.07 (losses ~0.3 db) the additional noise temperature due to input losses will constitute ~20° K, which is considerably greater than the inherent noise temperature of the amplifier T_n.

In the described traveling wave quantum amplifier [5] a noise temperature of ~20° K was obtained; the main part of this noise is due to losses in the input line of the amplifier and, theoretically, be further reduced.

The total noise temperature T'_Σ of a receiver with a quantum amplifier at the input is determined by formula

---

[5]For this derivation it is assumed that $G \gg 1$.

$$T'_{\Sigma} = (L_{\beta} - 1)\,T_0 + L_{\beta}\left(T_{\text{п}} + \frac{T_{\text{пг}}}{G}\right), \qquad (20)$$

where $T_{пг}$ is the noise temperature of the receiver, connected after the quantum amplifier; G is the gain coefficient (strength) of the quantum amplifier; L_β is the coefficient of losses in the waveguide, inherent to the quantum amplifier.

For complete characteristics of the entire receiver system including the antenna, to the quantity T'_Σ (given by equation 20) it is necessary to add the quantity (temperature) which characterizes the noise received by the antenna from the outside. These may include noise due to cosmic sources, noise due to atmospheric conditions, and finally noise radiated by the earth and "cached" by the side lobes of the antenna. It is customary to characterize the antenna noise by the effective noise temperature of the antenna T_A. In Figure 5, is given magnitude dependence of T_A, (which takes into account the first two of the mentioned noise sources) upon frequency for different angles of elevation φ of the antenna beam above the horizon.

With a wavelength longer than 30 cm the main source of antenna noise is cosmic radiation (Figure 5). With wavelengths shorter than 3 cm, the atmospheric absorption begin to play an important part. Therefore, the region between these two wavelengths is known as the "cosmic window".

From the above, it follows that for complete realization of the possibilities of noise reduction it is necessary to subdue noises due to the antenna and the antenna route.

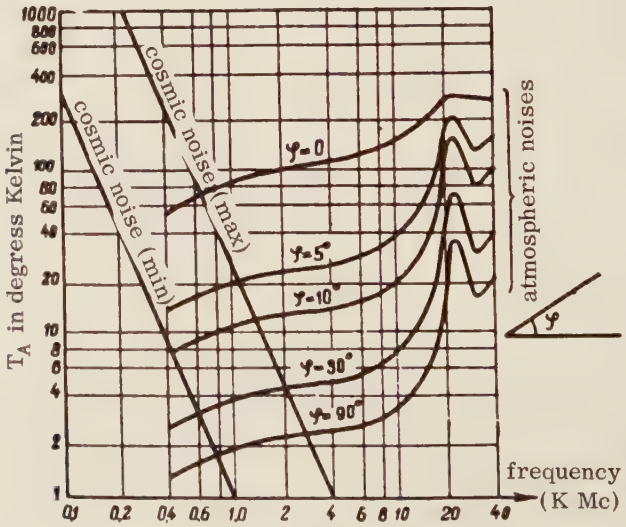

Figure 5

In the receiver system [6], in which a traveling wave quantum amplifier with a wavelength ~5-6 cm and a specially constructed antenna (with

exceptionally small lobes of — 70 db in the earth direction) were employed, a complete noise temperature of the entire receiver system (antenna plus receiver) was obtained. This was 18° to 20° K with the zenith direction of the antenna, and less than 30° K with a 12° angle of elevation. With this, the route losses which included the rotating stage yielded 3.5° K noise and the noise of the quantum amplifier did not exceed 10° K. With the given amplification factor of the quantum amplifier greater than 35 db, we may disregard the temperature noise in the receiver following it.

The gain in sensitivity from the use of quantum amplifier is approximately 100 times. In the future it is expected to reduce the total noise temperature of the system to 10° K, for the zenith direction of the antenna.

CONCLUSION

Quantum paramagnetic amplifiers permit a sharp increase in the sensitivity of the receiver systems andachieve practical limits which are restricted only by the noise external to the receiver.

In recent times the quantum paramagnetic amplifiers have found application in practical systems — in radio telescopes [1], in long range communication systems [6] and others. Hand in hand with this, work is continued toward further development of these amplifiers in connection with portable systems [10]. Progress in this direction will yield a substantial solution in the field of quantum paramagnetic amplifier application.

It should be pointed out that the shortening of the wavelength, which constitutes greater difficulties in other types of amplifiers (in electrical setups and parametric semiconductor amplifiers) is not difficult in maser amplifiers. In recent time quantum amplifiers have appeared which operate in the millimeter wavelength, and under development are amplifiers in the sub-millimeter range, as well as in the infrared and visual range [3].

Presently, intensive development is devoted to low noise generating amplifiers of ultra high frequencies. Without doubt, in this new field of radiophysics, and mainly in the field of maser amplifiers there will appear new important results.

Original article submitted June 30, 1960

LITERATURE

1. Giordmaine, Alsop, Mayer, Townes, "A maser amplifier for Radio Astronomy at X-Band." Proc. IRE, v. 47, No. 6, 1959.
2. Maiman, "Maser behavior: temperature and concentration effect." Journal Appl. Physics, v. 31, No. 1, 1960.
3. Maiman. Brown, "Ruby maser amplifier extends range of electronic systems tenfold." Electronics and Communications, V. 1960.
4. V.B. Shteinshleiger, "Paramagnetic (quantum) amplifier with two resonators." Radiotekhnika i Elektronika, V. 4, No. 11, 1959.
5. De Grasse, Schulz-Du Bois, Scovil, "The three level solid state traveling Wave maser." BSTJ, V. 38, No. 2, 1959.
6. De Grasse, Hogg, Ohm, Scovil, "Ultra-low-noise antenna and receiver combination for satellite or space communication." Proc. Nat. Electronic Conference, V. XV, 1959.
7. Van der Zil, Fluctuation Noise in Radio Engineering and Physics, Gosenergoizdat, 1958.

8. Radarscope (New Maser). Electronic Industries, II, 1960.
9. Schawlow, Towners, "Infrared and optical masers." Phys. Review V. 112, No. 6, 1958.
10. Senf., "Masers for system applications." IRE Wescon Conv. Rec. part 1, Aug., 1960.

HIGH-FREQUENCY TELEPHONE COMMUNICATIONS WITH SEMICONDUCTOR TRIODES

K.P. Egorov and I.V. Sukhodoev

Presented are the fundamental principals for building a three-channel system of high frequency telephoning of type K-3, which system is intended to tighten the intraregional communication lines. Individual semiconductor junctions of the apparatus are described, and a concise basis is given for the decisions undertaken.

At the present time, in low frequency broadcasting and communication networks, a single paired cable of type NPBNM-1, 2, composed of a pair of copper conductors with a diameter of 1.2 mm with a polychloric insulator, is commonly employed. The distance of communication on such a cable with tuned telephoning without amplifiers, does not exceed 13-16 km.

Connections utilizing audio frequency with cable NPBNM-1, 2 do not give satisfactory solutions to problems of intraregional connection because of the inadequate number of channels as well, as their low quality.

In the intraregional communication networks, connections of 50 km and, in a number of cases up to 100 km in length, can be found. In one direction it is desirable to have at least two channels suitable to be used as an end section-link of complicated between-city connections, insuring the transmission of speech signal in the frequency band of 300 to 3,400 cps.

The solution, insuring the development of intraregional connections via cables of simple construction, is the use of high-frequency telephone communication methods.

Toward this goal, development of apparatus for tri-channel system of the low frequency cable communication of the type K-3, has been realized.

System K-3 is actually composed of two independent systems: the single-channel system (channel 1/3) and the two channel group system (channels 2/3 and 3/3). Both systems can work simultaneously on the same NPBNM-1, 2 cable, and their spacing of transmission is established at the same points. The maximum length of the repeater section in this case is 16.5 km, which corresponds to a line attenuation b = 4.5 nepers at the highest frequency of the linear range.

The longest span of connection on any of three channels during re-reception at low frequency across 50 km, may reach 100 km.

Channels 2/3 and 3/3, which constitute the fundamental two-channel system, are designed for a band of 300-3400 cps, characteristics of channel 1/3 permit the transmission of the spectrum of frequencies 300-3700 cps.

The basis of selection for the transmission range and network construction of the two channel system is the decision to use in this system receiver-transmitters and the signal channel of the newly developed 30-channel apparatus KPP [1], assigned for the condensation of junction lines between ATC and suburban network lines.

Modulation in a receiver-transmitter is realized by the phase-difference method. Phase relations in the audiofrequency networks and the feeding networks are determined by calculating the transmission of the upper side-bands into the circuit line and the attenuation of the lower bands (not smaller than 3 nepers [2]).

In the apparatus KPP for a one-side action channel, a frequency band of 8 Kc is formed; in system K-3, with a sharp slope rise in line attenuation with increase in frequency, a band half that size is designated for one channel. Such a switch in general is impossible; however it is permissible in a particular case by the use of a group from two adjacent channels. With this, one of the two receiver-transmitters retains transmission of the upper sideband, while in the other a switch to transmission on a lower sideband is performed. In order to realize such a switch, it is sufficient to switch the circuits in one of the network branches of the phase-difference modulation.

A group of two channels permits the construction of a two-channel system with intervals of 4 Kc per channel.

For cable operation it is necessary to translate this group from comparatively high frequency range (328.3 - 335.7 Kc) to a lower frequency range (8.3 - 26.3 Kc), suitable for transmission via a cable of the type NPBNM.

Thus, it is necessary to consider the following requirements:

a) transmission must be performed on a two-way transmission line electrically by a four-way conduction network.

b) the interval between channels of one group corresponding to the transmission direction must be as narrow as possible with the aim of filter-simplification of intermediate stations.

c) it is desirable to have comparatively narrow ranges of two-channel groups for each transmission direction, which simplifies the correction of frequency distortions and facilitates countermeasures against nonlinear distortions in common amplifiers.

d) the upper limit of the linear range of transmission must be as low as possible since the attenuation in the cable rises sharply with frequency.

e) in the lower part of the range it is imperative to arrange the operating regions of a one-channel system.

The above given requirements are contradictory. For example, for the narrowing of the relative band of the two-channel groups and for the creation of easier working conditions for the first channel apparatus, the spectrum of a two-channel system must be moved up higher. However from the point of view of amplifier simplification and increasing the band of the amplification regions, this spectrum must be moved down. The final distribution of transmission range, which represents a compromise solution in which all the above mentioned points were thoroughly weighed, is shown in Figure 1.

For each direction of transmission, a separate group of two channels is applied, created by the frequency shaping of the high-frequency group 328.3 - 335.7 Kc, into the linear range of the transmission.

The one-channel system is actually a perfected channel of audio

telephoning. In one direction, the transmission is carried by audiofrequencies 0.3 - 2.7 Kc; in the other, transmission is realized in the 3.7 - 6.0 Kc band with frequency shaping of the audio spectum. The directions of transmission are divided with the aid of filters. In this manner, the system of transmission becomes equivalent to a four-way conduction circuit.

The width of the telephone channel band in a one-channel system is somewhat narrower than ina two-channel system. This is done for the following reasons:

a) the narrowing of the band in a one-channel system permits lowering of the upper limit of the linear range of the system by lowering the upper frequency limit of the first channel,

b) the use of a receiver-transmitter unit, or similar, in this case is not in order, since one of the channels is working in the audio range.

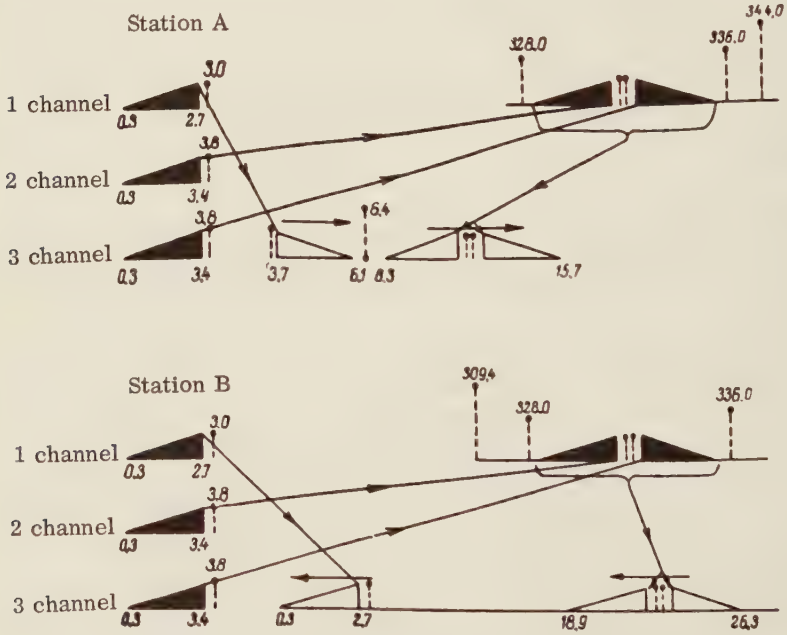

Figure 1

A singular characteristic of the two channel network portion of the end station, is the presence of the second stage of frequency shaping and group amplifiers for reception and transmission.

Group frequency shaping, realized with the aid of a simple network, introduces insignificant complications in the end apparatus, which is justified by saving on common units in the reception and transmission routes of the two-channel group, as well as by the use of the unified receiver-transmitter. Savings on the main units for one end station with individual and group shaping, is presented in Table 1.

It is also advisable to note that the mixed (individual - group) principal

of construction gives the K-3 system a flexibility in relation to the possibility of increasing the number of channels from one to three and a separate use of the first channel 1/3 from the other two 2/3 and 3/3.

To transmit excitation, dialing, and signal currents of the ATC control, a narrow band signal channel is constructed next to the upper edge of each of the audio channels. The carrier frequency of these channels, corresponding to their tuning center, is selected equal to 3,800 cps for a two-channel system and 3,000 cps for a one-channel system.

The extension of frequency transmission of the control signals into the range, in which the appearance of audio components is not probable, permits a considerable simplification of the receiver networks of control signals.

The apparatus of system K-3 is accomplished without the use of electron tubes. Semiconductor units (diodes and triodes) are used which enables a wide application of miniaturization.

Table 1

Junction	Individual system	Group system
Carrier-frequency generator	4 comp**	4 comp*
Receiving and sending amplifiers	4 comp	2 comp
Directional filters	4 comp****	1 assem***
Line equalizers	2 comp	1 comp
Filter equalizers	2 comp	1 comp
Frequency converters	4 comp**	4 comp*

Notes: *-high frequency, **-low frequency, ***-type DK, ****-bandpass.

Miniaturization, in particular the use of miniature inductance coils in tuned and linear filters, has effected the choice of value of the output level of transmission. It is that level which is permissible from the point of view of mutual nonlinear effects between channels. This is explained by the inconsistency of existing magnetic materials used in miniature construction, which at high levels, introduces nonlinear effects.

The level of one telephone cable at the output of end and interval stations with a load of 600 ohms in system K-3 is taken as equal to 0.4 nepers. With this an isolation between any two channels is achieved, corresponding to crosstalk attenuation $B_{per} \geqslant 6.7$ nepers.

Transmission of signals with an output level of 0.4 neper also insures an adequate noise protectiveness of channels. At the output of a telephone cable, at the point of a measured level of 0.8 neper, the circuit noise meter voltage of the set noise (during operation with two interval stations) does not exceed 1.0 mv.

The minimal level of reception at the station input constitutes 4.9 nepers at the highest linear frequency of range under the worst operating condition of the system from the point of view of protection against interference (cable temperatures plus 20° C). Attenuation of the cable installed 0.8 m deep from the surface of the ground, falls with the decrease in

temperature. Preliminary analysis has shown that these changes for cable type NPBNM-1, 2, which is installed in dry, sandy ground, constitute at the upper limit of the operating frequency range approximately $2 \cdot 10^{-3}$ neper/km per 1° C.

At the end and interval stations, the possibility is foreseen correcting for attentuation changes due to temperature of the cable, from the point of view of maintaining original channel attenuation within ±0.2 nepers from the average value of 0.8 nepers at a frequency of 800 cps. The aim of this correction is to prevent amplifier overloading.

Amplitude frequency distortions of the cable are corrected by linear rectifiers at the input of receiving amplifiers of end and interval stations. Channels 2/3 and 3/3 have joint group rectifiers in both directions, which are designed for a frequency range of 8.3 to 26.3 Kc.

The most complicated and important parts of the apparatus are the oscillator and amplifier units, which have considerable importance within the apparatus, and in many cases determine the quality of channel indicators.

According to their designation and performed function, oscillator units can be divided into main and supporting ones. The first of these is used in the system to feed carrying currents to the individual and group frequency converter.

In channels 2/3 and 3/3, to create a two-channel group in the 328.3 - 335.7 Kc spectrum, individual oscillators employing 328.0 and 336.0 Kc are used. The two-channel group, with the aid of those employing 309.4 and 344.0 Kc is frequency converted into the linear range of the direct 8.3 - 15.7 Kc or the reverse 18.9 - 26.3 Kc direction of transmission. In channel 1/3, which has one stage of frequency shaping, an oscillator with 6.4 Kc carrying frequency is used.

The supporting oscillators of 3.8 Kc and 3.0 Kc serve to transmit directive signals on the signal channel carried beyond the audio spectrum.

To oscillators of carrying frequencies, comparatively high requirements are made in respect to frequency stability of generated oscillations. The stability of carrying frequencies of an order of $5 \cdot 10^{-5}$ in the temperature range of +15° C to +40° C is achieved in the oscillators by way of quartz crystal stabilization.

The principal network of a generator carrier oscillations is presented in Figure 2.

The oscillator consists of the master and terminal stages. The division of functions, oscillation generation and amplification insures the least dependence of the operation range of the first stage, on the load oscillation at the output, and has a favorable effect on the frequency stability of generated oscillations.

The oscillator is constructed with semiconductor triodes of type D-14, utilizing a common emitter network. Negative bias on the base of triodes is supplied from voltage dividers R_1, R_2 and R_7, R_8. To achieve temperature stabilization of oscillator parameters, the operating points of triodes are stabilized by R_1, R_2, R_4, and R_7, R_8, R_{10}.

According to the theory of temperature stabilization of semiconductor networks, the stability coefficient of the amplifcation stage is determined by the expression

$$S = \frac{\alpha Ik}{\alpha Ik_0} = 1 + \frac{\alpha}{R_1/R_2 + R_1/R_3 + 1 - \alpha}, \qquad (1)$$

where R_1, R_2, and R_3 are the network impedances for temperature stabilization.

Impedances R_1 and R_2 produce the greatest effect, the choice of which

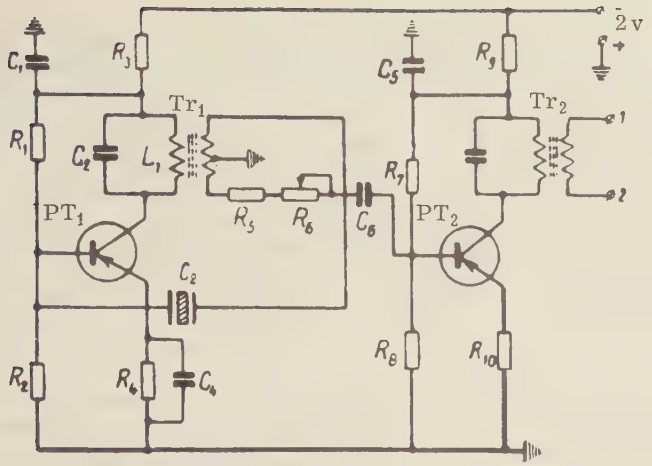

Figure 2

to a great extent affects the characteristics of the amplification stage. In the network of the carrying frequency oscillator, the temperature stabilization coefficient is selected equal to $S_t = 2.8$, which completely insures sufficient stability of oscillator characteristics. As an additional measure of oscillator stability, the local negative feedback network is put to use through resistances R_4 and R_{10} in the emitter triode networks.

Tuned circuits L_1C_2, and L_2C_7 are the collector loads, and circuit L_1C_2 is tuned to a frequency which is close to the frequency of generated oscillations, and the tuning of the second circuit coincides with the generated frequency. The inductive coil in the circuit of the master stage has an excitation winding through the aid of which, a positive feedback is realized. Thus a quartz crystal resonator (QR), which mainly determines the frequency of generated oscillations, is connected to the positive feedback network. The regulation of the output oscillator level is realized by the potentiometer R_6.

Assisting oscillators differ schematically from the others by their lack of a quartz crystal oscillator in the positive feedback network, and the parameters of tuned circuits L_1C_2 and L_2C_7 which are connected to the triode collectors.

One of the most important and critical units of apparatus K-3 is the group linear amplifier, which is installed at the remote amplifier stations. Its chief requirements are high linearity and low noise level. During the development of the amplifier, special attention was given to the fulfillment of these conditions. The principal network of the group amplifier is presented in Figure 3.

The amplifier was constructed using type P-13 B triodes for the first stage and P-14 triodes for subsequent stages. These semiconductor triodes are hooked into a circuit with a common emitter. Among the many advantages of a circuit with a common emitter are the broad possibility of using the good features of local negative feedback, and the setting up of the simplest form of an intercascade circuit. This is explained by the fact that the input resistance of a stage with a common emitter is completely adequate

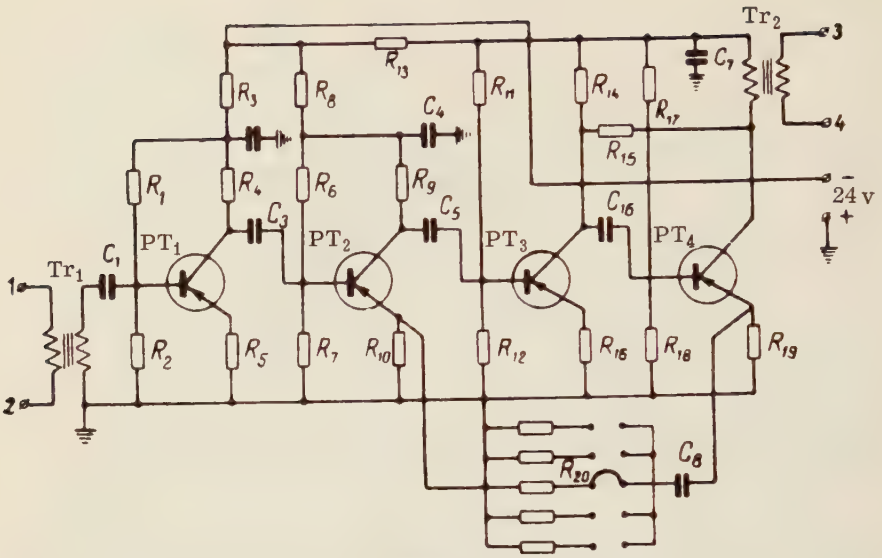

Figure 3

for obtaining amplification of 1.5 to 2 nepers without intercascade matching transformers. As in the oscillator circuits, the semiconductor triodes in the amplifier are temperature — stabilized. Furthermore, local negative feedback is available in each of the stages through resistances in the emitter circuits of the triodes. The operating regime of the first stage is built around the low-noise triode P-13 B, selected after calculation of the least noise value. Analysis of the semiconductor triode, using a linear self contained quadrupole system shows that one method of bettering the signal-to-noise ratio is to match source noise with that of the triode. Noise matching of a circuit with a common emitter utilizes the real component of the internal resistance of the signal source:

$$R_{n\,1\,opt} = \left(\frac{|\bar{e}_{n11}|^2}{|\bar{e}_{n22}|^2} \; |z_e - az_c|^2 + |z_0 + z_e|^2 + |X_1|^2 \right)^{\frac{1}{2}}, \qquad (2)$$

thus, the optimal value of the excess noise coefficient is

$$K_{n\,1\,opt} = \frac{1}{2cT\Delta f} |\bar{e}_{n22}|^2 \left| \frac{1}{z_e - az_c} \right|^2 \left(\frac{|\bar{e}_{n11}|^2}{|\bar{e}_{n22}|^2} |z_e - az_c|^2 + \right.$$

$$\left. + |z_0 + z|^2 + |X_1|^2 \right)^{\frac{1}{2}}, \qquad (3)$$

Equations (2) and (3) are simplified and do not take into account the correlation relationship between internal sources of noise in the semiconductor triode. Calculation shows that the optimal value of the real component of internal resistance of the signal source usually lies in the region $500 \leqslant R_{n\,1\,opt} \leqslant 1000$ ohms; thus, the excess noise coefficient can be of the same order as that in electron tubes.

The best results were obtained when, in conjunction with noise matching and the use of low-noise triodes, an optimal DC operating regime was established. Investigations preceding development work established that the

optimal operating range for p-n-p junction triodes is a collector bias voltage not exceeding 1.0 v and an emitter bias current within the limits 0.2 to 1.0 ma.

Thanks to the application of the indicated measures for lowering the inherent noise of the triodes, a sufficient low noise value was achieved for the linear amplifier. The set noise of the amplifier in the band of one telephone channel, calculated after allowance for input noise data, did not exceed — 14.5 nepers. The last stage of the amplifier works in a regime stipulated by the requirement of linearity for the amplifier. The attenuation of nonlinearity in the second and third harmonics constitutes, respectively $b_{h2} \geq 7.5$ nepers and $b_{h3} \geq 8.5$ nepers for zero level of the signal at the amplifier output. The last three stages of the amplifier have a total

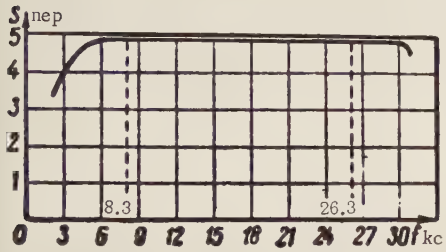

Figure 4

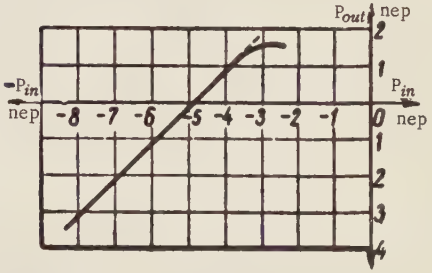

Figure 5

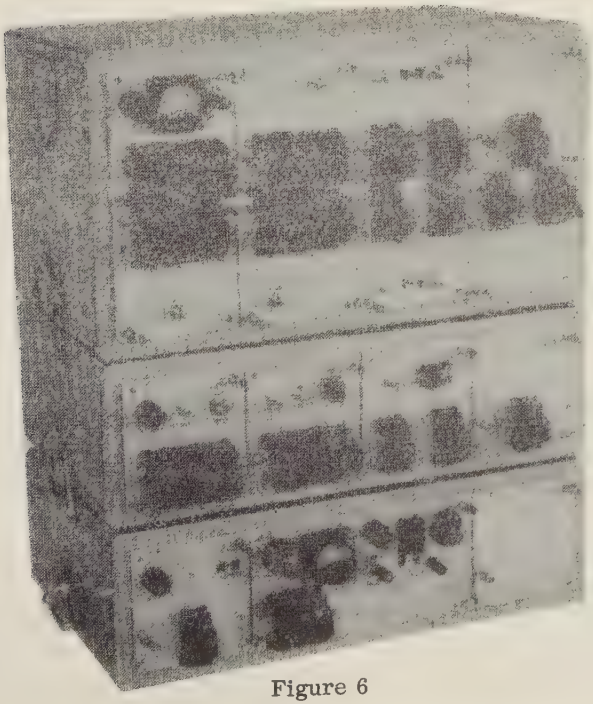

Figure 6

negative feedback which is passed on from the second — stage emitter to the next by resistance R_{20}. By changing the value of this resistance, stepwise control of amplification within the limits of 10.3 nepers to an average value of 5.0 nepers is produced. The frequency and amplitude characteristics of the amplifier are presented in Figures 4 and 5.

The apparatus of system K-3, a general view of which is shown in Figure 6, is constructed with due consideration for the conditions under which it will be used in local communication networks. Thus, the necessity of stipulating simplicity of replacing individual blocks and units, the accessibility of available controls, and the possibility of setting up intermediate stations in unheated locations and underground are all considered. The over-all size of the terminal station is 370 x 470 x 290.

Because of the use of semiconductor triodes, the apparatus of a three-channel system is highly economical in power consumption. The terminal stations require batteries with a load of 24 v and, on the average, 120 ma, which is less than one watt of power per channel. The intermediate stations are remotely supplied from a 60 v DC source according to a wire-to-wire system. The principle involved in this system is that each terminal station feeds one intermediate. The average consumption for all three channels of an intermediate station is 45 ma.

LITERATURE

1. M.U. Polyak, K.P. Egorov, L.T. Kim and Yu. G. Lopushnyan, "Multichannel System KRR 30/60 for Telephone Communication over Short Distances — A Lecture on Communication Technique" Svyaz'-izdat, 1960.
2. K.P. Egorov and M.U. Polyak, "Principles of Construction of Multichannel Communication Apparatus of Simplest Design for Cable and Radio Relay Lines," Elektrosvyaz', No. 4, 1957.

SELECTION OF SEMICONDUCTOR AMPLIFIER CIRCUITS FOR MULTIPLEX BALANCED CABLES

Yu. D. Farber

A circuit consisting of two amplifying elements and a line equalizer is considered and the operating conditions of an amplifier built around such a circuit and used as a high frequency line repeater for multichannel telephony is investigated.

In tube amplifiers for multiplex balanced cables, the desired slope of the frequency characteristic of amplification is obtained by using a frequency

dependent network connected, at least partly, into the OOS circuit (Figure 1a). In semiconductor amplifiers this kind of hookup creates difficulties in obtaining the required characteristic. Therefore, a circuit (Figure 1b) is used which contains two amplifying elements S_1 and S_2, not dependent on frequency, with a line equalizer of attenuation b_{le} connected between them. On replacement of amplifier circuit 1a with circuit 1b the conditions of signal transmission (especially noise-reducing features) are changed. Correspondingly, the relationships used for selection of the basic parameters of the amplifier and calculation of the channel's performance quality should be expected to change. To confirm the aforesaid, we compare amplifiers based on both circuits. We will consider amplifiers to be equivalent for this purpose if, for identical signal values at the input and output of the high frequency channel, the set and nonlinear noise powers are equal. Designating the levels at points 1, 2, 3, 4 (Figure 1) by the letter p with a corresponding subscript, we note that the quantities p_1 and, p_2 in both circuits are correspondingly equal. In order that for identical requirements in the set noise levels of the amplifiers we may obtain practically equivalent minimization of noise interference, it is necessary that

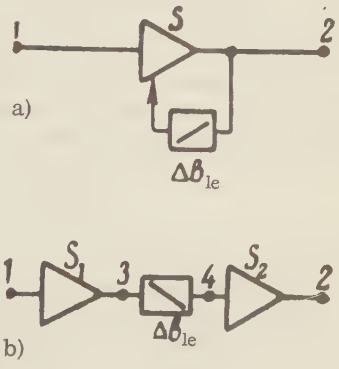

Figure 1

$$p_4 > p_1.$$

In order to obtain practically equivalent reduction of nonlinear noise, given equal requirements of linearity in the amplifiers, it is necessary that

$$p_2 > p_3.$$

Further, since, (Figure 1b) $p_3 = p_4 + b_{le}(f)$, then, total amplification must satisfy the condition

$$S = S_1 + S_2 - b_{le}(f) = p_2 - p_1 > p_3 - p_1 = p_4 + b_{le}(f) - p_1 > b_{le}(f). \quad (1)$$

However, an amplifier must compensate for loss in the part of the cable preceding it. This requires that

$$S_f = \beta_f l \text{ and } b_{le}(f) \geqslant (\beta_u - \beta_f) l. \quad (2)$$

where β_u and β_f are losses in the cable per kilometer at, respectively the upper frequency and an arbitrary intermediate frequency within the transmission band, and l is the length (in km) of the preceding part of the cable.

From (2) and (1) we obtain the condition $S_f = \beta_f l > (\beta_u - \beta_f) l$

$$\text{or } 2\beta_f - \beta_u > 0, \quad (3)$$

which must be met for any frequency in the band, including the lowest. We may take the following values (in round numbers) for the linear spectrum of existing balanced — cable systems: for the lower frequency $\beta_l = 0.09 \frac{\text{neper}}{\text{km}}$ and for the upper frequency of the K-12, K-24 and K-60

systems $\beta_u = 0.15$, 0.19 and 0.29 $\frac{\text{neper}}{\text{km}}$, respectively.

Thus, condition (3) is not fulfilled in the K-24 and K-60 systems and therefore, the circuit in Figure 1b is not equivalent to that in Figure 1a. To use circuit 1b it is necessary either to raise the requirements for the amplifiers (as far as the level of set noise and attenuation of nonlinearities) or to shorten the length of the amplification section. Thus, it is important to determine the parameters of the amplifier for which the given complications will be minimal. In particular, since the required amplification may be obtained using several different values of S_1, it is necessary to find the most suitable of these values. Furthermore, since reduction of noise in signals transmitted along a particular channel depends on predistortion of levels at the output of the terminal station, the magnitude of predistortion most expedient for a given multiplex system must be determined.

If, as is assumed at the present time, the measured levels at the output of the station vary according to a straight — line law, and are, respectively, p_{2u} and p_{2l}, for the upper and lower channels of the system, such that $p_{2u} - p_{2l} = \Delta p_2$ (line 2, Figure 2), then the levels at the amplifier input are

$$\left.\begin{aligned} p_{1l} &= p_{2l} - \beta_l l;\ p_{1u} = p_{2u} - \beta_u l; \\ p_{1l} - p_{1u} &= p_{2l} - \beta_l l - p_{2u} + \beta_u l = \Delta b_{1e} - \Delta p_2, \end{aligned}\right\} \quad (4),$$

where $\Delta b_{1e} = (\beta_u - \beta_l)$ is the loss difference of the line equalizer for the upper and lower frequencies of the transmission band.

The frequency characteristic of the level at point 1 is indicated by line 1 in Figure 2. Lines 3 and 4 of this figure (showing characteristics at corresponding points) were obtained by drawing a line parallel to line 1 upward to the value S_1 and another parallel to line 2 downward to S_2. Let us explain that for construction of Figure 2, the loss characteristics of the cable and the equalizer were assumed to be straight lines, and the losses in the linear equalizer for the higher transmission frequencies were assumed to be equal to zero. As is well known, these assumptions correspond to reality with an accuracy sufficient for practical considerations. The conclusion obtained earlier that condition (3) is not fulfilled is accounted for by the fact that in Figure 2, $\beta_l l < \Delta b_{1e}$, and lines 2 and 3 (and, also, lines 1 and 4) intersect.

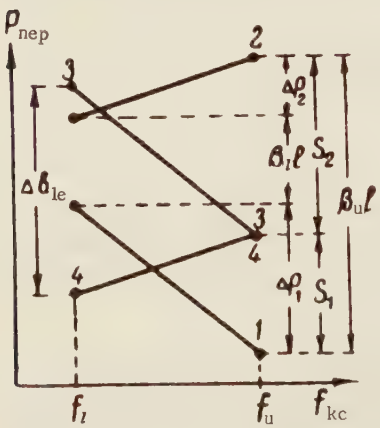

Figure 2

If the set noise level at the input of an amplifier, measured in the frequency band of one channel, has a constant value p_n in all channels of the system, then the set noise reduction introduced into any channel by an amplifier of the circuit in Figure 1b will be

$$\begin{aligned} \delta &= p_{2f} - 1/2 \ln [e^{2(p_n + \beta_f l)} + e^{2(p_n + S_1)}] = \\ &= p_{2f} - (p_n + \beta_f l) - 1/2 \ln [1 + e^{2(S_1 - \beta_f l)}] = \\ &= p_{1f} - \{p_n + 1/2 \ln [1 + e^{2[b_{1e}(f) - S_1]}]\} = p_{1f} - p_n. \end{aligned} \quad (5)$$

From (5) it follows that the method recommended earlier for determining the permissible length of the amplifying section [1] can be expanded to include the considered amplifier, under condition that the set noise level measured at the input in the frequency band of one channel be replaced by the the equivalent expression

$$p_n' = p_n + 1/2 \ln \{1 + e^{2[b_{1e}(f) - S_1]}\}.$$

Expression (5) can be rewritten in the following form, for the upper and lower channels of the system:

$$\begin{aligned} \delta_u &= p_{1u} - p_n - 1/2 \ln (1 + e^{-2S_1}); \\ \delta_l &= p_{1l} - p_n - 1/2 \ln [1 + e^{2(\Delta b_{1e} - S_1)}] = \\ &= p_{1u} + (\Delta b_{1e} - \Delta p_2) - p_n - 1/2 \ln [1 + e^{2(\Delta b_{1e} - S_1)}]. \end{aligned} \tag{5'}$$

Since there is no physical basis for $\delta_l < \delta_u$ we may require that

$$\delta_l \geqslant \delta_u$$

or

$$\Delta b_{1e} - \Delta p_2 - 1/2 \ln [1 + e^{2(\Delta b_{1e} - S_1)}] \geqslant -1/2 \ln [1 + e^{-2S_1}],$$

whence,

$$S_1 \geqslant 1/2 \ln \frac{e^{2\Delta p_2} - 1}{1 - e^{2(\Delta p_2 - \Delta b_{1e})}}. \tag{6}$$

From (6) it is evident that for $\Delta p_2 \to 0$, $S_1 \to -\infty$, and for $\Delta p_2 \to \Delta b_{1e}$ $S_1 \to \infty$. Consequently, the condition $\delta_l \geqslant \delta_u$ is fulfilled only for values of Δp_2 lying within the limits $0 < \Delta p_2 < \Delta b_{1e}$. From the relationship

$$\frac{dS_1}{d\Delta p_2} = -1 + \frac{e^{2\Delta p_2}}{e^{2\Delta p_2} - 1} + \frac{e^{2(\Delta b_{1e} - \Delta p_2)}}{e^{2(\Delta b_{1e} - \Delta p_2)} - 1}$$

and the fact that for

$$0 < \Delta p_2 < \Delta b_{1e} \quad \frac{e^{2\Delta p_2}}{e^{2\Delta p_2} - 1} > 1 \text{ and } \frac{e^{2(\Delta b_{1e} - \Delta p_2)}}{e^{2(\Delta b_{1e} - \Delta p_2)} - 1} > 1, \quad \frac{dS_1}{d\Delta p_2} > 0$$

we are convinced that the value of S_1, should also monotonically increase with increase of Δp_2. But we see from (5) that when S_1 increases set noise is reduced. Therefore, it is expedient to increase Δp_2 and S_1 along with it, thus fulfilling condition (6). In this way, if there is an inequality sign in (6), set noise reduction in the upper and lower channels of the system is identical.

On further increase of S_1 noise reduction in the lower channels becomes larger than that in the upper.

However, on increasing S_1, the quantity p_3 and the specified value of undistorted output power in the first amplifying element are correspondingly increased. To require that the undistorted power of amplifier S_1 should exceed that of S_2 is inexpedient, since then there would be no excuse for a second amplifying element. This obviously limits the applicable values of p_3 and, consequently, those of S_1.

If the permissible value of the transmission level, without predistortion, at the output of a multichannel amplifier with band frequency x, lying within the limits 0 and 1, is p_{tr}, then the total power corresponding to this level will be $e^{2p_{tr}}$.

On introduction of predistortion with a difference between upper and

lower levels equal to Δp and variation of the levels according to the equation of a straight line $p = p_{min} + \Delta px$ (for $0 < x < 1$), the total power is $\int_0^1 e^{2(p_{min} + \Delta px)} dx$. Thus, in order that, on introduction of predistortion, the total power should remain unchanged, we require that

$$e^{2p_{tr}} = \int_0^1 e^{2p_{min}} e^{2\Delta px}\, dx = e^{2p_{min}} \frac{e^{2\Delta p} - 1}{2\Delta p},$$

whence

$$p_{tr} = p_{min} + \frac{1}{2} \ln \frac{e^{2\Delta p} - 1}{2\Delta p}. \qquad (7)$$

A graph of the function

$$(p_{min} - p_{tr}) = \varphi(\Delta p)$$
$$\text{and } (p_{min} + \Delta p - p_{tr}) = \psi(\Delta p)$$

for values of Δp having practical significance, is presented in Figure 3.

Explanations of formula (7) and Figure 3 are presented in Appendix 1.

For points 2 and 3, Figure 2, the difference in the upper and lower channels are Δp_2 and $\Delta p_1 = \Delta b_{1e} - \Delta p_2$. For these points, expression (7) may be rewritten in the form

$$p_{tr} = p_{2l} + \frac{1}{2} \ln \frac{e^{2\Delta p_2} - 1}{2\Delta p_2}\ ;\ p_{tr} = p_{3u} + \frac{1}{2} \ln \frac{e^{2(\Delta b_{1e} - \Delta p_2)} - 1}{2(\Delta b_{1e} - \Delta p_2)}, \qquad (7')$$

whence,

$$p_{2l} - p_{3u} = \frac{1}{2} \ln \frac{[e^{2(\Delta b_{1e} - \Delta p_2)} - 1]\,\Delta p_2}{[e^{2\Delta p_2} - 1]\,[\Delta b_{1e} - \Delta p_2]} = \frac{1}{2} \ln D, \qquad (8)$$

and, thus, (Figure 2),

$$S_1 = \beta_u l - \Delta p_2 - (p_{2l} - p_{3u}),$$

so that

$$\left.\begin{aligned} S_1 &\leqslant \beta_u l - \Delta p_2 - \frac{1}{2} \ln D \\ S_2 &= \beta_u l - S_1 \geqslant \Delta p_2 + \frac{1}{2} \ln D \end{aligned}\right\}. \qquad (9)$$

If there is an inequality sign in (9), then the utilization factors of S_1 and S_2 are identical and they are determined by the value of the output level p_{tr}. On decreasing the amplification of the first element by ΔS, to the value

$$S_1 = \beta_u l - \Delta p_2 - \frac{1}{2} \ln D - \Delta S_1$$

the level at the output of this amplifier is also reduced by the value ΔS_1.

The total power of the nonlinear products of second and third order, forming at the output of an amplifier in the frequency band of one channel, can be determined from the expression

$$W_{nl} = W_2 + W_{32} + W_{31} = 4 \frac{\Delta f}{\Delta F} y_2(\sigma, \Delta p)\, e^{-2b_2(0) + 4p_0 + 4p_{tr}} +$$
$$+ 24 \frac{\Delta f}{\Delta F} y_{32}(\sigma, \Delta p) e^{-2b_3(0) + 6p_0 + p_{tr}} .$$
$$+ 24 \frac{\Delta f}{\Delta F} y_{31}(\sigma, \Delta p)\, e^{-2b_3(0) + 6p_0 + 6p_{tr}} .$$

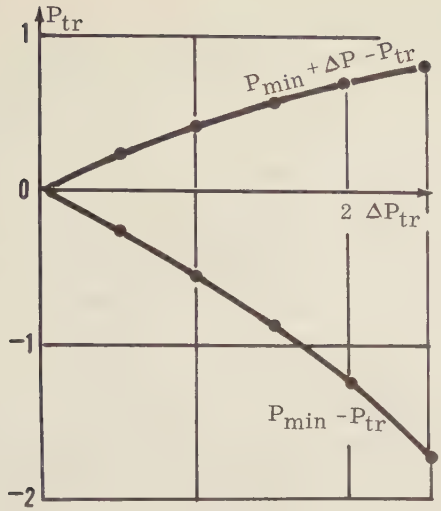

Figure 3

In this expression ΔF and Δf are the width of the frequency band used in the given system, and the bandwidth of the channel, respectively; $b_{2(0)}$ and $b_{3(0)}$ are the nonlinear losses due to second and third harmonics at an output level of the first harmonic equal to 0 neper; p_0 is the level of the multichannel system (in the given multiplex system) at the 0 neper level; $y_2(\sigma, \Delta p)$, $y_{32}(\sigma, \Delta p)$, $y_{31}(\sigma, \Delta p)$ are coefficients indicating what part of the total power of the nonlinear products of a particular order and kind passes through a given channel. The magnitude of these coefficients depends on an auxiliary variable σ $(0 < \sigma < 1)$, which characterizes the position of a given channel in the linear spectrum of the system, and on the spectral distribution of the signal power of the applied amplifiers.

On changing the output level of an individual channel according to a straight-line relationship, the signal power distribution monotonically follows the changing difference between the limiting frequencies Δp'. In calculations of the power of nonlinear products, this difference between the upper and lower channels of the system $\Delta p' = p_u - p$ is taken into consideration (as distinct from the value taken earlier $\Delta p = p_{max} - p_{min}$.

Values of p_0 for systems with different numbers of channels are given in [2]. In [3] graphs of the function $y_2 = \varphi(\sigma)$, $y_{32} = \phi(\sigma)$, $y_{31} = \Theta(\sigma)$ for various values of Δp' are presented.

In the considered circuit nonlinear products arise at both amplifiers. At the output of the second element, where the tranmission level p_{tr} can be determined from the quantities Δp_2 and p_2 with the aid of (7) and $\Delta p' = \Delta p_2$, $b_{2(0)} = b''_{2(0)}$, $b_3\ 0 = b''_{3(0)}$, the total power of the nonlinear products is

$$W''_{n1} = W''_2 + W''_{32} + W''_{31} = 4\frac{\Delta f}{\Delta F} y_2(\sigma, \Delta p_2)\, e^{-4b''_{2(0)} + 4p_0 + 4p_{tr}} + \\ + 24\frac{\Delta f}{\Delta F} y_{32}(\sigma, \Delta p_2) e^{-2b''_{3(0)} + 6p_0 + 6p_{tr}} + 24\frac{\Delta f}{\Delta F} y_{31}(\sigma, \Delta p_2)\, e^{-2b''_{3(0)} + 6p_0 + 6p_{tr}}. \quad (10')$$

For determination of the power of nonlinearities at the input of the

first amplifying element, we assume that, for amplification at S_1, the calculated transmission level is

$$p'_{tr} = p_{tr} - \Delta S_1 = p_{tr} - \left(\beta_0 l - \Delta p_2 - \frac{1}{2}\ln D - S_1\right) \qquad (11)$$

and for

$$b_{2(0)} = b'_{2(0)},\ b_{3(0)} = b'_{3(0)},\ \Delta p' = p_{3u} - p_{3l} = \Delta p_2 - \Delta b_{le}$$

the total power of the nonlinear products will be

$$W'_{nl} = W'_2 + W'_{32} + W'_{31} = 4\frac{\Delta f}{\Delta F} y_2(\sigma, \Delta p_2 - \Delta b_{le})\, e^{-2b'_{2(0)} + 4p_0 + 4p'_{tr}} +$$
$$+ 24\frac{\Delta f}{\Delta F} y_{32}(\sigma, \Delta p_2 - \Delta b_{le})\, e^{-2b'_{3(0)} + 6p_0 + 6p'_{tr}} +$$
$$+ 24\frac{\Delta f}{\Delta F} y_{31}(\sigma, \Delta p_2 - \Delta b_{le})\, e^{-2b'_{3(0)} + 6p_0 + 6p'_{tr}}. \qquad (10'')$$

In passing from the output of the first amplifier to that of the second, the transmission level is changed by the value $p - p_3 = S_2 - b_{le}(f) = \beta_f l - S_1$.

Therefore, the power of the nonlinearities arising at the first amplifier and passing to the second becomes $W'_{nl}\, e^{2(\beta_f l - S_1)}$. The additive law for nonlinear products arising at particular amplifiers depends on the frequency phase characteristic of the element of the transmission line included between them and should be determined experimentally for amplifiers of a given type. In design work, where experimental data cannot be obtained and special measures for correcting the phase characteristic have not been provided, it is assumed [4] that nonlinear products of the second order and of the third order, second kind, are added according to power, but products of the third order, first kind, are added according to a law which is intermediate between power and voltage addition. If we accept this for amplifying elements of the circuit under consideration, then the total power of nonliner products at the output of the second amplifier, determined in the frequency band of one channel, will be found within the limits from

$$W_{nl\,min} = W'_{nl}\, e^{2(\beta_f l - S_1)} + W''_{nl} \qquad (12)$$

to

$$W_{nl\,max} = (W'_2 + W'_{32})\, e^{2(\beta_f l - S_1)} + W''_2 + W''_{32} + W'_{31}\, e^{2(\beta_f l - S_1)} +$$
$$+ W''_{31} + 2\sqrt{W''_{31} W'_{31}\, e^{2(\beta_f l - S_1)}}. \qquad (12')$$

Substituting into (12) the values of W''_{nl} and W'_{nl} from (10') and (10'') we obtain

$$W_{nl\,min} = 4\frac{\Delta f}{\Delta F} e^{-2b''_{2(0)} + 4p_0 + 4p_{tr}} \left[y_2(\sigma, \Delta p_2) + y_2(\sigma, \Delta p_2 - \Delta b_{le}) \times\right.$$
$$\left. \times e^{-2\left[b'_{2(0)} - b''_{2(0)}\right] - 4\Delta S_1 + 2(\beta_f l - S_1)}\right] + 24\frac{\Delta f}{\Delta F} e^{-2b''_{3(0)} + 6p_0 + 6p_{tr}} \times$$
$$\times \left[y_{32}(\sigma, \Delta p_2) + y_{32}(\sigma, \Delta p_2 - \Delta b_{le})\, e^{-2\left[b'_{3(0)} - b''_{3(0)}\right] - 6\Delta S_1 + 2(\beta_f l - S_1)}\right] +$$
$$+ 24\frac{\Delta f}{\Delta F} e^{-2b''_{3(0)} + 6p_0 + 6p_{tr}} \left[y_{31}(\sigma, \Delta p_2) + y_{31}(\sigma, \Delta p_2 - \Delta b_{le}) \times\right.$$
$$\left. \times e^{-2\left[b'_{3(0)} - b''_{3(0)}\right] - 6\Delta S_1 + 2(\beta_f l - S_1)}\right]. \qquad (13)$$

Comparing (13) and (10) we see that (10) can be extended to include the considered amplifier under condition that the values of the coefficients y_2, y_{32} and y_{31} are replaced by equivalent values obtained from the expression

$$y_2 = y_2(\sigma, \Delta p_2) + y_2(\sigma, \Delta p_2 - \Delta b_{1e})\, e^{-2[b'_{3(0)} - b''_{3(0)}]-4\Delta S_1+2[\beta_f l - S_1]}$$
$$y_{32} = y_{32}(\sigma, \Delta p_2) + y_{32}(\sigma, \Delta p_2 - \Delta b_{1e})\, e^{-2[b'_{3(0)} - b''_{3(0)}]-6\Delta S_1+2[\beta_f l - S_1]} \qquad (14)$$
$$y_{31} = y_{31}(\sigma, \Delta p_2) + y_{31}(\sigma, \Delta p_2 - \Delta b_{1e})\, e^{-2[b'_{3(0)} - b''_{3(0)}]-6\Delta S_1+2[\beta_f l - S_1]}$$

for power addition, and

$$y_{31} = y_{31}(\sigma, \Delta p_2) + y_{31}(\sigma, \Delta p_2 - \Delta b_{1e})\, e^{-2[b'_{3(0)} - b''_{3(0)}]-6\Delta S_1+2[\beta_f l - S_1]} +$$
$$+ 2\sqrt{y_{31}(\sigma, \Delta p_2)\, y_{31}(\sigma, \Delta p_2 - \Delta b_{1e})\, e^{-2[b'_{3(0)} - b''_{3(0)}]-6\Delta S_1+2[\beta_f l - S_1]}} \qquad (14)$$

for voltage addition.

From the aforesaid it follows that the method presented earlier [4] for the most part remains in force. However, introduction of auxiliary variables S_1 and Δp_2 substantially complicates the problem. Substituting into (14) the values of ΔS_1 from (11) clearly demonstrates that, on increase of S_1, the total power of the nonlinearities are increased, which, for a given reduction of nonlinear noise, compels the lowering of the transmission level p_{tr}. This circumstance in its turn limits the applicable values of S_1. Varying Δp_2 occasions various changes in the power of the nonlinear products of different kinds. As investigations [3] indicate, on increase of Δp_2, the power of the nonlinearities of the second order increase in the lower and decrease in the upper channels of the system, the power of those of third order, second kind, decrease in all channels, and the power of the products of the third order first kind, increase in the upper and decrease in the lower channels. Furthermore, as has been pointed out, the dependences of the coefficients y_2, y_{32} and y_{31} on the magnitude of predistortion Δp are expressed not in analytical, but graphic form. Therefore, the values of S_1 and Δp_2 chosen in accordance with nonlinear noise reduction factors must be determined separately for each concrete multiplex system. This requirement is a basic criterion, if the suppression of nonlinear noise in the upper channels of the system is to equal the suppression of set noise. An auxiliary criterion (for fulfillment of the basic one) is noise reduction in the lower channels. As an illustration, Figure 4 shows the results of calculations

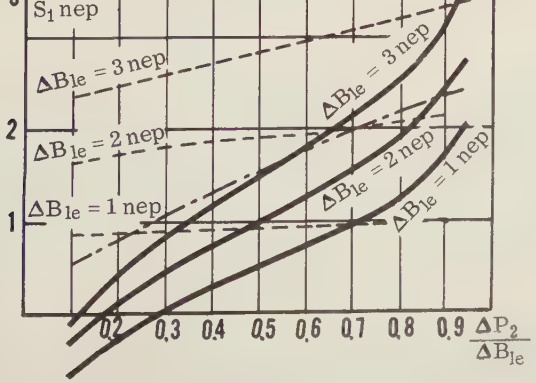

Figure 4

made for the K-60 system, using MKSB-60 cables and section lengths of approximately 5, 10 and 15 km (for which Δb_{1e} are 1, 2 and 3 nepers, respectively). The values of the ratio $\frac{\Delta p_2}{\Delta b_{1e}}$ are laid off along the horizontal axis, and values of S_1, along the vertical. Solid lines indicate minimal values of S_1, found from (6). Dashed lines represent maximal values of S_1, found from (9). Dotted and dashed lines show values of S_1 for which there is equality of nonlinear and set noise in the upper channel (for $\Delta b_{1e} = 2.0$ nepers).

As the calculations indicated, loss from replacement of amplifiers in the circuit Figure 1a by amplifers in Figure 1b is quite considerable. Therefore, introduction of a frequency dependence into the OOS circuit of a semiconductor amplifier is wholly to be desired.

In conclusion, the practical interest of a variant of the circuit with two amplifiers should be noted, in which the equalizer is placed partly at the input and partly between the amplifying elements.

APPENDIX

It is necessary to explain that the expression presented in [5]

$$p_{tr} = p_{min} + 1/2 \ln \frac{e^{2\Delta p} - 1}{e^{2\frac{\Delta f}{\Delta F}\Delta p} - 1} - 1/2 \ln \frac{\Delta F}{\Delta f}$$

takes into consideration the absence of power in the intervals between channels.

Rewriting it in the form

$$p_{tr} = p_{min} + 1/2 \ln \frac{e^{2\Delta p} - 1}{\left[e^{2\frac{\Delta f}{\Delta F}\Delta p} - 1\right]\frac{\Delta F}{\Delta f}}$$

and expanding $e^{2\frac{\Delta f}{\Delta F}\Delta p}$ in series form, we obtain in the denominator on the right

$$\left[1 + 2\frac{\Delta f}{\Delta F}\Delta p + \frac{1}{2!}\left(2\frac{\Delta f}{\Delta F}\Delta p\right)^2 + \frac{1}{3!}\left(2\frac{\Delta f}{\Delta F}\Delta p\right)^3 + \ldots - 1\right]\frac{\Delta F}{\Delta f} =$$

$$= 2\Delta p + 2\Delta p^2\frac{\Delta f}{\Delta F} + \frac{4}{3}\Delta p^3\left(\frac{\Delta f}{\Delta F}\right)^2 + \ldots$$

For the K-24 $\frac{\Delta f}{\Delta F} = \frac{3.1}{96} = 3.23 \cdot 10^{-2}$, and for the K-60 system it equals $\frac{\Delta f}{\Delta F} = \frac{3.1}{240} = 1.3 \cdot 10^{-2}$. Therefore, the terms containing $(\frac{\Delta f}{\Delta F})$ in any degree higher than the first are negligible in comparison with the first term. As for the first two terms, they can be presented in the form

$$2\Delta p\left[1 + \Delta p\frac{\Delta f}{\Delta F}\right].$$

Even at $\Delta p = 2.5$ nepers, the quantity in brackets does not exceed 1.081 in the K-24 system and 1.033 in K-60. Thus, by taking only the first term in the denominator into the calculation we decrease the denominator by no more than 8% in K-24, and by no more than 3.3% in the K-60 system.

Consequently, the error in the determination of p_{min} does not exceed 0.04 neper in K-24 and 0.02 neper in K-60. This permits us to recommend expression (7) as the simplest for practical calculations.

Original article submitted July 5, 1960

LITERATURE

1. Yu. D. Farber, "Selection of Parameters in High-Frequency Semiconductor Amplifiers for Cable Lines" Elektrosvyaz, No. 11, 1958.
2. A.A. Leshchinski, High-Frequency Telephone Communication along Coaxial Cables, Svyaz'izdat, 1955.
3. N.E. Popova, "Distribution of Nonlinear Distortions at the Output of an Amplifier for Oblique Frequency Characteristics of the Transmission Level" TsNIIS Ministry of Communications of the USSR, "Information Bulletin" No. 4, 1954.
4. A.I. Borisov, "Determination of the Basic Parameters of Multichannel Transistor Amplifiers for Cable Lines" Elektrosvyaz, No. 2, 1960.
5. S.A. Dvorkin, "Determination of the Transmission Level in High-Frequency Telephone Systems Operating with Predistortion" Elektrosvyaz, No. 10, 1960.

APPLICATION OF VARISTORS TO ARC QUENCHING

E.E. Raukas

The volt-ampere characteristics of varistors are investigated in connection with their application to arc quenching. A nomogram is set up permitting the selection of suitable parameters. A method for calculation of the power dissipated by the varistor is presented.

On breaking a circuit containing a large inductance, a spark discharge is observed, under certain conditions, at the moment the contact is broken. This phenomenon is in many respects undesirable (it hastens deterioration of the contacts, etc.).

For quenching the arc, usually, a resistance is connected across the inductance or contacts, or, an RC circuit, or, finally, a varistor is used. The advantage of a resistance is its economy; its disadvantages are the delay in making and breaking the contact and the large power requirement. An RC circuit is free from these defects, but it is much more expensive. The varistor has the advantage of simplicity, economy (in mass production)

and a significant decrease in the delay in operation of the contact in comparison with a resistance having the same power requirement.

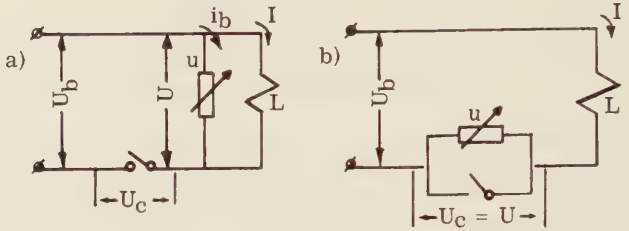

Figure 1

Let us consider an arc — quenching circuit based on a varistor. Let the varistor be connected in parallel to the inductance L (case a). The operating voltage of the system is equal to u_b; we will call the voltage arising at the contact on breaking the circuit u_c. As is well known, at the moment the circuit is broken, the current I following through the induction does not change, and the circuit is completed, not through the power supply, but through the varistor. A voltage pulse u arises in the varistor. As seen from the Figure, $u_c = u_b + u$. When the varistor is connected in parallel to the contacts (Figure 1b) $u_c = u$.

In order to avoid an arc the inequality $u_c < u_s$ must be fulfilled, where u_s is usually found within the limits 270 - 330 v [1, 2].

According to investigations, the optimum voltage u_c for longest life varies from 180 to 240 v, depending on the material of the contacts.

VOLT - AMPERE CHARACTERISTICS OF VARISTORS

A nonlinear semiconductor resistance whose value depends on the applied voltage is called a varistor.

The low-power varistors produced by our industry are prepared from silicon carbide and are disks 10, 15, 20 and 25 mm in diameter and 2 - 3 mm thick.

According to [3, 4, 5] one of the following empirical formulas may be used as an approximation of the volt - ampere characteristic of a varistor:

$$i = \sigma u, \quad \sigma = \sigma_0 e^{b\sqrt{u}}, \tag{1}$$

where σ is the electrical conductivity, σ_0 is the conductivity for u = 0 v, b is an experimental constant; or

$$i = Cu^{\beta}, \tag{2}$$

and, finally

$$u = Bi^{\alpha}, \tag{3}$$

where C, B, α and β are experimental constants.

In the general case, nonlinearity is determined from the ratio of the static resistance to the dynamic

$$\beta = \frac{u}{i}\,\frac{di}{du}.$$

When approximation (2) is used β takes the form

$$\beta = \frac{\lg \frac{i_1}{i_2}}{\lg \frac{u_1}{u_2}},$$

where u_1, i_1 and u_2, i_2 are related values of the current and voltage lying close to one another.

Volt - ampere characteristics of the type NPS varistor made at the Pegel'man Radiotechnical Factory at Tallinn was studied in the circuit (Figure 2). The capacitor C (20 - 160 μf) was first charged through a resistance R_1 to a voltage u, measured by voltmeter V_1 and subsequently discharged through the varistor circuit.

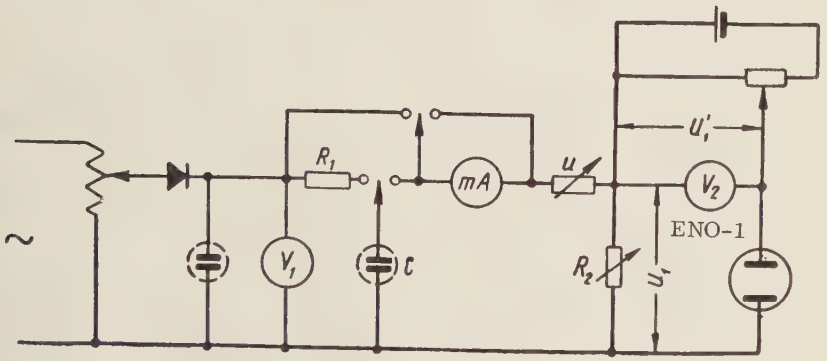

Figure 2

For measuring the current by the compensation method, an inductanceless resistance R_2 was connected in the circuit, chosen so that the voltage pulse from R_2 was compensated by the voltage u'_1. An ENO-1 oscilloscope was used as an indicator. The volt - ampere characteristic at low voltages was read directly using a milliammeter connected into the circuit. Depending on the varistor current, characteristics were taken from 200 - 400 v (approximately corresponds to a field intensity of 1400 v/cm in the varistor).

A typical volt - ampere characteristic is presented in Figure 3 on a logarithmic scale. As seen from the figure, beginning

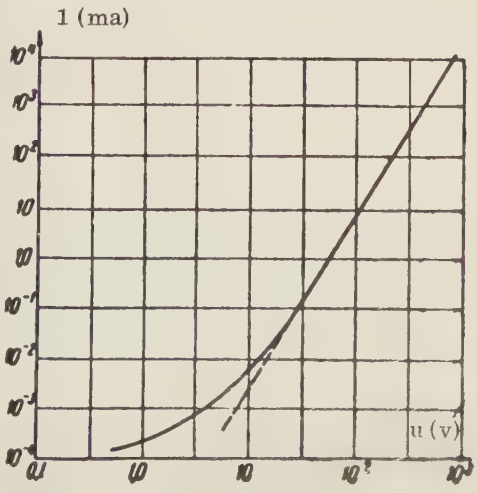

Figure 3

with a certain value of the voltage, the experimental curve becomes a straight line, which indicates the constancy of β at high voltages.

From many measurements on different samples the lower limit of constancy of β was determined for the particular type of varistor. It varied from 16 to 40 v (approximately 50 - 300 v/cm).[1] Thus, for voltage above this, formulas (2) and (3) give the best approximation to the characteristics.

Investigations at much lower voltages showed that from 1.5 to 35 v (5 v/cm to 130 v/cm) formula (1) gives the best approximation. The volt - ampere characteristic expressed in (σ, $\sqrt{u}$) coordinates (Figure 4) shows this, being a straight line in the indicated voltage interval.

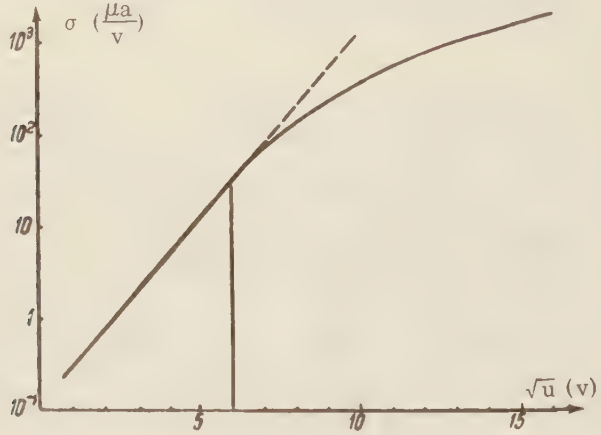

Figure 4

CHOICE OF PARAMETERS

As the above makes clear, the most suitable expressions for the characteristic of a varistor, from the point of view of arc quenching, are formulas (2) and (3). Using formula (2) we express C in terms of i_0 and u_0

$$i = i_0\left(\frac{u}{u_0}\right)^5, \tag{4}$$

where i_0 is the current at voltage u_0.

The parameters of the varistor in this case are i_0 and β, fixed for a given u_0. In order to keep β constant, u_0 should be sufficiently high (for varistors from the Tallinn factory, greater than 16 to 40 v). For quality control the voltage u_0 = 50 v is used, then i_0 = 0.1 to 30 ma, β = 2.5 to 4.0.

---

[1] The figures given relate to varistors prepared at the Tallinn Radiotechnical Factory according to LETI technology. Similar experiments on varistors prepared by other techniques gave approximately 100 v for the lower limit of constancy of β.

Let us set up a nomogram for determining suitable parameters for an arc quenching varistor, given the parameters of a relay-coil circuit. At the first instant of contact separation, the current through the varistor is equal to the operating current of the inductive element and formula (4) can be given as

$$I = i_0 \left(\frac{u}{u_0}\right)^{\beta}.$$

Formulas (1) and (2) give

$$u_c = u_b + u < u_s \text{ or } u_c = u < u_s.$$

Noting that $u_0 = 50$ v and the optimal value of $u_c \approx 200$ v, for circuits with supply voltages $u_b = 48$ and $u_b = 60$ v, parallel connection of the varistor to the inductance gives $u/u_0 = 3$. Thus, the voltages upon contact separation, $u_c = u_b + u = 3\,u_0 + u_b$, will be 198 and 210 v, respectively.

In systems operating at 6, 12 and 24 v, a varistor connection leads to $u/u_0 = 4$. The corresponding voltage at the contacts is then from 206 to 224 v.

In connecting the varistor across the contacts, the ratio u/u_0 is independent of the operating voltage and is approximately equal to 4.

The nomogram (Figure 5) consists of four scales: one each for I and β, and two for i_0. Depending on the conditions noted above, we use either the left ($u/u_0 = 3$) or the right ($u/u_0 = 4$) scale for i_0. Any line

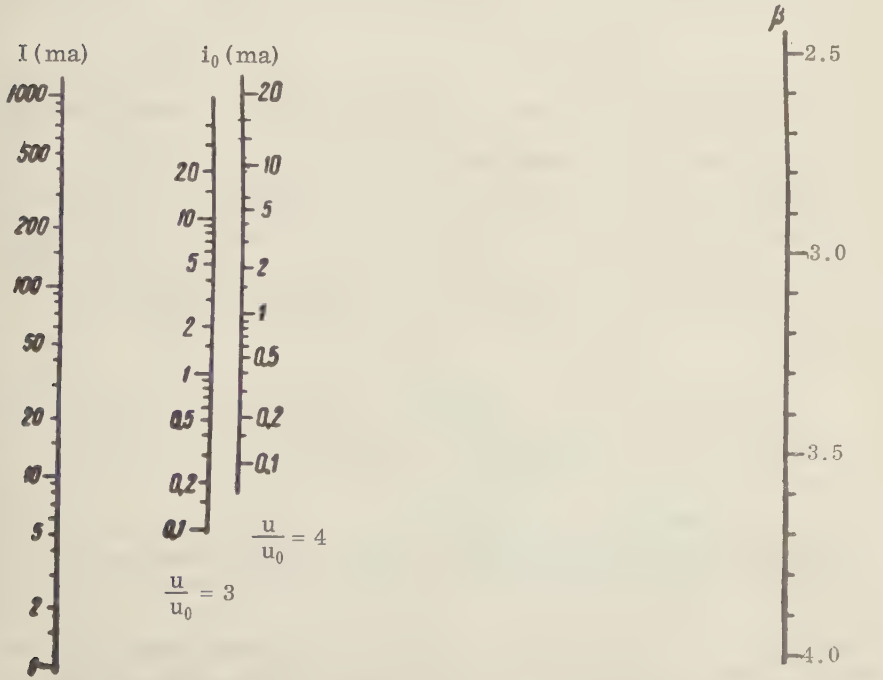

Figure 5

passing through the given value of I and intersecting the i_0 and β axes gives the desired parametric values. These i_0 and β pairs are innumerable, as seen from the nomogram. It is most economical to use varistors with large β and small i_0. As a result of connection of the varistor into the circuit, an additional power consumption arises

$$\Delta N = i_b u_b,$$

where i_b and u_b are the operating current and voltage of the varistor.

The ratio $\Delta N/N$ can be called the power-loss coefficient.

$$K = \frac{\Delta N}{N} = \frac{i_b}{I}, \tag{5}$$

where N is the power stored in the induction coil.

On connecting the varistor across the contacts

$$K = \frac{\Delta N}{N} = \frac{i_b}{I} \frac{1-p}{p}, \tag{6}$$

where p is the ratio of the inductive loading time to the total time.

i_b is calculated from the formula

$$i_b = i_0 \left(\frac{u_b}{u_0}\right)^{\beta}. \tag{7}$$

At low voltages (below 15 v) a wide divergence from the true value of the current i_b as a result of the inconstancy of β can appear.

Thus, after selecting suitable parameters according to the nomogram (Figure 5) we can calculate the power loss occasioned by the varistor from formulas (5), (6) and (7).

CHOICE OF PARAMETERS, INCLUDING TEMPERATURE CORRECTIONS

The calculations are somewhat more complicated if we consider the relatively large temperature coefficient of the varistor's resistance (on the average $-0.6\%/^\circ C$).

With each pulse, with the varistor hooked up to the circuit of Figure 1, almost all of the energy stored in the inductance is dissipated. If we designate the number of circuit breaks per minute by n, the inductance of the circuit by L, and the current through the inductance by I, then the power loss will be

$$N_u = \frac{nLI^2}{120}.$$

The total power dissipated by the varistor is equal to

$$N_0 = N_u + \Delta N.$$

Assuming the relationship between current and temperature of the varistor to be linear and considering that, to a first approximation, the varistor temperature depends linearly on the power dissipated by it, we may write

$$i'_\delta = i_\delta [1 + \delta (N_u + \Delta N) + \gamma \Delta t] = i_\delta [1 + \delta (N_u + i'_\delta u_\delta p) + \gamma \Delta t], \tag{8}$$

where i'_δ is the operating current of the varistor with temperature correction, δ is an experimental coefficient, reflecting the increase of current with increase of power dissipated, γ is the temperature coefficient of the varistor

current ($\sim +0.6\%\,^{\circ}$ C), $\Delta t = t - 20^{\circ}$ C is the number of degrees above room temperature. The term $\gamma \Delta t$ is concerned with the effect of the temperature of the medium; it is used for large differences between the medium and room temperature. For a disk-shaped varistor with diameters 10, 15, 20 and 25 mm, the coefficient δ is equal to 0.60, 0.35, 0.27 and 0.21 respectively. The error introduced by using formula (8) does not exceed 15% if the difference between the temperature of the varistor and that of the medium does not exceed 70° C.

Taking i'_{δ}/i_{δ} from (8) we obtain

$$\frac{i'_{\delta}}{i_{\delta}} = F,$$

where

$$F = \frac{1 + \delta N_u + \gamma \Delta t}{1 - \delta i_{\delta} u_{\delta p}},$$

i_{δ} is calculated from (7).

Comparing the result with equations (5) and (6) we see that the power loss coefficient K is multiplied by a factor F when a temperature correction is applied.

Again, making calculations similar to (8) we obtain for the current i_0 the expression

where

$$i_0 = \frac{i'_0}{G},$$

$$G = 1 + \delta \left(N_u + i'_0 \frac{u_{\delta}^{\beta+1}}{u_0^{\beta}} p \right) + \gamma \Delta t. \qquad (9)$$

If the varistor is connected across the contacts, it is necessary to replace the quantity p by 1-p.

To take account of the temperature correction it is necessary to use the nomogram (Figure 5) in the following manner:

Let it be given that I = 100 ma, $u_{\delta} = 60$ v, $\beta = 3.2$; a varistor with diameter 15 mm ($\delta = 0.35$) connected across the inductance; $N_u = 0.55$ watt, $p = 0.5$; temperature of surroundings equal to that of the room.

Using the scale $u/u_0 = 3$ on the nomogram (thus, $u_c = u + u_{\delta} = 3u_0 + u_{\delta} = 210$ v) we find $i'_0 = 3$ ma. Finally, from equation (9) we obtain

$$G = 1 + 0.35 \left(0.55 + 3 \cdot 10^{-3} \frac{60^{4.2}}{50^{3.2}} 0.5 \right) = 1.72,$$

$$i_0 = \frac{3}{1.72} \approx 1.75 \text{ ma}.$$

Consequently, in the given case for $\beta = 3.2$, a varistor with $i_0 = 1.75$ ma (measured at a voltage $u_0 = 50$ v) is suitable for arc quenching.

The author gives thanks to Professor Kh. Sillam for his many useful suggestions.

Original article submitted April 25, 1960

LITERATURE

1. M.I. Vitenberg, Electromagnetic Relay Calculations for Automation and Communiction, Gosenergoizdat, 1956.
2. F.F. Zhdanov, "Calculations for Arc Quenching Circuits," Elektrosvyaz' No. 6, 1957.

3. V.V. Pasynkov, Nonlinear Semiconductor Resistors (Varistors), in the collection "Semiconductors in Science and Technology," Vol. 1, 1957, Izd. AN SSSR, 1957.
4. Rumpf, Bauelemente der Elektronik, Berlin, 1959.
5. Franke, "Eigenschaften und Anwendungen von Varistoren." Radio und Fernsenen, No. 4, 5, 1959.

LETTERS TO THE EDITOR

REMARKS CONCERNING THE ARTICLE BY S.I. SAMOILENKO, "OPTIMAL REGULATION OF THE PARAMETERS OF RADIO LINES"

In the journal "Elektrozvyaz" No. 12, 1957 was published an article by S.I. Samoilenko, "Optimal Regulation of the Parameters of Radio Lines." Since in certain later publications (e.g., A.M. Petrovskii, "A Scanning Method for Improving Radio Reception," Elektrosvyaz No. 5, 1959) references were made to this work and its results utilized, we feel it is necessary to call attention to an error which was allowed to stand in the previous article and was carried over into those that followed.

Samoilenko poses the problem of determining the conditions which will ensure optimal transmission of a binary code along a noisy channel. On the basis of this analysis of the capacity of a channel to transmit binary signals in equation (5) (here and subsequently, we use Samoilenko's enumeration of equations) the author comes to the conclusion that

"... for transmission of information by binary code under the condition that the probabilities of the appearance of the elementary symbols are equal, the greatest quantity of information per elementary symbol is achieved when the probabilities of distortion of each of these symbols are also equal."

This conclusion in no way follows from the discussion preceding it. Actually, to make a statement such as that quoted above, it would be necessary to express the quantity of information as the probability of distortion of the symbols, $P_{dist\,1}$ and $P_{dist\,0}$, under conditions of a priori equal probability of the symbols at the input [equation (5) represents the maximum quantity of information in all possible methods of coding that can be transmitted per channel, given the symbol distortion probabilities $P_{dist\,1}$ and $P_{dist\,0}$, and, therefore, generally speaking, is not equal to the quantity of information that can be transmitted by symbols with equal probabilities $P_0 = P_1 = \frac{1}{2}$]. Thus, assuming that the probability of distortion is a function of a certain parameter (in particular, this could be the limiting level of the signal) we can set up the equation for optimality

$$\frac{dI}{d\alpha} = 0.$$

The ratio between $P_{dist\,0}$ and $P_{dist\,1}$ obtained from this equation allows us to make the statement we require. Continuing this analysis, it is easily proved that neither equation (8) nor any other simple and physically

significant relationship between $P_{dist\,0}$ and $P_{dist\,1}$ can be obtained. This is an obvious consequence of the fact that "quantity of information" is not a very fortunate criterion for the problem considered. On the other hand, a generally adopted criterion of optimality exists: if the total probability of faulty reception $P = P_{dist\,0} + P_{dist\,1}$ is a function of some parameter α, then for optimal reception it is necessary that

$$\frac{dP}{d\alpha} = 0.$$

Returning to Samoilenko's work, we note that analysis of equations (5) and (6), under the condition of equiprobable transmitted symbols and leading to the conclusion formulated in equation (8), can be given in these words: a code with a priori probability of symbols $P_1 = P|_0| = 1/2$ is an optimal code when the probabilities of distortion of these symbols are equal.

It is obvious that this conclusion and that of S.I. Samoilenko are not identical. They would be identical if optimality of a code A for a channel with noise k_1 means that the amount of information transmitted in this code over any other channel k is also a maximum. In actuality, that a given code A is optimal for a given channel k signifies an extremal condition for the quantity of information transmitted over the channel only as far as the multiplicity of the code is concerned, not the multiplicity of channels.

L. Byalyi

ANSWER TO L.I. BYALYI

Analysis of equation (5) of the article in question shows if there is an equivalence in the maximum quantity of information per symbol per channel, then, for the case of equal a priori probability of the appearance of the symbols 0 and 1, the best channel is that in which the probabilities of distortion of the symbols 0 and 1 are equal.

This conclusion was presented in the article in a formulation which did not emphasize the importance of equivalence of the channels and this has led to the critical remarks.

Actually, we assume that on changing the regulating parameters and, correspondingly, $P_{dist\,1}$ and $P_{dist\,0}$, the channel is no longer equivalent i.e., the maximum amount of information per symbol, which can be achieved with the best code, is changed. In this case it would seem that matching the probabilities of distortion in the selected code would not lead to the greatest amount of information per symbol.

Considering that these questions were not treated in sufficient detail in the article considered, it would seem expedient to fill in the gaps somewhat. An analysis is presented below of some examples of the regulation of amplitude thresholds according to the criterion $P_{dist\,1} = P_{dist\,0}$ from the point of view of the minimality criterion ($P_{dist\,1} + P_{dist\,0}$).

Example 1. Transmission of binary information in the presence of white noise by amplitude modulation and envelope detection.

As is well known [1, 3], the probabilities of distortion of the symbols 0 and 1 with amplitude modulation are

$$P_{dist\,1} = e^{-h^2} F(z_0, h); \quad (1)$$

$$P_{dist\,0} = e^{-z_0^2/2}; \quad (2)$$

where $h = \frac{U_{mc}}{\sqrt{2}\, U_{n\,eff}}$ is the ratio of the effective values of the signal and noise voltages at the detector input.

$$z_0 = \frac{E_0}{U_{n\,eff}}$$

E_0 is the threshold.

$$F(z_0, h) = \int_0^{z_0} x e^{-x^2/2} I_0(x\sqrt{2}h)\, dx. \quad (3)$$

In Figure 1 is shown the dependence of the quantity $\frac{P_{dist\,1} + P_{dist\,0}}{2}$ on the threshold value for different signal-to-noise ratios. In the same figure, the circles represent threshold values corresponding to $P_{dist\,1} = P_{dist\,0}$.

As seen on the curves, the thresholds selected from the condition $P_{dist\,1} = P_{dist\,0}$ are found in immediate proximity to minimum values of P. Thus, use of the criterion minimum (p) is seen to lead to a decrease in the amount of transmitted information in comparison with a system of transmission in which the threshold satisfies the condition $P_{dist\,1} = P_{dist\,0}$ and where transmission of excess information is not required.

Example 2. Transmission of binary information in channels with white noise by amplitude modulation and synchronous detection.

The probability of distortion of the symbols 0 and 1 is in this case [3]

$$P_{dist\,0} = \frac{1}{2} - \frac{1}{2} I(a\sqrt{R}), \quad (4)$$

$$P_{dist\,1} = \frac{1}{2} - \frac{1}{2} I[(1-a)\sqrt{R}], \quad (5)$$

where $a = \frac{T}{S_0}$ is the relative threshold, T is the value of the threshold, S_0 is the effective value of the carrier envelope after a long time, R is the average signal-to-noise ratio and

$$I(z) = \frac{2}{\sqrt{\pi}} \int_0^z e^{-x^2} dx.$$

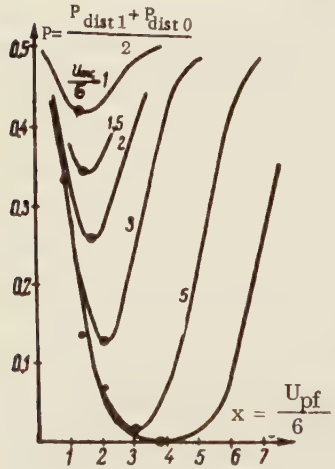

Figure 1

In this same work [3] it was shown that the minimum value of P takes place at a = 1/2. As seen from equations (4, 5) for this threshold value, distortion probabilities of the symbols 0 and 1 are equal. In other words, regulation of the threshold according to the criterion $P_{dist\,1} = P_{dist\,0}$ ensures an optimum for the criterion minimum (p).

Example 3. Transmission of binary information by video pulse in a channel with white noise.

The probability that the white noise will exceed the level U is equal to [4]

$$P\{|\xi| > U\} = 1 - I\left(\frac{U}{\sqrt{2}\sigma}\right). \quad (6)$$

This is evidenced by the fact that in the given examples the condition of equivalence of the channels is accurately, (Examples 2, 3), or, approximately (Example 1), fulfilled.

The probability of distortion of a video pulse with an amplitude U_{imp} for reception at the threshold level is equal to

$$P_{dist\,0} = 1 - I\left(\frac{U_{thresh}}{\sqrt{2}\,\sigma}\right) =$$

$$= 1 - I\left(\frac{U_{thresh}}{U_{imp}}\,\frac{U_{imp}}{\sigma\sqrt{2}}\right) = 1 - I\,(ka), \qquad (8)$$

where $a = \frac{U_{thresh}}{U_{imp}}$, $k = \frac{U_{imp}}{\sigma\sqrt{2}}$;

$$P_{dist\,1} = 1 - I\left(\frac{U_{imp} - U_{thresh}}{\sqrt{2}\,\sigma}\right) = 1 - I\left[\frac{U_{imp}}{\sqrt{2}\,\sigma}\left(1 - \frac{U_{thresh}}{U_{imp}}\right)\right] =$$

$$= 1 - I\left[k\,(1 - a)\right]. \qquad (9)$$

From a comparison of equations (8) and (9) with (4) and (5) it is seen that they are identical in structure. Consequently, minimum (p) will take place in the considered case at $P_{dist\,1} = P_{dist\,0}$. Regulation according to the criterion $P_{dist\,1} = P_{dist\,0}$ will be optimal in regard to the criterion minimum (p).

A consideration of the examples indicates that regulation of the threshold according to the criterion $P_{dist\,1} = P_{dist\,0}$ under the given conditions leads to the maintenance of the threshold level either in direct proximity to a value corresponding to minimum (p) (Example 1) or to some level for which the sum $P_{dist\,1} + P_{dist\,0}$ is a minimum (Examples 2 and 3). For other conditions of transmission, evaluation of the criterion $P_{dist\,1} = P_{dist\,0}$ may be conducted in analogous fashion.

In conclusion I would like to express gratitude to L.I. Byalyi for his useful criticism of my article.

LITERATURE

1. D.S. Lezin, Noiseproofing for Different Forms of Radiotelegraphy, Elektrosvyaz' No. 4, 1957.
2. N.L. Teplov, Maximum Noise Reduction in the Reception of Radio Signals with Amplitude, Frequency and Phase Modulation, Elektrosvyaz No. 1, 1959.
3. Montgomery, "A comparison of amplitude and angle modulation for narrow-band communication." Proc. IRE, Vol. 42, No. 2, 1954.
4. A.A. Kharkevich, Outline of General Communication Theory, Gostekhizdat, 1955.

AUTHOR'S CERTIFICATES (PATENTS)

Class $21a^1$, 30, No. 130062. R.G. Karpov, Device for producing two pulse series.

Class $21a^1$, 33_{11}, No. 130063. V.F. Vorob'ev, Method for improving the quality of the picture in magnetic recording television systems.

Class $21a^1$, 33_{31}, No. 130065. G.V. Braude, Method for limiting frequency band.

Class $21a^1$, 34_{31}, No. 130066. Ya. I. Efrussi, Method for reproducing color television images.

Class $21a^1$, 35_{30}, No. 130541. O.I. Yudzon, Method of compensating for the shift of the horizontal blanking pulses of a transmitting television tube during the operation of a camera with a long cable.

Class $21a^1$, 36, No. 129671. G.I. Isserlin, D.V. Katz and G.I. Sokolov, A frequency divider.

Class $21a^1$, 36, No. 129672. V.V. Zolotov, Method for differentiating (integrating) signal envelopes with amplitude modulation.

Class $21a^1$, 36, No. 129673. V.E. Vershin, Device for shaping pulses.

Class $21a^1$, 36, No. 130067. V.N. Glavnov, Current reverser in semiconductor triodes.

Class $21a^2$, 16_{01}, No. 129674. N.N. Labzin and R.A. Baranov, A distributing device.

Class $21a^2$, 18_{04}, No. 130068. B. Ya. Lur'e, Method for decreasing the thermal noise of a linear amplifier.

To reduce the noise in an amplifier connected to a main communication line, it is suggested that an active two-terminal network with a low noise level be connected to the input of the amplifier, along with a matching resistance.

Class $21a^2$, 18_{08}, No. 129675. F.S. Shapiro, Electromagnetic regulator.

Class $21a^2$, 18_{08}, No. 130542. S.P. Kolosov and E.B. Elagin, Device for introducing automatic regulation of a signal into a system, proportional to a derived mismatch in time.

Class $21a^4$, 8_{01}, No. 130069. B.M. Kublanov and I.M. Kublanov, Controlled blocking oscillator in a "transfluxer."

Class $21a^4$, 10, No. 129679. R.P. Poilov, Method of measuring the equivalent reactive electrical parameters of a piezoelectric resonator.

Class $21a^4$, 11, No. 130070. M.V. Artem'ev and P.I. Udalov, Device for suppressing arcs in transmitters.

Application of a thyratron relay is suggested for automatically switching off the transmitter when an arc appears.

Class $21a^4$, 13, No. 129680. V.M. Il'in, Ferroresonant generator of damped oscillations.

Class $21a^4$, 13, No. 129681. P.M. Sudakov, Electromechanical

generator for self-excitation.

Class $21a^4$, 14_{01}, No. 129682. L.G. Volkov, Magneto-tube pulse modulator with shaping device composed of antiresonance circuits.

Class $21a^4$, 14_{01}, No. 130071. A.S. Dadunashvili, Method and device for thermomagnetic pulse modulation.

Class $21a^4$, 29_{01}, No. 130072. Yu. N. Glukhov, V.L. Brailovskii and A.V. Datsko, Pulsed power amplifier.

Class $21a^4$, 29_{04}, No. 130543. Yu. F. Korobov, Method for synchronizing reception with double frequency conversion.

Class $21a^4$, 35_{14}, No. 130544. V.I. Aleksandrin, A voltage stabilizer.

Class $21a^4$, 36_{04}, No. 129683. V.I. Beketov, Antenna system operating in the microwave region.

Class $21a^4$, 48_{67}, No. 130073. Yu. S. Bondartsev, Method of adjusting the frequency characteristics of polarization gratings.

Class $21a^4$, 54, No. 129684. K.M. Kosikov, Method for determining the optimal operating frequency for a radio communication line of a given length.

Class $21a^4$, 64_{02}, No. 129685. K.P. Kharchenko, Method for strengthening the guy wires of a free standing communication pole.

Class $21a^4$, 70, No. 130076. A.A. Leonov, A differential capacitor.

Class $21a^4$, 71, No. 129686. M.I. Krivosheev, Method of measuring the ratio of the signal to the quasi-peak value of the noise by judging the moment of coincidence of the upper and lower noise peaks on an oscillograph.

Class $21a^4$, 71, No. 130077. R.A. Valitov and S.I. Pozdnyak, Method for determining the parameters of a dielectric.

Class 21b, 7_{01}, No. 130080. Related to Author's Certificate No. 55463. P.M. Spiridonov, Carbon-zinc dry cell using air depolarization.

Class 21b, 25_{04}, No. 129691. A.I. Koss, Airtight alkaline nickel-cadmium battery.

Class 21b, 26_{02}, No. 129692. K.P. Nefedov and S.F. Bugaev, Device for charging and discharging electrical batteries.

Class 21c, 46_{51}, No. 129703. Related to Author's Certificate No. 128053. V.G. Leskov, N.I. Chicherin and V.I. Turkin. System of dynamic automatic gain control.

Class 21c, 41_{01}, No. 130089. L.I. Gutenmakher, Contactless stepping switch.

Class 21c, 47_{01}, No. 130554. Related to Author's Certificate No. 130089. L.I. Gutenmakher, A contactless switch.

Class 21c, 54, No. 129705. M.D. Notarius, A.V. Abrosimov, S.M. Nikolaevskii and I.L. Rotbert, A temperature-compensated resistor.

Class 21c, 55_{02}, No. 129707. B.A. Piontkovskii, Device for voltage stabilization in a direct current supply circuit.

Class 21c, 59_{10}, No. 130094. A.A. Krugly, Ionic frequency converter.

Class 21c, 63_{20}, No. 129709. I.A. Stolovitskii, Regulator for two interrelated electrical quantities.

Class 21c, 67_{10}, No. 129711. Ya. S. Nesel', Device for automatic maintenance of the mean value of a rectified current.

Class 21c, 68_{60}, No. 130563. Related to Author's Certificate No. 91384. M.G. Koblentz, G.A. Bugaev and A.K. Sheshnev, An electromagnetic relay.

Class 21^2, 5, No. 130102. I.S. Rogachev and A.N. Tkachenko, Device for obtaining a unipolar voltage (current) pulse.

Class $21d^2$, 12_{03}, No. 129726. T.A. Suetin, A.A. Sokovich, A.V. Stukachev and N.S. Lazarev, A rectifier installation.

Class $21d^2$, 12_{03}, No. 130105. P.P. Litvinskii, Three-phase rectifier installation.

Class 21e, 11_{20}, No. 129739. A.A. Pirogov, Device for the automatic determination of the fundamental frequency of a current.

Class 21e, 11_{20}, No. 130110. D.M. Tas'man, Device for determination of instantaneous values and frequencies of an oscillogram.

Class 21e, 11_{20}, No. 130111. S.I. Krechmer, Device for cross-multiplying two voltages.

Class 21e, 12, No. 130112. M.E. Mazurov, Device for measuring alternating magnetic fields.

Class 21e, 12, No. 129741. Related to Author's Certificate No. 113185. N.N. Grekov and A.P. Ryabov, Method for measuring the ratio of the gradient to the intensity of a time varying magnetic field.

Class 21e, 27_{02}, No. 129742. V.S. Mel'nikov, Device for functional transformation of a DC voltage.

Class 21e, 28_{02}, No. 129743. Related to Author's Certificate No. 127392. V.A. Baramidze, Generator for linearly increasing voltages.

Class 21e, 29_{01}, No. 130576. Related to Author's Certificate No. 127750. L.S. Perel'man, Device for measuring the resistance, reactance and admittance of a load's impedance.

Class 21e, 29_{10}, No. 130578. S.P. Stryapunin, Method for determining the location of a break in a cable.

Class 21e, 29_{12}, No. 130580. N.I. Sverdlov, Device for determining the similarity of cable conductors.

Class 21e, 36, No. 129745. V.A. L'vov, A.A. Askinazi, O.I. Gurin and L.B. Beniaminson, Device for measuring the frequency characteristics of exchange channels.

Class 21e, 36_{01}, No. 129746. V.I. Bayunov and M.I. Demidov, Device for measuring small DC voltages.

Class 21e, 36_{10}, No. 129747. N.F. Vollernev and N.G. Gatkin, Method for measuring the spectral density modulus of a unit signal.

Class 21e, 36_{10}, No. 129749. I.A. Tsalkin, Method for measuring the RMS value of a periodic signal, the RMS value of the stationary noise, or the ratio of these quantities.

Class 21g, 11_{02}, No. 130119. V.E. Vershin and E.K. Zhivulin, Method for measuring the high-frequency parameters of a transistor.

Class 21g, 13_{01}, No. 129752. B.S. Marino, Device for connecting a tuning element, made in the form of a cluster of contacts, with a magnetron.

Class 21g, 29_{40}, No. 130122. S.I. Kochergin, Method for recording images on magnetic tape.

Class 21g, 30_{02}, No. 130591. Related to Author's Certificate No. 118055. Yu. B. shaub, Device for recording small AC voltages.

Class 21g, 34, No. 130124. V.K. Petrenko, Electromechanical band filter.

Class 21g, 38, No. 129755. Ya. K. Trokhimenko, A multistage multivibrator.

Class 42d, 1_{12}, No. 130688. R.G. Karpov, Device for obtaining a separation of the frequencies of two pulse series.

Class 42d, 10, No. 130200. V.M. Zakharov and B.V. Bolotov, memory device.

Class 42i, 20_{01}, No. 130696. I.E. Vedernikov, Device for recording electrical quantities photographically.

Class 42m, 14, No. 130238. L.I. Gutenmakher, AC trigger computer.

Class 42m, 14, No. 130239. E.I. Gurvich, Ferrotransistor with a "forbidden" logical circuit.

Class 42m, 14, No. 130241. G.P. Gorobchuk, Device for converting voltage into positional code.

Class 42m, 14, No. 130242. V.N. Zhovinskii and V.A. Koshelev, Device for obtaining a series of uncorrelated random voltage pulses.

Class 42m, 14, No. 130243. A.A. Bredov and I. Kh. Geller, Matrix device based on semiconductor diodes.

BIBLIOGRAPHY

1. General Communication Theory
2. Radio Communication Systems
3. Space Radio and Television
4. Radio Relay Lines
5. Noise and Interference
6. Propagation of Radio Waves
7. Antennas
8. Waveguides and Microwave Transmission
9. Parametric and Quantum Mechanical Amplifiers
10. Telephony and Telegraphy
11. Television
12. Electron-Tube and Semiconductor Instruments

---

1. GENERAL COMMUNICATION THEORY

Discrimination in continuous signals. Kharkevich, A.A. "Radiotekhnika," 1960, V. 15, No. 10, pp. 11-13, illustrations.

Design Methods for Maximum-Distance Error-Correcting Codes. MacDonald, J.E. "IBM J. Res. Develop," 1960, V. 4, No. 1. p. 43-57, 9 lit. cit.

Correlation Detection of Signals Perturbed by a Random Channel, Kailath, Th. "IRE Trans. of Information Theory," 1960, V. IT-6, VI, No. 3, p 361-366, illustrations.

Reliability of a system for spaced-antenna reception of two unequal correlated signals. Kibner, B.E. and M.F. Bakhareva, "Radiotekhnika i Elektronika," 1960, V. 5, No. 10, pp. 1726-1727, illustrations, 4 literature citations.

Rapid Detection of Coherent Signals in Noise. Metz, R.J. and others. "IRE Internat. Convent. Rec," 1960, V. 8, P. 8, p. 222-232, illustrations, 4 lit. cit.

Comparison of methods for detecting periodic pulses in the presence of noise. Zusammenstellung und vergleich bekannter Verfahren zur Auffindung periodischer Pulse bei Anwesenheit von Gerauschen. Haubig D. "Hochfrequenztechn. und Elektroakust.", 1960, Bd. 69, VI, No. 3, S. 94-103, illustrations, 10 lit. cit.

An Introduction to Matched Filters. Turin, G.L. "IRE Trans. on Information Theory." 1960, V. IT-6, VI, No. 3, p. 311-329, illustrations, 61 lit. cit.

A Matched Filter Communication System for Multipath Channels. Sussman, S.M. "IRE Trans. on Information Theory," 1960, V. IT-6, VI, No. 3, p. 367-373, illustrations.

On New Classes of Matched Filters and Generalization of the Matched Filter Concept. Middleton, D. "IRE Trans. on Information Theory," 1960. V. IT-6, VI, No. 3, p. 349-360, illustrations.

2. RADIO COMMUNICATION SYSTEMS

Development Trends in USAF Global Communications Systems in 1960 Kunze, A.A. and others. "IRE Internat. Convent. Rec." 1960, V. 8, P. 5 p. 194- 207, illustrations, 4 lit. cit.

Simple Methods for Designing Troposcatter Circuits. Yeh, L.P. "IRE Internat. Convent. Rec." 1960, V. 8, P. 5, p. 180-187, illustrations, 17 lit. cit.

Equipment Configuration and Performance Criteria for Fully Optimized Tropospheric-Scatter Systems. Parry, C.A. "IRE Internat. Convent. Rec." 1950, V. 8, P. 5, p. 169-178, illustrations, 16 lit. cit.

Analysis of a Phase Modulation Communications System. Choate, R.L. "IRE Internat. Convent. Rec." 1960, V. 8, P. 5, p. 208-218, ill.

New Communication System Cut Reaction Time. Speed Control Function "Aviat. Week," 1960, V. 72, VI, No. 25, p. 130-132, ill.

Multiple asynchronous communications systems employing "address" command. System Concepts for Address Communication Systems. "IRE Wescon Convent. Rec." 1960, P. 7, p. 102-106, illustrations.

Cryptographic Signaling Applied to Radio Communication Circuits. Thompson, O.E. "IRE Internat. Convent. Rec." 1960, V. 8, P. 8, p. 265-272, illustrations.

Optimized SSB Transmitter Loading by Multichannel Frequency Division Data. Brennan, A.T. and others. "IRE Internat. Convent. Rec." 1960, V. 8, P. 5, P. 188-193, illustrations.

An Improved Decision Technique for Frequency-Shift Communication Systems. Thomas, E. "IRE Internat. Convent. Rec." 1960, V. 8, P. 5, p. 219-227, illustrations, 3 lit. cit.

Sensitivity Receiving System for Frequency Modulated Wave. Morita, M. and Ito, S. "IRE Internat. Convent. Rec." 1960, V. 8, P. 5, p. 228-237, illustrations, 10 lit. cit.

3. SPACE RADIO AND TELEVISION COMMUNICATION

Use of waves of centimeter and millimeter length in outer space. Johnson, "Zarubezhnaya Radioelektronika," 1960, V. 8, No. 8, pp. 9-16.

Two Approaches Pressed to Crack Space Communications Barrier. "Electronic Design," 1960, V. 8, No. 7, p. 32-34, illustrations.

Radio relay system employing artificial earth satellites. Communication Relaying. Cutler, C.C. "IRE Internat. Convent. Rec." 1960, V. 8, P. 5, p. 275-276.

RFI in Satellite Communications Systems. Salati, O.M. "Electronic Ind." 1960, V. 19, VI, No. 4, p. 93-97, ill., 18 lit. cit.

HF Satellite Scatter. "Wire and Radio Communs." 1960, V. 7, VII,

No. 7, p. 43-44, 46, illustrations.

Communication Satellites. Pierce, J.R. "Wire and Radio Communs." 1960, V. 7, VII, No. 7, p. 9-10, 50, 54, illustrations.

Active Vs Passive Satellites for a Multi-Station Network. Pollack, L. and Campbell, D. "IRE Internat. Convent. Rec." 1960, V. 8, P. 5, p. 141-146, illustrations, 3 lit cit.

Moon Relay Communication. Radford, W.H. "IRE Internat. Convent. Rec." 1960, V. 8, P. 5, p. 277-283, illustrations.

Radio Relaying by Reflection from the Sun. Blattner, D.J. "IRE Internat. Convent. Rec." 1960, V. 8, P. 5, p. 135-140, ill., 7 lit. cit.

Television and Lunar Investigations. Spalding. "Radio Electronics Abroad" 1960, VIII, No. 8, p. 17-77, illustrations.

Design Consideration of Television Satellite Reconnaissance Systems. Zastrow, R. and Ritchie, R. "IRE Internat. Convent. Rec." 1960, V. 8, P.5, p. 87-107, illustrations, 27 lit. cit.

4. RADIO RELAY LINES

Radio Frequency Interference Consideration in the TD-2 Radio Relay System. Curtis, H.E. "Bell Sys. Tech. J." 1960, V. 39, No. 2, p. 369-387, 7 lit. cit.

Newfoundland's Microwave TV Network. Jarman, H.G. "Electronics World," 1960, V. 64, VII, No. 1, p. 54-55, 110, illustrations.

Use of television relays for telephone communication in the province of Saskatchewan (Canada). Television Microwave Facilities Included in SGT Expansion Program. "Electronics and Communs." 1960, V. 8, VI, No. 6, p. 40, 69.

Remote TV Control By Blanking-Interval Pulses. Kazamak and others. "Electronics," 1960, V. 33, V, No. 20, p. 79-81, illustrations.

Radio Coverage-Area Survey-Instrumentation Research. Sharp, C.E. and Lacy, R.E. "IRE Internat. Convent. Rec." 1960, V. 8, P. 8, p. 259-264, illustrations, 2 lit. cit.

Long-distance TV Transmission requirements and measurements. Anforderungen und Messungen an Fernseh-Weitverbindungen. Müller, J. "Nachr.-Techn. Zeitschr." 1960, VII, No. 7, S. 327-324, ill., 7 lit. cit.

Power Bridging for Microwave Stations. Feese, W.E. "Pipeline Engr." 1960, V. 32, IV, p. 3-23 - D-25, illustrations.

Power Supply for TJ Repeaters. Small, R.H. "Bell Labs. Rec." 1960, V. 38, VII, No. 7, p. 262-265, illustrations.

5. NOISE AND INTERFERENCE

Effects of Nuclear Tests on Radio Noise. "Wire and Radio Communs." 1960, V. 7, VII, No. 7, p. 26.

Electromagnetic Interference and Vulnerability Reduction. Egli, J.J. "IRE Internat. Convent. Rec." 1960, V. 8, P. 8, p. 48-53, ill., 8 lit. cit.

Making Transmitters RFI-Free. Blakely, C.E. and Bailey, R.N. "Electronic Ind." 1960, V. 19, No. 3, p. 133-141, ill., 36 lit. cit.

RFI I Everybody's Business. Hickey, J.E. "Electronic Ind." 1960, V. 19, No. 3, p. 131-132.

Radio interference in telephone lines and its permissible value. Funkstörungen durch Fernsprecheinrichtungen und ihre Grenzwerte. Kö-witsch, G. "Fernmeldepraxis," 1960, Bd. 37, VI, No. 12, S. 474-477, ill.

Disturbances in telephone connections caused by operating radio transmitters. Fernsprechstörungen, die durch Rundfunksender hervorgerufen werden. Köwitsch, G. "Fernmelde praxis," 1960, Bd. 37, VI, No. 12, S. 478-480, illustrations.

Appearance and reduction of noise in receivers. Entstehung und Einschränkung des Rauschens. Reinsch, H.H. "Fernmelde praxis," 1960, Bd. 37, VII, No. 14, S. 578-583.

Experimental study of the duration of noise peaks. Velichkin, A.I. and Ponomareva, V.C., "Radiotekhnika," 1960, V. 15, No. 10, pp. 21-26, illustrations, 3 lit. cit.

Reducing Interference in Ionospheric Sounding. Perry, K. "Electronics," 1960, V. 33, V, No. 22, p. 118-120, illustrations.

6. PROPAGATION OF RADIO WAVES

Long-distance scattering of short waves by the earth. Kobanov, N.I. "Radiotekhnika and Elektronika," V. 5, No. 10, p. 1578-1592, illust., 38 lit. cit.

Tropospheric Propagation at VHF. Dixon, J.M., "Proc. IRE Austr." 1960, V. 21, VI, No. 6, p. 398-406, illustrations.

Ultra-Low-Frequency Atmospherics. König, H., "IRE Internat. Convent. Rec." 1960, V. 8, P. 1, p. 128-133, illustrations, bibl. No. 15.

Anomalies in the Absorption of Radio Waves by Atmospheric Gases. Straiton A.W. "Proc. IRE," 1960, v. 48, V. No. 5, p. 898-903, illust.

Radio Forecasting. Jowett, J.K. S., "Post Off. Telecommuns. J." 1960, No. 3, p. 122-126, illustrations.

Some Medium Frequency Sky Wave Measurements. Dixon, J.M., "Proc. IRE Austr." 1960, V. 21, VI, No. 6, p. 407-409, illustrations.

Observations of Sudden Ionospheric Disturbances. Morris, R.W., "Proc. Phys. Soc.," 1960, V. 76, VII, No. 487, p. 79-92, illust., bibl.

Radio Frequency Scattering from the Surface of the Moon. Leadabrand R.L. "Proc. IRE," 1960, V. 48, V. No. 5, p. 932-933, illustrations.

Propagation Measurements in Shock-Ionized Media. Sukhia, D.E. and Hampton, G.H. "IRE Internat. Convent. Rec." 1960, V. 8, P. 1, p. 115-127, illust., 8 lit. cit.

7. ANTENNAS

A Broadband Spherical Satellite Antenna. "IRE Internat. Convent. Rec." 1960, V. 8, P. 5, p. 63-73, illustrations.

Powerhandling Capability of Antennas at High Altitude. Scharfman, W.E. and Morita, T., "IRE Internat. Convent. Rec." 1960, V. 8, P. 1, p. 103-114, illust., 9 lit. cit.

Fresnel Region Field Distributions of Circular Aperture Antennas. Ming-Kuei Hu. "IRE Trnas. on Antennas and Propag." 1960, V. AP-8, V, No. 3, p. 344-346, illust., 3 lit. cit.

Some New Methods of Analysis and Synthesis of Near-zone Fields. Ming-Kuei Hu. "IRE Internat. Convent Rec." 1960, V. 8, P. 1, p. 13-21, 8 lit. cit

The Spiral Antenna. Bower, R. and Wolfe, J.J., "IRE Internat. Convent. Rec." 1960, V. 8, P. 1, p. 84-93, illust., 10 lit. cit.

The Archimedean Two-Wire Spiral Antenna. Kaiser, J.A., "IRE Trans. on Antennas and Propag." 1960, V. AP-8, V. No. 3, p. 312-322,

illustrations, 15 lit. cit.

Parasitic Spiral Arrays. Brown, R.M., "IRE Internat. Convent Rec." 1960, V. 8, P. 1, p. 51-66, illustrations, 6 lit. cit.

Experimental Study of a Diffraction Reflector. Provencher, J.H., "IRE Trans. on Antennas and Propag." 1960, V. AP-8, V. No. 3, p. 331-336, illustrations, 3 lit. cit.

Corner-Reflector Antenna Design. "Electronic Design." 1960, V. 8, V, No. 10, p. 250-251, illustrations.

Log Periodic Dipole Arrays. Isbell, D.E., "IRE Trans. on Antennas and Propag." 1960, V. AP-8, V, No. 3, p. 260-267, illust., 7 lit. cit.

Some Consideration in the Design of the Horizontal Rhombic Antenna. Rac, K.L., "J. Inst. Telecommun. Engrs." 1960, V. 6, No. 3, p. 123-126, illust., 9 lit. cit.

Simulation Tests on an Interference Rejection Antenna System. Ball, C.O. and White, W.D., "IRE Internat. Convent. Rec." 1960, V. 8, P. 8, p. 3-9, illustrations.

Derivative Control in Shaping Antenna Patterns. Ksienski, A., "IRE Internat. Convent. Rec." 1960, V. 8, P. 1, p. 3-12, illustrations, 5 lit. cit.

Phase shift in balanced antenna switches caused by lightning protectors. Rubinshtein, B.E., "Radiotekhnika," 1960, V. 15, No. 10, pp. 14-16, illustrations, 4 lit. cit.

8. WAVEGUIDES AND MICROWAVE TRANSMISSION

Waveguide for long-range Signal Transmission. Wellenleiter für die Nachrichtenübertragung über grosse Distanzen. "Rev. PTT," 1960, VII, No. 7, p. 186-187, illustrations.

Spiral Waveguides. Die Wendel als Übertragungsleitung für Hohlleiterwellen. Piefke, G., "Nachr.-Techn. Zeitscher." 1960, VII, No. 7, S. 335-341, illustrations, 9 lit. cit.

Excitation of a circular waveguide by the H_{01} Wave of a Magnetron Resonator. Minich, V.V., "Izv. Sibirsk. Otd. AN SSSR," 1960, No. 7, p. 19-24, illust., 7 lit. cit.

Impedance Measurements by Propagation Constant Perturbation. "Proc. IRE," 1960, V. 48, V. No. 5, S. 904-911, illust.

Calculation of the propagation constant of an H-waveguide with a TM ferrite plate. Kovtun, N.M. and Tereshchonko, A.I., "Zh. Tekh. Fiz." 1960, V. 30, No. 9, p. 1077-1080, illust., 9 lit. cit.

Variational method for calculating symmetrical four-pole discontinuities in rectangular waveguides, Il'in, V.S., "Izv. Vyssh. Ucheb. Zavedenii" (Radiofizika), 1960, V. 3. No. 4, p. 683-693, illust., 7 lit. cit.

Analysis of certain Transmission-line Networks in the Time Design. Getsinger, M.J., "IRE Trans. on Microwave Theory and Techniques," 1960, V. MTT-8, No. 3, p, 301-309, illustrations.

A Y-Junction Strip-Line Circulator. Milano, U. and others. "IRE Trans. on Microwave Theory and Techniques," 1960, V. MTT-8, V. No. 3, p. 346-351, illustrations.

Discontinuities in the Center Conductor of Symmetric Strip Transmission Line. "IRE Trans. on Microwave Theory and Techniques." 1960, V. MTT-8, V. No. 3, p. 328-339, illustrations.

9. PARAMETRIC AND QUANTUM MECHANICAL AMPLIFIERS

Parametric Amplification. Power Control and Frequency Multiplication at Microwave Frequencies Using Cyclotron-Frequency Devices. Cussic, C.L., "RCA Rev." 1960, V. 21, VI, No. 2, p. 228-244, illust.

Noise in parametric semiconductor amplifiers with variable capacitance. Uenohara, "Zarubezhnaya Radioelektronika," 1960, V. 8, No. 8, p. 214-142, illust., 12 lit. cit.

Theory of Masers with Traveling Waves. Kontorovich, V.M., "Izv. Vyssh. Ucheb. Zavedenii" (Radiofizika), 1960, V. 3, No. 4, p. 656-666, illust., 11 lit. cit.

Measurement of the thermal noise of a Traveling-Wave Amplifier. "Zarubezhnaya Radioelektronika," 1960, V. 8, No. 8, p. 120-123, illust., 7 lit. cit.

Packaged Tunable L-Band Maser System. "Proc. IRE," 1960, V. 48, V. No. 5, p. 866-874, illustrations.

10. TELEPHONY AND TELEGRAPHY

The Complexity of the Transmission Network. Abraham, L.G., "Bell Labs. Rec." 1960, V. 38, No. 2, p. 43-48, illustrations.

An Improved Multiplex Voice Frequency Carrier System. Tennent, B., "IRE Internat. Convent. Rec." 1960, V. 8, P. 5, p. 238-246, illust., 5 lit. cit.

Transistorized Carrier Telephone Equipment. "Philips Telecommuns. Rev." 1960, V. 21, No. 4, p. 183-193, illustrations.

Transistorized Carrier and Multiplex System. Wagner, T.T., "Pipeline Engr." 1960, V. 32, No. 4, p. D-30-D-32, illustrations.

TASI Boots Cable Capacity. Reed, J.S. "Telephone Engineer and Management," 1960, V. 64, No. 5, p. 44-45.

Detail Design of an Operational Missile Detail Design of an Operational Missile Voice Frequency Communications System. Cayott, W.S., "IRE Internat. Convnet. Rec." 1960, V. 8, P. 5, p. 148-158, illustrations.

The UR49A Automatic Telephone System. Westerveld, F., "Philips Telecommuns. Rev." 1960, V. 21, No. 4, p. 145-154, bibl. No. 5.

Electronic telephone exchange with 240 lines. "Mecanique Electricite," 1960, V, No. 133, p. 73, illustrations.

A Central Control for ESS. Drew, G.G., "Bell Labs. Rec." 1960, V. 38, No. 2, p. 49-53, illust.

Wiring of Data Systems for Minimum Noise. White, J.V., "IRE Internat. Convent. Rec." 1960, V. 8, Pt. 8, p. 28-34, illust.

Cables for Local Communication Lines. Böhme, G., "Fernmelde praxis," 1960, Bd. 37, VIII, No. 15, p. 601-619.

Gas Tracers Locate Cable Leaks. "Telephone Engineer and Management," 1960, V. 64, No. 6, p. 68-71, illust.

Device for Cable Measurements Between Inter-city Telephone Stations. Kabelmesseinrichtung für Fernämter, Kallen, R., "Techn. Mitt. PTT," 1960, No. 4, p. 118-121, illust.

Measurement of Pulse Distortion in Carrier-Frequency Transmission by Means of a Test Loop Through the Source (telegraph) Station. Impulsverzerrungs-Messungen an TF-Systemen mit systemeigener Signalübertragung als Schleifenmessung über die Gegenstelle. Falk, W., "Fernmelde praxis," 1960, Bd. 37, VI, No. 12, p. 485-494, illust., 3 lit. cit.

Low-Frequency Noise Generator. Bell, D.A. and Rosie, A.M.,

"Electronic Technology," 1960, V. 37, VI, No. 6, p. 241-243, illust., 7 lit cit.

Redesign of Low-Frequency Network. Steiff, L.H., Bell Labs. Rec." 1960, V. 38, No. 2, p. 68-71, illustrations.

Transmission of Photo-telegrams by Frequency Keying. "J. Inst. Telecommuns. Engrs." 1960, V. 6, No. 3, p. 132-139, illust., 7 lit. cit.

11. TELEVISION

Compression of the Frequency band of a Television Signal by the Frequency-shift Method. Whasson and Bell. "Zarubezhnaya Radioelektronika," 1960, VII, V. 8, p. 28-40, illust., 7 lit. cit.

Noise Limitations to Resolving Power in Electronic Imaging. Coltt-man, J.W. and Anderson, A.E., "Proc. IRE," 1960, V. 48, V. No. 5. p. 858-865, illustrations.

Sine-Squared Pulses in Television System Analysis. Kennedy, R., "RCA Rev." 1960, V. 21, VI, No. 2, p. 253-265, illust.

A Transversal Equalizer for Televison Circuits. "Bell Sys. Tech. J." 1960, V. 39, No. 2, p. 405-422, 8 lit. cit.

Transistorized Carrier System for TV. Schimp, L.G., "Bell Labs. Rec." 1960, V. 38, VII, No. 7, p. 253-255, illust.

Coaxial Transmission of Television Programs. Fernsehübertragung auf Fraht-Wegen. Reinsch R. "Fernmelde praxis," 1960, Bd. 37, VIII, No. 16, p. 647-656, illust.

12. ELECTRON-TUBE AND SEMICONDUCTOR INSTRUMENTS

Small-Signal Performance and Noise Properties of Microwave Triodes. "Philips Res. Reps." 1960, V. 15, No. 2, p. 124-221, illust., 63 lit. cit.

Modern-Trends in Magnetron Design. "Electronic Technology," 1960, V. 37, VI, No. 6, p. 234-237, illust., 3 lit. cit.

Future developments in Transistors and Electron Tubes (a review of new instruments). Weiterentwicklungen von Transistoren und Röhren. Reinseh, H., "Fernmelde praxis," 1960, Bd. 37, VIII, No. 16, p. 668-673, illust.

Patent Review of Semiconductor Devices, Fabrication Techniques and Processes and Circuits and Applications. Marshall, S., "Semiconductor Products," 1960, V. 3, No. 5, p. 56-57.

Characteristics Chart of New Transistors. "Semiconductor Products," 1960, V. 3, No. 5, p. 58-61.

TELECOMMUNICATIONS

1961

A.S. Popov Technical Society of Radio Engineering and Telecommunications
Svyaz'izdat, Moscow

EDITORIAL BOARD

A. Ch. Pukhal'skiy, Editor

B.F. Anosovich
S.V. Borodich
N.I. Chistyakov
A.D. Fortushenko
P.T. Gobets
I. Ye. Golubtsov
V.A. Kuz'min
G.A. Levin
Ye. V. Markhay
Ye. S. Medvedev
Ye. A. Rizkin
P.V. Shmakov
V.M. Shteyn
N.N. Shumskaya
V.I. Siforov
B.P. Terent'yev
G.S. Tsykin
N.B. Zeliger
E.V. Zelyakh

The English Edition of Telecommunications is mailed to subscribers within 18 weeks after the publication of the original Russian issue.

Russian Electronic Journals published by the
American Institute of Electrical Engineers
Translated by Royer and Roger, Inc.

	Subscription rates			
	Individuals		Libraries	
	$	£	$	£
Telecommunications	14.25	5	28.50	10
Radio Engineering and Electronics	28.50	10	57.00	20
Radio Engineering	14.25	5	28.50	10

Royer and Roger translates and produces
the following Russian scientific journals:

Biophysics
Entomological Review
Geochemistry
Geodesy and Cartography
Izvestiya, Academy of Sciences of the USSR, Geologic Series
Pavlov Journal of Higher Nervous Activity
Problems of Oncology
Radio Engineering
Radio Engineering and Electronics
Refractories
Sechenov Physiological Journal of the USSR
Soil Science
Telecommunications

Comments and inquires regarding *Telecommunications* and other translation journals should be sent to:

International Division
Royer and Roger, Inc.

1000 Vermont Avenue, N.W.
Washington 5, D.C.

41 East 28th Street
New York 16, New York

TELECOMMUNICATIONS
ЭЛЕКТРОСВЯЗЬ

NUMBER 1 1961

CONTENTS

Page

V.A. Smirnov: Application of Null-Deviation for the Evaluation of Noise and Distortion 1

V.S. Andreev, B.P. Burdzeiko and V.I. Vasil'ev: Low Frequency Regenerative Divider 7

V.V. Shirokov: Interference Effects on a Two-Channel Receiver Installation With AGC 16

G.B. Al'tshuler and V.A. Prokhorov: Selection of Network Elements to Compensate for Frequency Changes Due to Temperature in Quartz-Crystal Oscillators 24

A.A. Glukhov: Investigation of the Effect of Phase Distortion Instantaneous Signal Value in a Radio Transmission Channel 35

V.B. Shteinshleiger: Quantum Paramagnetic Amplifiers of Ultrahigh Frequencies 43

K.P. Egorov and I.V. Sukhodoev: High-Frequency Telephone Communications with Semiconductor Triodes 54

Yu. D. Farber: Selection of Semiconductor Amplifier Circuits For Multiplex Balanced Cables 62

E.E. Raukas: Application of Varistors to Arc Quenching Circuits 71

Letters to the Editor 78

Author's Certificates (Patents) 82

Bibliography 85